EXPERIMENTAL INVESTIGATION OF RECOVERING GOLD FROM MAGHEMITE-RICH MAGNETIC CONCENTRATES BY ROASTING

by

Bernard Fosu

A thesis submitted to the Faculty and the Board of Trustees of the Colorado School of Mines in partial fulfillment of the requirements for the degree of Master of Science (Metallurgical and Materials Engineering).

Golden, Colorado

Date: _____

Signed: _____

Bernard Fosu

Signed: _____

Dr. Patrick R. Taylor

Thesis Advisor

Golden, Colorado

Date: _____

Signed: _____

Dr. Ivar Reimanis

Professor and Head

Department of Metallurgical & Material Engineering

ABSTRACT

Roasting of double refractory ores found in the Carlin Trend is necessary to oxidize the sulfides and remove the organic matter prior to leaching for gold extraction. Oxidation of the iron sulfides often leads to the formation of maghemite, an intermediary product of non-porous calcine, which negatively affects cyanide leaching. Magnetic recovery circuits are often used to capture the highly magnetic maghemite from the leach tails. The magnetic concentrates are either routed to autoclaves for pretreatment or as part of the raw feed to the roasters. The component that goes into the autoclave is ground finer prior to pressure oxidation. This fine grinding presents an added processing cost.

The main objective of this project was to explore the possibility of recovering gold from the maghemite-rich magnetic concentrates by roasting. Preliminary roasting tests were conducted on pure maghemite standard samples and the results obtained were used as a basis for further roasting the magnetic concentrate samples. The magnetic concentrates were characterized before and after the experiments to determine any changes in mineralogy, composition, and surface characteristics. Roasting at 650^{o}C or higher resulted in at least 50% maghemite-to-hematite conversion. The roast calcines were cyanide-leached for gold recovery. Results suggest that roasting improves gold recovery from the magnetic concentrates from no extraction to about 85% extraction. Enriching the roast air with oxygen did not yield in any appreciable increase in gold recovery. Additional test results have also shown that finer grinding of the magnetic concentrates and/or prolonging the roasting time barely reduces the arsenic, organic carbon and sulfide sulfur content of the resulting calcine. Therefore, these processes do not result in any appreciable increase in gold recovery. Even though roasting has been proven as a feasible means of recovering appreciable amount of the gold held in the maghemite-rich magnetic concentrates, it is highly recommended that its application on a large scale be preceded by a detailed economic analysis.

Keywords: Roasting, refractory gold ores, magnetic concentrates, maghemite, calcine, cyanide leaching, pressure oxidation, organic matter, sulfide sulfur, arsenic

TABLE OF CONTENTS

LIST OF FIGURES

LIST OF TABLES

ACKNOWLEDGMENTS

I am greatly indebted to my advisor Dr. Patrick Taylor for the incredible guidance, support, supervision, opportunities and inspiration that he continues to give me. I am confident of succeeding wherever I find myself because of the priceless coaching and training he has given me. To him I say “I remain extremely grateful!”

Special thanks go to my thesis committee members, Dr. Corby Anderson and Prof. Erik Spiller for their valuable insight and time in reviewing my work and providing me with useful feedback which has made this work a success story.

This work was made possible by funding from Newmont Mining Corporation. I really appreciate the contributions made by Dr. Scott Shuey, Matthew Jeffrey, and the entire metallurgy team at the Newmont Metallurgical Services facility in Englewood, CO. To the metallurgy team at Newmont, Carlin, NV, I say “I am grateful for the internship opportunity…thanks for providing me with the samples for this work.”

I am also grateful to all the members of the Kroll Institute for Extractive Metallurgy for their help regarding experimental set-up and data analysis. Thank you all for providing me with a warm and cordial atmosphere to learn and grow. Special thanks go to Phil Lowe, Dane Hyer-Peterson, Scott Pawelka, Patrick Eduafo, Hunter Sceats and Will Friesinger for their respective supports.

I greatly appreciate all of my friends for providing me with a home away from home.

DEDICATION

This work is dedicated to;

My awesome parents and siblings for their continued love and support…to my lovely brother Prince Boateng, I say "You keep me motivated! I love you!"

Charles Bissue, my mentor, for his invaluable support and coaching. Charles, I say "You are definitely worth dedicating this work to." and to

Esther Kwekie Kwenortey, my very special friend, for her priceless friendship and encouragements…I say "Knowing you makes a lot of difference."

CHAPTER 1

INTRODUCTION

This chapter introduces the background of the project and outlines the objectives and motivations.

1.1 Background

Gold ores are generally classified into non-refractory and refractory ores. The non-refractory ores are said to be ‘free milling’ as significant proportion of the gold (>90%) can be recovered by milling followed by direct cyanidation. The refractory ores are characterized by poor gold recoveries, even with ultrafine milling and enhanced reagents addition. The refractory ores are not economically amenable to direct cyanidation owing to several reasons including; the gold being locked up in sulfide matrices, presence of organic carbonaceous matter, and presence of reactive minerals in the ore that react with leach reagents in side reactions that deplete the reagents available for gold dissolution. Refractory ores are characterized by poor gold extractions which do not normally allow economic recovery of the gold metal.

The refractory ores are said to be double refractory when in addition to the presence of sulfide components, the ore also contains organic carbonaceous matter. This naturally occurring carbon competes with the activated carbon used in carbon-in-leach (CIL) circuits and absorb the metal cyanide complexes in a process called ‘preg-robbing’. Ores in the Carlin Trend are known refractory ores.

Unfortunately, mining costs have been increasing but as mining progresses, the non-refractory ores are being depleted, and the encountered gold ore bodies are decreasing in grade. These coupled with the recent global volatility in gold prices have made the luxury of not treating

double refractory ores no longer an acceptable business option. According to Taylor [1], "The increasing trend towards lower grade and more complex ores and the need for lower cost processes especially for small deposits have resulted in the introduction of a variety of new processes." Pretreatment steps are therefore required to make extraction from refractory gold ores economically viable.

The pretreatment methods that have been used commercially include Pressure Oxidation, Biological Oxidation, Roasting [1-7]. According to Paktunc et al [4], roasting is the oldest technique employed to recover Au from double refractory ores. Newmont Mining Corporation's Gold Quarry Mine in Carlin, Nevada employs roasting in a two-train circulated fluidized bed reactors at solid feed rate of between 440 tph – 500 tph to oxidize the sulfides and remove the organic matter prior to carbon-in-leach process for gold extraction. According to Hammerschmidt et al [5], "The processed gold ore consists mainly of quartz (70%), with 1.5–2.5% sulfur and approximately 0.4% organic carbon."

Following dry grinding, roaster oxidation is performed at conditions that, in addition to oxidizing sulfides, combust the organic carbon. Ideally, the oxidation transformation from pyrite to pyrrhotite should be followed by conversion to magnetite and the magnetite further oxidized to hematite [5, 8] and the gold that was present as solid solution in the pyrite forms colloids within the hematite. The ideal texture of the produced hematite is porous to allow for the penetration of cyanide for gold dissolution. Douglas and Semenyna [10] have noted that "Temperature and other conditions of roasting, as well as ore characteristics (pyrite mineral associations, arsenic) can affect the texture and the type of iron oxide formed. Many of these alternate iron oxide minerals result in incomplete leaching." A commonly known intermediate phase known as maghemite (γFe_2O_3) is usually formed during the transformation from magnetite to hematite [5, 8, 10-12]. Maghemite

is an intermediary product of non-porous calcine and is detrimental to subsequent cyanide leaching. Gold deportment to tails, caused mainly by entrapments in maghemite, requires that the maghemite component of the leached tails be further reprocessed to recover the included gold. After cyanide leaching, maghemite containing gold, and tailing hematite from which gold has been dissolved make up the leach tails. Owing to the highly magnetic nature of maghemite, Newmont Carlin has designed a magnetic recovery circuit to capture these iron oxides from the leach tails, and with subsequent reprocessing, recover the lost gold. The magnetic concentrates are either routed to autoclaves or as part of the feed to the rosters. The component that goes into the autoclave is ground finer prior to pressure oxidation. This fine grinding presents an added processing costs as can be seen from Figure 1.1. It is therefore imperative to assess options of recovering gold from maghemite to ensure that the overall process is technically feasible and economically viable.

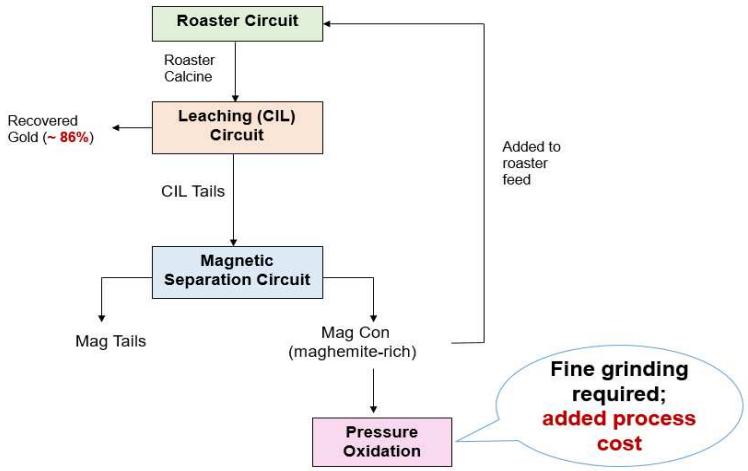

Figure 1.1 Processing route for maghemite-rich magnetic concentrates

1.2 Research Objectives

The goal of this research will be to assess the possibility of recovering gold from maghemite-rich magnetic concentrates by roasting.

CHAPTER 2

LITERATURE REVIEW

In this chapter, relevant literature has been reviewed.

2.1 Classification of Gold Ores

Gold is a lustrous, yellow metal which is malleable and relatively chemically inert [2, 13]. Mudd et al [13] noted that throughout human history, gold has enjoyed a special place as a preferred metal for jewellery and signifying wealth and power – with widespread gold use by the ancient Egyptians and across Europe and Asia. According to the United States Geological Survey [14], "Estimates of the gold content of the earth's crust are in the range of 0.001 to 0.006 parts per million." Marsden and House [2] put the average concentration of gold in the earth's crust at about 0.005 g/t, which is much lower than most other metals, for example, silver (0.07 g/t) and copper (50 g/t).

According to Neuvonen [15], "Gold is recovered from sources such as: alluvial and placer deposits, veins associated with quartz and various sulfides; also from refining residues of nonferrous metals." Gold appears normally as a trace element in several common sulfide and sulfarsenide minerals [15]. This kind of gold is called submicroscopic or invisible gold [2, 3, 16, 17]. Gold concentration in common gold minerals [15] is presented in Table 2.1.

Table 2.1 Concentrations of gold in common minerals (Neuvonen [15])

Mineral		Gold concentration
Arsenopyrite	FeAsS	< 0.3 ppm-1.7 wt-%
Loellingite	$FeAs_2$	1.5 – 1.087 ppm
Pyrite	FeS_2	< 0.25 – 800 ppm
Tetrahedrite	$Cu_{12}As_4S_{13}$	< 0.25 – 59 ppm
Pyrrhotite	$Fe_{x-1}S$	0.006 – 1.8 ppm
Marcasite	FeS_2	0.05 – 4.1 ppm
Chalcopyrite	$CuFeS_2$	0.01 – 20 ppm

The primary and secondary gold bearing materials can be divided into fifteen groups, based on their mineralogical characteristics [18]. La Brooy et al [17] noted that gold ores are characterized as “free milling”, "complex" or "refractory", as illustrated in Figure 2.1 below. Refractoriness simply means stubbornness or not easily yielded. They referred to those gold ores that give acceptable economic gold recovery only with the use of significantly higher cyanide or oxygen requirements as “complex”. Several other authors however, simply classify gold ores as either refractory or non-refractory [1, 2, 6, 19, 20]. In non-refractory gold ores, significant proportion of the gold (>90%) can be recovered by milling followed by direct cyanidation [2]. The non-refractory ores are said to be free milling. Gold ores are considered refractory if gold recoveries from a conventional cyanidation process are less than 80% even after fine grinding [2, 21]. These low extractions do not normally allow economic recovery of the metal. Pretreatment steps are therefore required to make extraction from refractory gold ores economically viable.

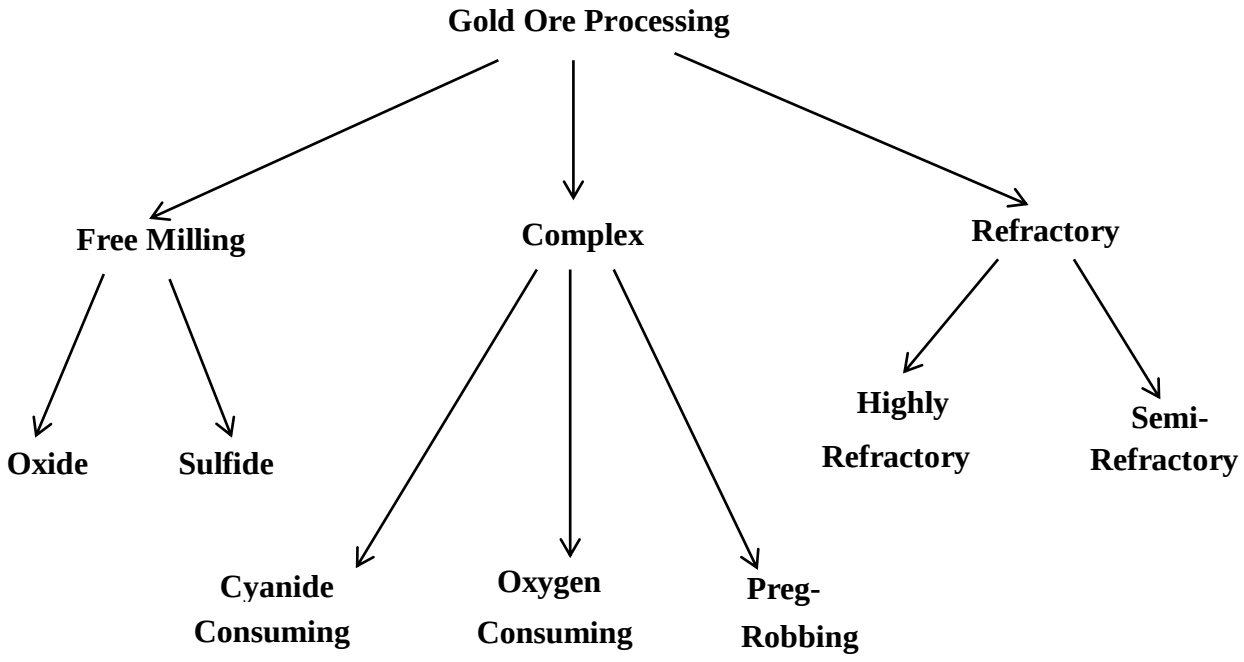

Figure 2.1 Classification of gold ores (Modified after La Brooy et al [17])

2.2 Non-refractory Ores

Non-refractory ores are said to be “free milling”. In free milling gold ores, significant proportion of the gold is recovered by gravity concentration and direct cyanidation [22]. Marsden and House [2] argued that the gold in non-refractory ores is not locked in the sulfides and is available for leaching. Free milling ores are easy to treat. Gold in such ores is recovered by gravity separating techniques or direct cyanidation [2, 6]. Processing options for free milling and semi-refractory ores are shown in Figure 2.2.

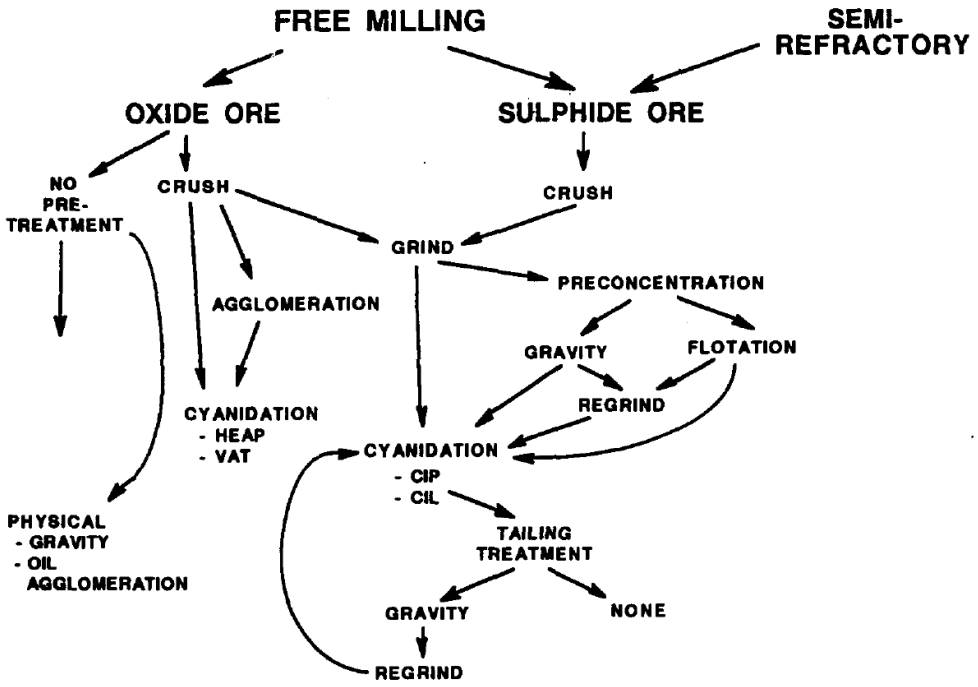

Figure 2.2 Gold processing options for free milling and semi-refractory ores (Modified after La Brooy et al [17])

The major processing route for free milling ores in is agitation cyanide leaching with gold recovery by CIP/CIL [2, 17]. In free milling ores, the ore is first prepared by a comminution step that usually consists of 2-3 stages of crushing and 1 or 2 stages of SAG or rod and ball milling to

produce a product typically 80% passing 75 µm [2, 13, 17]. In some cases, the nugget sized gold particles are recovered by a gravity concentration step [17].

2.3 Complex Ores

La Brooy et al [17] submitted that complex ores may be characterized by high cyanide or oxygen consumption or preg-robbing behavior caused mainly by carbonaceous matter; see Figure 2.3 below. Poor gold extraction by cyanide from these ores is attributed to preg-robbing characteristic of carbonaceous matter, gold locked in sulfide minerals and siliceous gangue. The active carbonaceous matter present has the ability of adsorbing dissolved gold from cyanide solutions and so rendering the leach liquor barren [2, 6, 20].

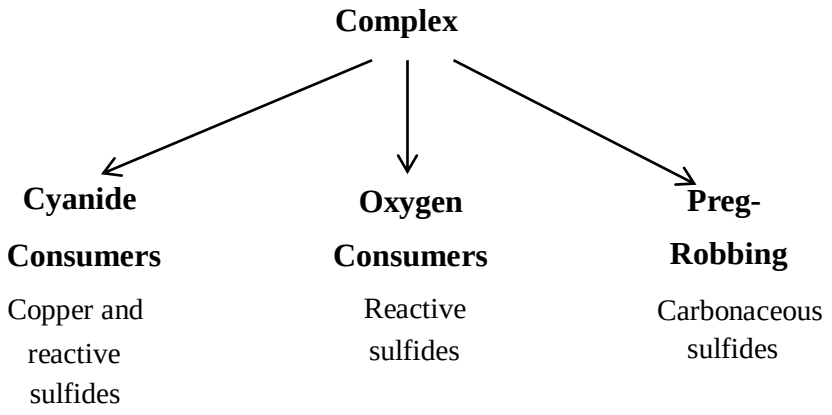

Figure 2.3 Complex ore classification (Modified after La Brooy [17])

Carbonaceous refractory gold ores contain organic carbon and inorganic carbon from black (or carbonaceous) and sedimentary rock series [6]. The carbonaceous gold ores are complex because dissolved aurocyanide complex is robbed by adsorption of carbonaceous matter, and this phenomenon is termed preg-robbing [2, 6, 17]. According to Afenya [6], the famous carbonaceous

gold ores include those at the Carlin gold mine in Nevada of USA, the Kerr Anderson mine in Canada, the Ashanti and Prestea Gold Mines in Ghana and the Bakyrchik and Natalkinsk mines of the Soviet Union. The mineralogy of some important carbonaceous gold ores have been presented in Figure 2.4 below.

Ore Type:	Carlin Ore	Gold Quarry	Jerritt Canyon	McLaughlin
Ref:	Guay[2]	Rota & Ekburg[5]	Birak & Deter[4]	Kunter et al.[6]
	%Wt	%WT	%WT	
Minerals:	Dolomite 39 Calcite 14 Quartz 36 Illite 8 Kaolin 13 Carbon 1 Pyrite	Calcite Dolomite Clay Minerals Quartz Chert Carbon 0.2-1% Pyrite 1.5-2%	Dolomite Calcite Sericite Quartz Carbon 0.7-2% Pyrite 2-4%	Pyrite Marcasite Pyrargyrite Miargyrite Chalcopyrite Sphalerite Galena Carbon-asphalt
Gold Size:	Submicroscopic Gold in carbonaceous matter, pyrite, illite	Submicroscopic Gold in chert and Pyrite.	Submicroscopic Gold associated with carbonaceous matter.	Gold locked in Sulphides.

Figure 2.4 Mineralogy of some important carbonaceous gold ores (Afenya [6])

2.4 Refractory Gold Ores

With reference to gold ores, the gold content is not released from the ore by milling and cyanidation [2, 23]. Fraser et al [7] have defined a refractory gold ore as one where gold recovery is less than 80% after conventional cyanidation. Barnes [23] reckoned that refractory ores are characterized by poor gold recoveries, even with ultrafine milling. La Brooy et al [17] added that even with enhanced reagent addition, refractory gold ores still give partial gold recovery. This has been confirmed by Taylor et al [4] as well as several other authors [2, 6].

When both sulfides and carbonaceous matter are present then the ore is classified as a double refractory ore [2, 3, 18, 22]. Unlike free milling ores, refractory ores require pre-treatment prior to cyanidation, in order to achieve optimum metal extraction [6]. As mining advances, the non-refractory ores become increasingly depleted. Marsden and House [2] and Yang et al [22] have suggested that with the increasing exhaustion of non-refractory gold ores, refractory gold ores have become main materials of the gold industry, and nearly one third of gold comes from refractory gold ores all over the world.

Again, free milling ores are not only being depleted, according to Mudd et al [13], gold ore grades are gradually declining. As can be seen from Figure 2.5, there has been a global decline in the grade of gold ores.

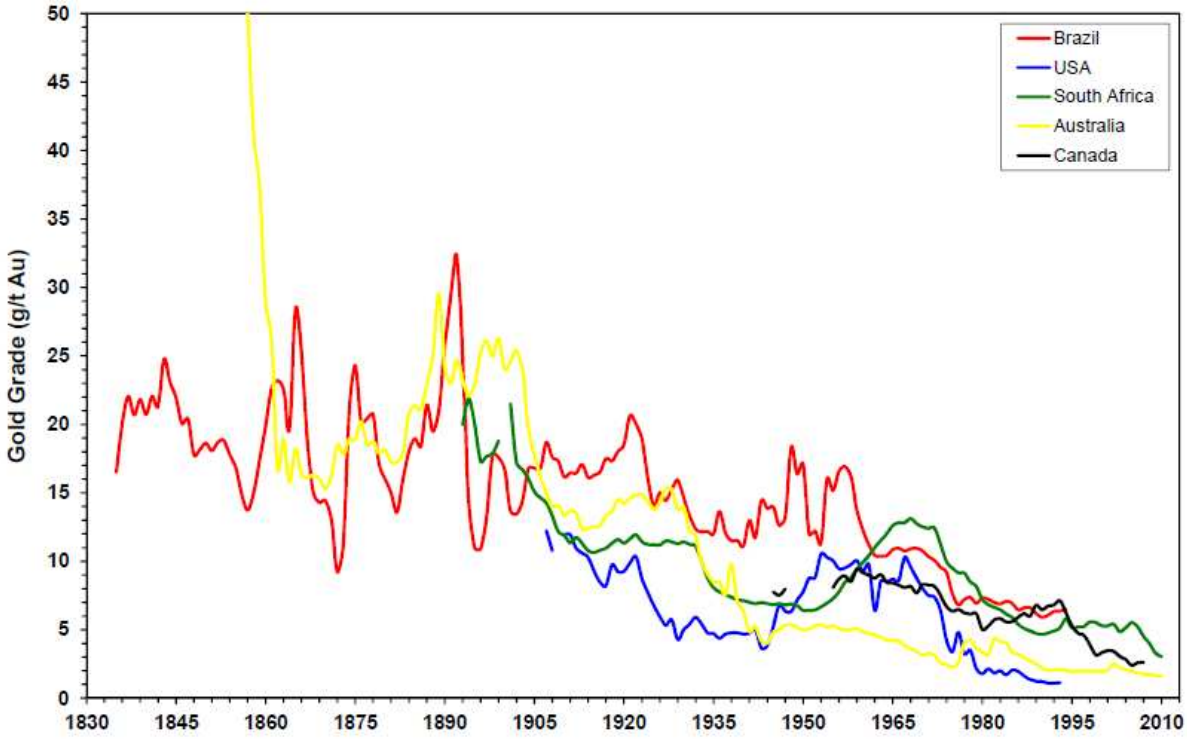

Figure 2.5 Gold ore grades over time (Modified after Mudd et al [13])

Afenya [6] has argued that because of the availability of considerable reserves of refractory gold ores in many parts of the world , there is the need for better understanding of their mineralogy if these ores are to be successfully treated.

2.5 Causes of Refractoriness

Ores may not respond to conventional cyanidation for three basic reasons [1, 2, 17].

- Gold can be locked up in the mineral matrix so that leach reagents are unable to reach it. Ellis [24] noted that gold can be finely disseminated in sulfide minerals, such as pyrite as can be seen from Figure 2.6.
- Reactive minerals in the ore can consume the leach reagents in side reactions and there may be insufficient cyanide and/or oxygen in the pulp to leach the gold.
- Components of the ore may adsorb or precipitate the dissolved gold cyanide complex so that it is lost from the leach liquor.

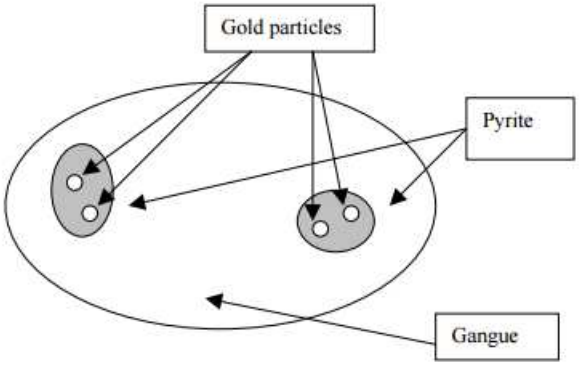

Figure 2.6 Pyrite locked gold within an ore (Modified after Ellis [24])

Some ores may have contributions from each of these factors, which will influence the processing strategy.

Ore mineralogy determines the degree of refractoriness [6, 17]. La Brooy et al [17] have graded and classified ore refractoriness as shown in Table 2.2.

Table 2.2 Classification of ore refractoriness (Modified after La Brooy [17])

< 50 % recovery	Highly refractory
50-80 % recovery	Moderately refractory
80-90 % recovery	Mildly refractory
> 90 % recovery	Non-refractory (Free Milling)

Developing an economic technology that is environmentally acceptable for treating refractory gold ores is crucial to the continued growth of the gold industry in the United States [6, 18].

2.6 Process Options for Refractory Gold Ores

According Fraser [7], the recovery of gold from refractory ores has received considerable attention in recent years. More and more ore bodies have been found where the gold is not amenable to simple cyanidation, and low recoveries have been indicated from various metallurgical test work [3, 7].

According to Taylor [1], "The increasing trend towards lower grade and more complex ores and the need for lower cost processes especially for small deposits have resulted in the introduction of a variety of new processes."

In the last several years, enormous research attention has been given to determining appropriate technically feasible, economically viable, and environmentally acceptable ways of treating refractory gold ores. According to La Brooy et al [17] "The options for processing

refractory sulfidic ores are complex and depend greatly on location and mineralogy." Fraser [7] noted that "quite a large number of possible processes have been developed, tested or considered."

These include: Pressure Oxidation (both acidic and alkaline), Biological Oxidation, Roasting (of which there are now several techniques), Chlorination and Ultra Fine Grinding [1-7]. According to Fraser [7] "Much development effort has also been expended on methods utilizing nitric acid." Pretreatment options for dealing with refractory ores as presented by La Brooy et al [17] is shown in Figure 2.7 below;

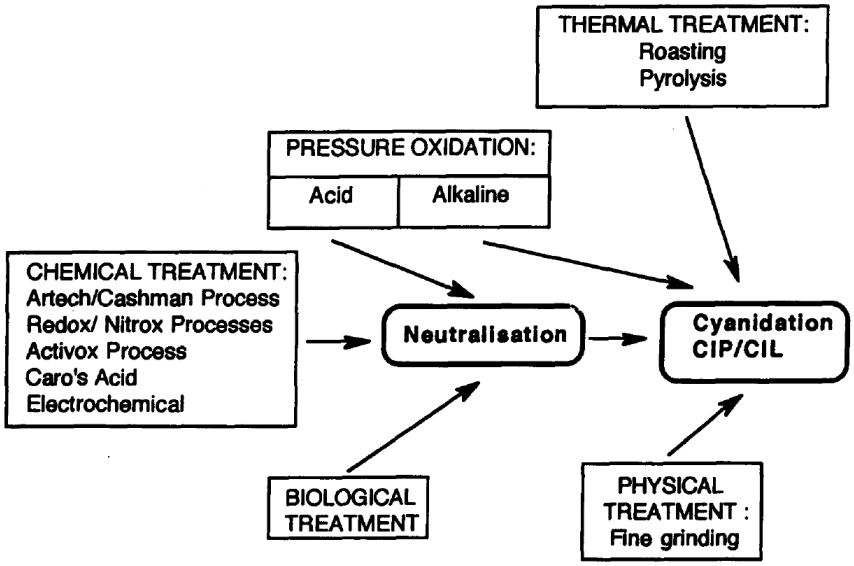

Figure 2.7 General process options for pretreating refractory ores (La Brooy et al [17])

2.6.1 Physical Treatment – Ultra Fine Grinding

A means of liberating disseminated gold from its host mineral is to further reduce the particle size of the host mineral [24]. Ultrafine grinding exposes a fragment of the gold surface which maximizes contact with cyanide solution during cyanidation [2, 17, 24].

According to Ellis [24] "A benefit of this technique is that the host mineral is not destroyed in an oxidative chemical reaction with the resultant problems of treatment of the reaction products." Ultra-fine grinding is normally done in mills such as vibratory mills, stirred mills and jet mills and can produce particle sizes as fine as 1 – 10 µm [17, 24]. Ultra-fine grinding is characterized by a high energy requirement and this has limited the process generally to pretreating higher grade concentrates rather than whole ores [24].

2.6.2 Chemical Pretreatment

The various chemical pretreatment methods for refractory ores have been discussed below.

Nitrox/Redox Processes

The overall chemistry of the Nitrox/Redox processes is generally the same. Differences however exist the operating temperatures and pressures [6, 17]. In these processes, the oxidant is nitric acid, and is mostly recycled [17]. According to La Brooy et al [17] "The Nitrox process uses soluble calcium nitrate and the Redox process regenerates spent nitric acid with oxygen." A simplified flowsheet for the Nitrox/Redox process is shown in Figure 2.8.

La Brooy et al [17] denoted the oxidation reactions for pyrite and arsenopyrite as follows:

$$3FeS_2 + 18HNO_3 \rightarrow Fe_2(SO_4)_3 + Fe(NO_3)_3 + 3H_2SO_4 + 6H_20 + 15NO \quad (2.1)$$

$$3FeAsS + 14HNO_3 + 2H_2O \rightarrow 3FeAsO_4.2H_2O + 3H_2SO_4 + 14NO \quad (2.2)$$

During recycling of the nitric acid, there is a reoxidation of NO to nitric acid as follows [17]:

$$2NO + O_2 \rightarrow 2NO_2 \quad (2.3)$$

$$3NO_2 + H_20 \rightarrow 2HNO_3 + NO \quad (2.4)$$

The operating conditions for both processes are around a pressure of 100-400 kPa, a temperature range of 90-110°C and a pH < 1 [17].

The formation of elemental sulfur must be avoided in the Nitrox process since this species reacts with cyanide [25]. According to Afenya [6] "The sulfur has to be converted into a soluble compound prior to cyanidation." Flatt and Woods [25] reported that the formation of elemental sulfur could be minimized by adding silver ions but this resulted in a decrease in the overall leaching rate.

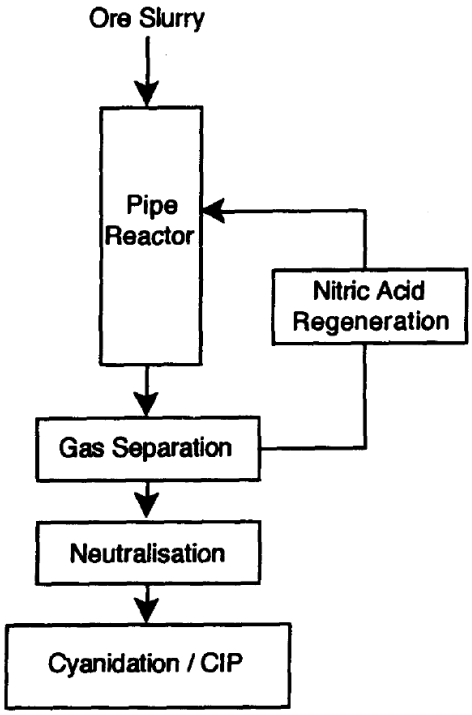

Figure 2.8 Simplified schematic flowsheet of the Nitrox/Redox process (La Brooy et al [17])

HMC Process

The HMC process is a single stage nitric-acid salt leach process and is carried out at 100°C and up to 1400 kPa in a pipe reactor [17]. The reactor is made of polyethylene coils enclosed in

concrete in a tank [17]. According to La Brooy et al [17] “The oxidizing solution is 10-30% w/w HNO_3 and 10% w/w NaCl solution.”

Iron ores containing gold (chalcopyrite, pyrite and arsenopyrite) is ground fine (< 50 µm) and pulped into a 30-60% w/w slurry. Nitric acid dissolves the gold and the gold-chloride complex $Au(Cl)_4^-$ is adsorbed onto activated carbon [17]. According to La Brooy *et al* [17] “High gold recoveries (> 90 %) have been claimed for various test ores and the process has been patented in several countries (eg Aust. Pat 580768, 4/2/89); but, there is no known commercial application of this technology.”

The Artech/Cashman Process

This process was developed to treat base metal flue dusts that contains arsenic [17]. In the process, Ca^{2+} is used as a reactant in acidic chloride solution at a temperature of 110°C and a pressure of 350 kPa [17] at an operating pH of 1-2 and a reaction time in the range of 30 – 60 mins [17]. This process is claimed to produce an environmentally acceptable arsenic-iron-calcium residue [17]. According to La Brooy *et al* [17] “The process could therefore be suitable for treating arsenopyritic gold ore in environmentally sensitive areas.”

However, “doubt has been expressed about the long term stability of the arsenic-iron-calcium residue due to its conversion to calcium carbonate by reaction with CO_2 in air releasing the arsenic.” La Brooy *et al* [17] noted.

The Caro's Acid Process

In the Caro's acid process, the sulfide is pulped in H_2SO_4 solution after Caro's acid is introduced as the oxidant [17]. According to La Brooy et al [17] “Caro's acid contains the species

H_2SO_5 and H_2O_2 and is a source of free oxygen in solution." La Brooy et al [17] added that the Caro's acid process can be expressed in the following equations:

$$H_2SO_5 + H_2O_2 \rightarrow H_2SO_4 + H_2O + O_2 \quad (2.5)$$

$$2H_2O_2 \rightarrow H_2O + O_2 \quad (2.6)$$

The oxidation of the sulfides results in sulfates and arsenates and some elemental sulfur [17].

However, it is reported that the high cost of the Caro's acid process makes the process less applicable on a large industrial scale. This is magnified substantially in the treatment of sulfide ores than for oxides. [26].

Electrochemical Processing of Ore Slurries

It is widely accepted that the electrical conducting properties of metal sulfide and telluride ore particles make their electrochemical processing feasible [2, 11, 17]. The oxidation of sulfide to either sulfate or sulfur and gold telluride can be described as follows [17]:

$$MS \rightarrow M^+ + S^0 + e^- \quad (2.7)$$

$$MS + 4H_2O \rightarrow M^+ + SO_4^{2-} + 8H^+ + 7e^- \quad (2.8)$$

$$AuTe_2 + 4H_2O \rightarrow Au^+ 2HTeO_2 + 6H^+ + 6e^- \quad (2.9)$$

According to La Brooy *et al* [17] "It is usually difficult to produce compacted or cast electrodes from ores and direct electrolysis of slurries is more practical." Figure 2.9 below summarizes the oxidation reaction mechanism. O denotes the oxidant form of the redox couple in solution and R denotes the reduced form of the redox couple in solution [17].

Slurry electrolysis is performed on a sample in its as-received form and the powder presents much needed surface area for the reaction [17]. According to La Brooy *et al* [17] "Slurry electrolysis has been applied at a laboratory, pilot plant and plant level involving the following

systems: chalcopyrite ($CuFeS_2$) reduction, pyrolusite (β-MnO_2) reduction, coal oxidation and chalcopyrite oxidation."

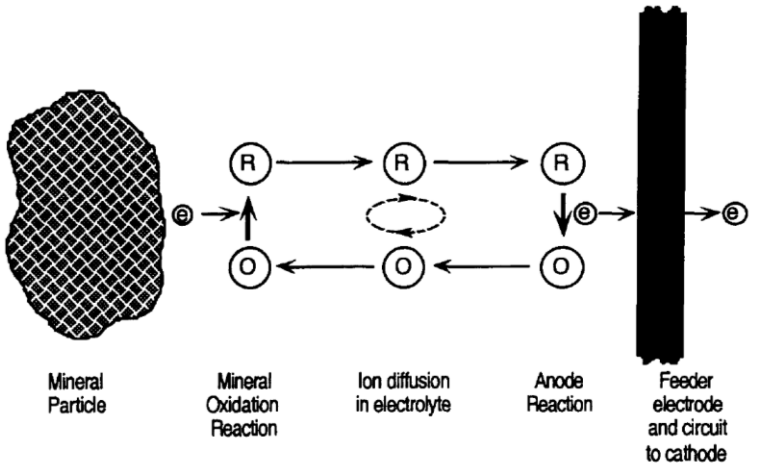

Figure 2.9 Anode reaction modes for oxidative slurry electrolysis (La Brooy et al [17])

Activox Process

La Brooy et al [17] noted that prior to applying the Activox process, ultra-fine grinding (discussed in section 2.6.1 above) is used to pretreat the material. This activates the ore prior to leaching. The "activated" material is leached at oxygen overpressures < 900 kPa and, temperatures under 100°C with a retention time in the range of 30 – 60 mins [17].

The advantage of this process is that because the process operates below the melting point of sulfur (120°C), the sulfur which is formed does not coat gold. Higher laboratory gold recoveries (98-99 %) from ultra-fine pretreated pyrite/arsenopyrite concentrates have been reported [17].

Bacterial Oxidation

In biooxidation of sulfide ores and concentrates, a number of bacteria such as *Thiobacillus ferrooxidans, Thiobacillus thiooxidans and Leptospirillum ferrooxidans* are mainly used to

improve the rate of oxidation [2, 3, 17, 27, 28]. During bacteria interaction with the minerals, the sulfide sulfur in the ore is ultimately converted to sulfate and sulfuric acid and ferrous iron in the ore is converted to the ferric state [2, 3, 28]. According to Marsden and House [2] the general oxidation reactions for iron sulfide mineral (FeS_x) in acidic media are given as follows:

$$FeS_x + xO_2 + 2xH_2O \rightleftharpoons FeSO_4 + 4xH^+ + (x-1)SO_4^{2-} + (2x+2)e \quad (2.10)$$

$$4FeSO_4 + O_2 + 2H_2SO_4 \rightleftharpoons 2Fe_2(SO_4)_3 + 2H_2O \quad (2.11)$$

$$FeS_x + Fe_2(SO_4)_3 \rightleftharpoons 3FeSO_4 + xS \quad (2.12)$$

$$2S + 3O_2 + 2H_2O \rightleftharpoons 2H_2SO_4 \quad (2.13)$$

The reaction chemistry for arsenopyrite and chalcopyrite is as follows [2]:

$$4FeAsS + 13O_2 + 6H_2O \rightleftharpoons 4H_3AsO_4 + 4FeSO_4 \quad (2.14)$$
bacteria-catalyzed

$$2FeAsS + 7O_2 + H_2SO_4 + 2H_2O \rightleftharpoons Fe_2(SO_4)_3 + 2H_3AsO_4 \quad (2.15)$$
bacteria-catalyzed

$$2FeAsS + Fe_2(SO_4)_3 + 4H_2O + 6O_2 \rightleftharpoons 4FeSO_4 + H_2SO_4 + 2H_3AsO_4 \quad (2.16)$$
chemical

The reaction chemistry for charcopyrite and chalcopyrite is as follows [2]:

$$CuFeS_2 + O_2 + 2H_2SO_4 \rightleftharpoons CuSO_4 + FeSO_4 + 2S + 2H_2O \quad (2.17)$$
bacteria-catalyzed

$$4CuFeS_2 + 17O_2 + 2H_2SO_4 \rightleftharpoons 4CuSO_4 + 2Fe_2(SO_4)_3 + 2H_2O \quad (2.18)$$
bacteria-catalyzed

$$CuFeS_2 + 2Fe_2(SO_4)_3 \rightleftharpoons CuSO_4 + 5FeSO_4 + 2S \quad (2.19)$$
chemical

Marsden and House [2] noted that "A number of mechanisms have been proposed for bacterial oxidation of sulfides, but the exact mechanism is the subject of debate and controversy."

A generalized; simplified mechanism for bacteria-catalyzed sulfide oxidation is shown on Figure 2.10 below [2].

In a pulp suspension containing sulfide and gangue minerals, *Thiobacillii* bacteria attach to the surfaces of the sulfides [2, 7]. According to Marsden and House [2] "It has been proposed that the attached bacteria serve to oxidize elemental sulfur that is formed at the surface of the sulfide mineral as a result of chemical oxidation reactions involving Fe^{3+} and the sulfide mineral itself, rather than playing a 'direct' role in the mineral oxidation." It can therefore be inferred that the bacteria play an 'indirect' role in sulfide mineral oxidation by converting sulfur to sulfate [2].

Again, the bacteria also oxidize Fe^{2+} to Fe^{3+}, in the bulk solution phase, and therefore derive energy from this reaction to create valuable oxidant to complement the direct action of bacteria on the sulfide minerals [2, 7].

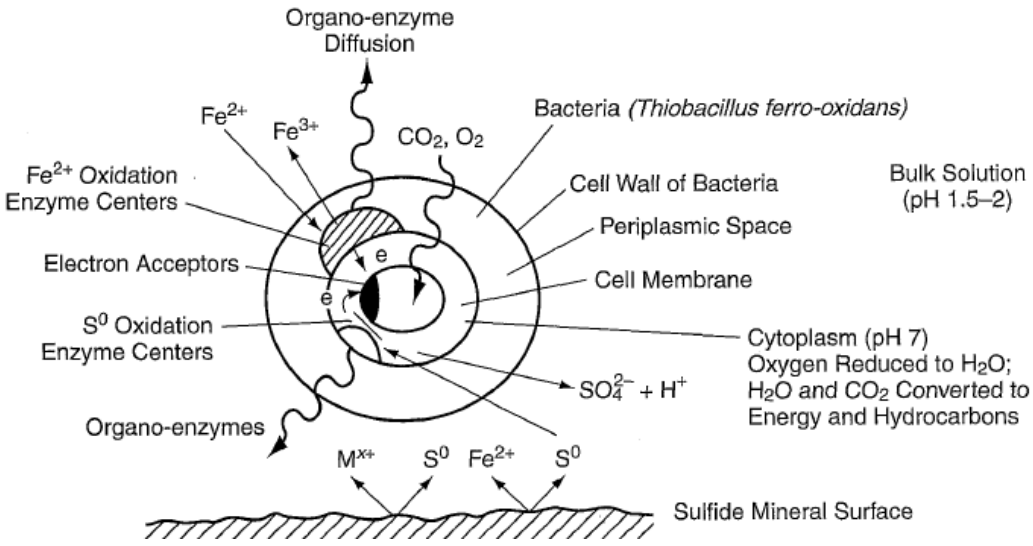

Figure 2.10 Simplified mechanism for bacteria-catalyzed sulfide oxidation (Marsden and House [2])

Cui et al [28] noted that "The efficiency of the bacterial attack is strongly dependent upon the mineralogical characteristics of the ores and concentrates."

Biological oxidation has several large scale applications [2, 6, 17]. According to La Brooy et al [17], Gencor's proprietary BIOX® has been used to process arsenopyrite concentrates at the Harbor Lights gold mine at Leonora in Western Australia since June 1992. The authors added that pyritic/arsenopyritic concentrates are being treated using the same technology at Wiluna in Australia. One of the best known biological oxidation operations is at Fairview in the Eastern Transvaal [7]. According to Fraser et al [7] the plant at Fairview treats arsenopyrite concentrate at a design rate of 10 tpd.

For sulfide ores in which gold is concentrated at grain boundaries, a major advantage of biooxidation is that only partial oxidation of the sulfide is required [2, 28]. The bacteria attacks preferentially at such sites liberating gold very efficiently [17]. Fraser et al [7] noted that "The high redox potentials obtained in biological oxidation due to the high ferric to ferrous ion ratios also improve precipitated arsenate stability as the arsenic is present in the "pentavalent" rather than the "trivalent" oxidation state." Unfortunately, according to Amankwah et al [3] "carbonaceous materials present in the ore are not oxidized by bacterial oxidation and continue to serve as preg-robbers in the subsequent gold leaching process."

La Brooy et al [17] have underscored the following as potential challenges that bacterial oxidation pose:

- Slow rate of reaction, e.g. days are required for effective treatment of sulfide concentrates.
- Careful temperature control required.
- Corrosion due to low pH pulps.
- The possibility of carbon deactivation in the CIP section of the plant due to fouling by dissolved organic residues from the bacterial reaction.
- Possible foaming problems.

Pressure Oxidation Pretreatment

In pressure oxidation, the sulfides are completely oxidized to sulfates by pressure leaching with oxygen at high temperature [20]. According to Fraser et al [7] "Pressure oxidation of gold ores and flotation concentrates is a commercially proven, effective pretreatment process for liberating refractory gold." Figure 2.11 illustrates process options for high pressure oxidation [17]. According to La Brooy et al [17] "Whilst the normal route for gold recovery following pressure oxidation is still cyanidation-CIL/CIP, much research has been carried out on acid leach systems to avoid the need for pre-leach neutralization."

Fraser et al [7] "Pressure oxidation flowsheets typically begin with a solid-liquid separation step, the purpose of which is to extract water from the ore following grinding. From an energy standpoint the removal of water is necessary since this water must ultimately be raised to the reaction temperature. Ground and classified ore is either thickened directly or following a flotation regrind step." Following ore preparation, the next two major steps are oxidation and neutralization [2].

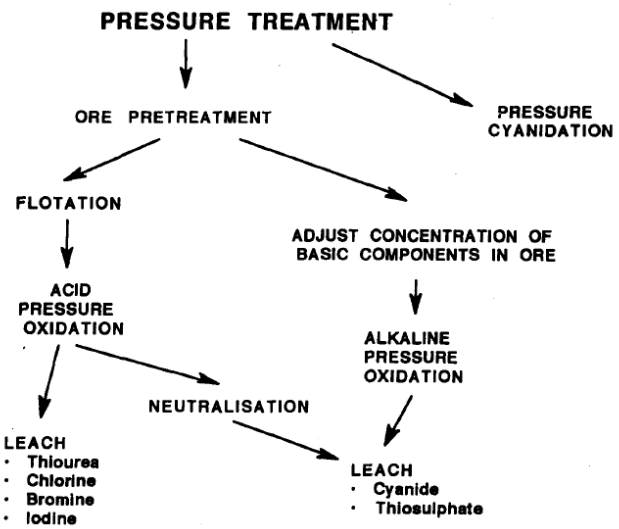

Figure 2.11 Process options for pressure pretreatment-leaching of refractory materials (La Brooy et al [17])

Komnitsas and Pooley [27] noted that pressure oxidation is done in autoclaves with the addition of H_2SO_4 and O_2 and a temperature range of 180-210°C (pressure 1800-2200 kPa) with residence times in the region of 1 to 3 hours [27].

The main reactions that take place in high temperatures are:

$$2FeS_2 + 7O_2 + 2H_2O = 2FeSO_4 + 2H_2SO_4 \quad (2.20)$$

$$4FeAsS + 11O_2 + 2H_2O = 4HAsO_2 + 4FeSO_4 \quad (2.21)$$

$$4FeSO_4 + 2H_2SO_4 + O2 = 2Fe_2(SO_4)_3 + 2H_2O \quad (2.22)$$

$$4HAsO_2 + FeSO_4)_3 + O_2 + 2H_2O = 2FeAsO4 + 3H_2SO_4 \quad (2.23)$$

Pressure oxidation has been successfully applied on large scale operations as can be seen from Tables 2.3 and 2.4 below. Newmont's Twin Creek operations in Nevada, USA, pressure oxidation is employed to pretreat the magnetic concentrates in the leaching tails of double refractory ores. pressure oxidation to treat tailings leached According to Marsden and House [2] "The ore is ground to 80% <22 μm to ensure effective oxidation and/or passivation of the preg-robbing organic constituents in the ore.

Pressure oxidation at 225°C is applied successfully to treat highly preg-robbing material containing 0.4% to 1.5% organic carbon and 2% to 6% sulfide sulfur. At the finer grind size, pressure oxidation achieves 97% to 98% sulfide sulfur oxidation and 30% carbon oxidation, compared with about 95% and 14%, respectively, at 80% <74 μm. Subsequent gold recovery by cyanidation has increased from 65% at 80% <74 μm to 85% to 90% at the 80% <22 μm size."

The main parameters that affect leaching are acidity and temperature [2, 17, 27]. According to Komnitsas and Pooley [27] "High acidity promotes sulfide oxidation, whereas high temperature can lead to the formation of elemental sulfur, which may adversely affect gold recovery and the

formation of jarosite and other basic salts which trap silver and minimize its recovery during the cyanidation step."

Iglesias and Carranza [20] noted that pressure oxidation pretreatment has been successfully used for the pretreatment of refractory gold ores with typical residence times in the range of 45-200 min. "In many instances, however, their use is precluded by capital and operating cost relative to the value of the ore." Iglesias and Carranza [20] added. According to La Brooy et al [17] "The technology is mature but it is still regarded a high technology-high capital cost option. The process is best suited to ores that require complete sulfide destruction."

Table 2.3 Operating conditions for selected commercial (past and present) pressure oxidation plants (Modified after Marsden and House [2])

Plant	McLaughlin	Sao Bento	Mercur	Getchell	Goldstrike	Porgera
Country	U.S.	Brazil	U.S.	U.S.	U.S.	PNG*
Start-up date	1985	1986	1988	1989	1990	1991
Media type	Acid	Acid	Alkali	Acid	Acid	Acid
Feed type	Ore	Concentrate	Ore	Ore	Ore	Concentrate
Feed rate (tpd)	2,450	240	720	2,500	~18,000	2,150
Particle size	80% −75 µm	90% −44 µm	75%–80% −75 µm	80% −75 µm	80% −75 µm	80% −38 µm
Sulfide sulfur (%)	3.0	18.0	0.95	2.0–4.0	1.7	14.0
CO_3 (%)	—	8.0	16.0	1.5–7.5	3.5	1.0–3.0
Organic carbon (%)	—	—	0.3	0.4	0.75	—
Total pressure (kPa)	1,700–2,200	1,600	3,200	3,200	2,500–3,000	1,725
Oxygen pressure (kPa)	140–280	—	380	700	340	325–350†
Temperature (°C)	180	190	220	210	225	190–200
Retention time (min)	90	120	112	90	75	110
Sulfide oxidation (%)	>85	—	>70	—	86.0–97.0	99.0–99.5
Reference(s)	[28]	[27]	[22]	[28, 32]	[26]	[35]

NOTE: Dashes = not available.

* PNG: Papua New Guinea.

† Inferred data.

Table 2.4 Operating conditions for selected commercial (past and present) pressure oxidation plants (Modified after Marsden and House [2])

Plant	Campbell Red Lake	Lone Tree	Twin Creeks	Lihir
Country	Canada	U.S.	U.S.	PNG*
Start-up date	1991	1994	1997	1997
Media type	Acid	Acid	Acid	Acid
Feed type	Concentrate	Ore + concentrate	Ore	Ore
Feed rate (tpd)	70	2,270	3,600	~10,000
Particle size	80% −75 μm†	80% −75 μm	80% −20 μm	80% −105 μm
Sulfide sulfur (%)	13.0–15.0	2.0–4.0	3.0–8.0	7.2
CO_3 (%)	~7.5†	—	0.5–12.0	—
Organic carbon (%)	—	—	0.1–1.0	—
Total pressure (kPa)	2,100	1,860	3,170	2,400–2,700
Oxygen pressure (kPa)	300–400†	520	690	300–500†
Temperature (°C)	190–195	195	225	210
Retention time (min)	120	48	50	65
Sulfide oxidation (%)	—	75.0	97.0	98.0
Reference(s)	[104, 105]	[106]	[34]	[36]

2.6.3 Thermal Pretreatment

According to La Brooy et al [17] “Thermal treatment can be applied to break down the sulfide phase to make gold accessible.” Roasting and pyrolysis are two main thermal means for pretreating refractory gold ores [2, 17].

Roasting, which is done in the presence of oxygen, converts the sulfide to an oxide whereas in pyrolysis, which is conducted in the absence of oxygen, transforms sulfide into a variety of reaction products [17]. Figure 2.12 illustrates the process options for thermal pretreatment of refractory ores or concentrates [17].

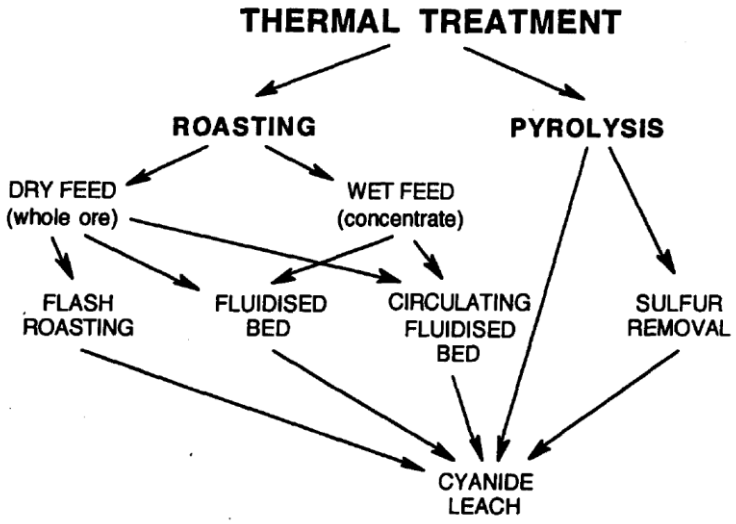

Figure 2.12 Process options for thermal pretreatment of refractory ores (La Brooy et al [17])

Pyrolysis

Cleyle and Caley [29] studied the pyrolysis of the high sulfur content of Eastern Canadian coals. As can be seen from Figure 2.13 below, pyrite decomposed entirely to pyrrhotite at 600°C [17]. Though Cleyle and Caley [29] observed complete pyrite to pyrrhotite transformation, it was not until after 15.5 hours of pyrolysis.

La Brooy et al [17] enlisted the following equations for the pyrolysis transformation of pyrite and arsenopyrite minerals:

$$FeS_2 \text{ (solid)} + \text{heat} \rightarrow FeS \text{ (solid)} + S \text{ (gas)} \quad (2.24)$$

$$FeAsS \text{ (solid)} + \text{heat} \rightarrow FeS \text{ (solid)} + As \text{ (gas)} \quad (2.25)$$

In these reactions, gold is liberated and triolite (FeS), non-stoichiometric pyrrhotite ($FeS_{[1+X]}$), or both is formed [17]. During the pyrolysis of pyrite and arsenopyrite, the metal sulfides that are produced react with cyanide, that is meant for leaching, and to form ferricyanide-ferrocyanide

species [17]. According to La Brooy et al [17] “The consumption of cyanide increases the processing cost unless the metal sulphide can be stabilized.

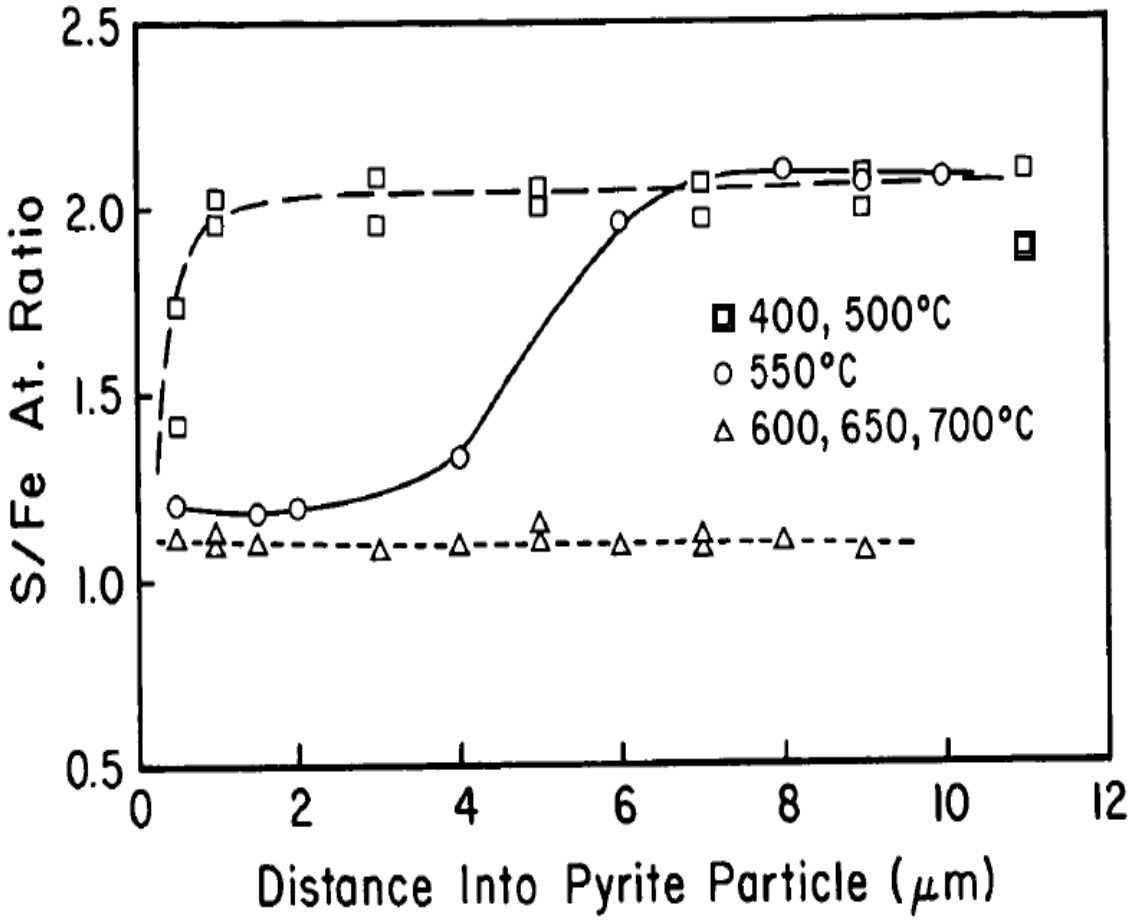

Figure 2.13 Decomposition of FeS_2 to FeS as coal is heated above 500°C [29]

Roasting

Maycock et al [30] quoted the definition of roasting from The USBM dictionary of mining, mineral and related terms as "heating a material to a point somewhat short of fusing with access of air to expel volatile matter or effect oxidation. According to Paktunc et al [8], roasting is the most commonly employed technique to recover Au from double refractory ores. Aylmore and de

Klerk [5] submitted that "During the roasting process the physical, chemical and mineralogical properties of the ore constituents are altered to an extent determined by the roasting conditions (eg temperature, pressure, feed composition, etc)."

Roasting is done to oxidize the sulfide matrix (host sulfide minerals) to liberate the structural and submicroscopic gold [1, 2, 7, 8, 19, 31]. Komnitsas and Pooley [27] noted that "The objective of the method is the transformation of the iron sulfides to high porosity iron oxides in order that cyanide ions can penetrate the calcine and increase extraction of the contained gold." The contained sulfur serves as fuel source for the reaction [19]. According to Charitos et al [19], "The roasting process transforms the main side element sulfur into SO_2, which is then converted into the saleable product sulfuric acid. Hence, S is utilised to a high-value product instead of a potential waste product such as gypsum." Roasting effectively oxidizes any organic carbon that may be present in the ore [2, 6, 32, 33]. The ore is roasted with the aim of achieving 96–98% oxidation of sulfide-based sulfur [8]. This makes roasting an effective pretreatment process method for double refractory gold ores.

Since roasting is a high-temperature process it has the advantage of removing additional minor elements from the concentrate, making them available for further treatment [19].

The efficiency of roasting is strongly dependent on the roasting kinetics, which are largely a function of temperature, partial pressure of oxidising gas and particle size. The rate of volatilisation and oxidation of sulfur and arsenic minerals increases with increasing temperature and increasing partial pressure of oxygen in the gas phase [5].

The form and deportment of gold in the ore matrix, as well as the conditions of roasting, impact the behavior of gold during roasting [5]. Charitos et al [19] contrasted how roasting compares with other refractory pretreatment methods as shown on Table 2.5 below.

Table 2.5 Attributes of different refractory ore-handling technologies [19].

	Roasting	Pressure oxidation	Bio-oxidation	Ultra-fine grinding
Energy recovery	Excess heat of reaction is used to produce high-pressure steam for energy recovery	Energy consumption is determined by oxygen generation	Low in energy consumption, no heat recovery	No heat recovery, energy consumption defined by mill
Sulfur	S fully oxidised as SO_2 in gas or partial sulfidation	S partially oxidised as H_2SO_4 in slurry	Partially oxidised as sulfate in slurry	Minimal oxidisation
Carbon type Lignite Anthracite	Oxidation >700°C to CO_2	No reaction Limited success with chlorination or fuel blanket	No reaction	No impact
Arsenic	Oxidation and separation to arsenic trioxide	Oxidation in slurry	Oxidation in slurry	No impact
Mercury	Almost complete evaporation Gas cleaning for Hg with the Boliden Norzink Process Almost Hg-free calcine	Majority remains in solids Some contamination of liquid	Remains in solids Partly dissolved in liquid	No impact
Residence time	0.5 h	1 h	4 - 5 days	Not applicable
Cyanide consumption	1 - 2 kg/t	1 - 2 kg/t	10 - 20 kg/t	No comparison available

2.7 Roasting Kinetics and Efficiency

The response of the calcine product to cyanide leaching is a measure of the efficiency of roasting [2, 5, 8, 17]. Several authors have presented that roasting efficiency strongly depends on the roasting kinetics, which is primarily a function of temperature, partial pressure of oxidizing gas, and particle size [1-6, 8, 15].

According to Marsden and House [2] "During the oxidation of gold-bearing sulfide minerals, the gold, which may be present either as fine particles or in solid solution, migrates toward pores or grain boundaries in the direction of diffusion of sulfur or arsenic. As migration occurs, the gold coalesces in the liquid phase. Further coalescence is thought to occur at the mineral surface, as arsenic and sulfur volatilize, and gold particles up to 1 μm diameter can be formed." Figure 2.14 below illustrates this phenomenon.

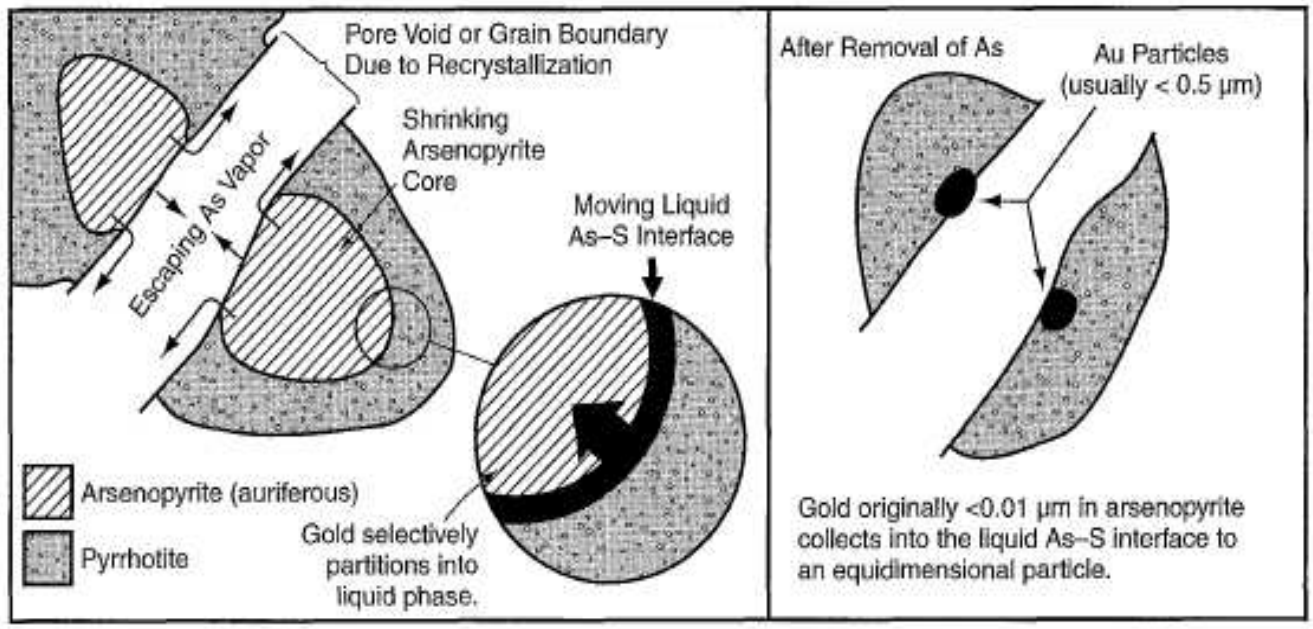

Figure 2.14 Mechanism for aggregation of gold particles during the roasting of auriferous Arsenopyrite [2]

2.7.1 Temperature and Gas Phase Composition

According to Marsden and House [2] "The rate of volatilization and oxidation of sulfur and arsenic minerals increases with increasing temperature and increasing partial pressure of oxygen in the gas phase." This has been proven by several othe authors [1, 6, 17, 19, 21]. The rate of reaction for roasting of pyrite and arsenopyrite are very slow at low temperatures (<400°C – 450°C). As can be seen from Figures 2.15 and 2.16, Acceptable reaction rates, for roasting of pyrite and arsenopyrite, can therefore be achieved by increasing roasting temperatures above 450°C [2, 5, 17].

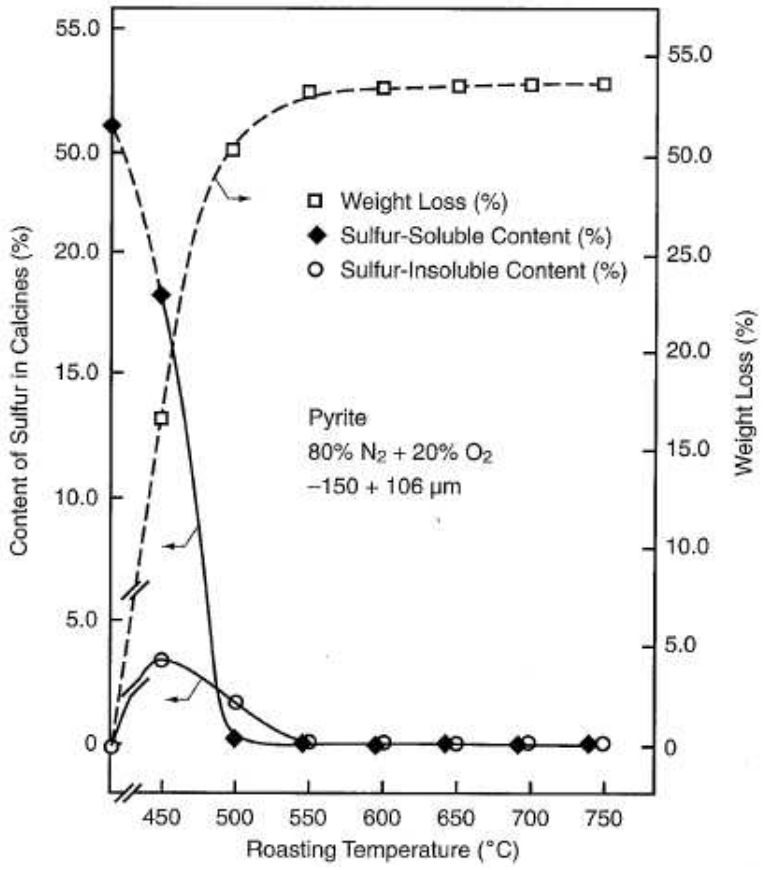

Figure 2.15 Content of sulfur (soluble and insoluble) in the calcines and weight losses in the roasting of pyrite at different temperatures [2]

However, at very high temperatures (above 700°C), “the porous iron oxide structure that is developed during oxidation may collapse, encapsulating gold within the particle and reducing subsequent gold recovery, possibly by as much as 50%.” According to Marsden and House [2]. This process is often referred to as "sintering" [2].

Marsden and House [2] noted that “Sintering may occur as a result of high overall temperature conditions in the roaster bed, the development of hot spots in the bed due to locally high sulfur content, or poor temperature control within different regions of the bed. Similar effects may be produced by roasting for too long at high, or even marginally high, temperatures, commonly referred to as "overroasting."

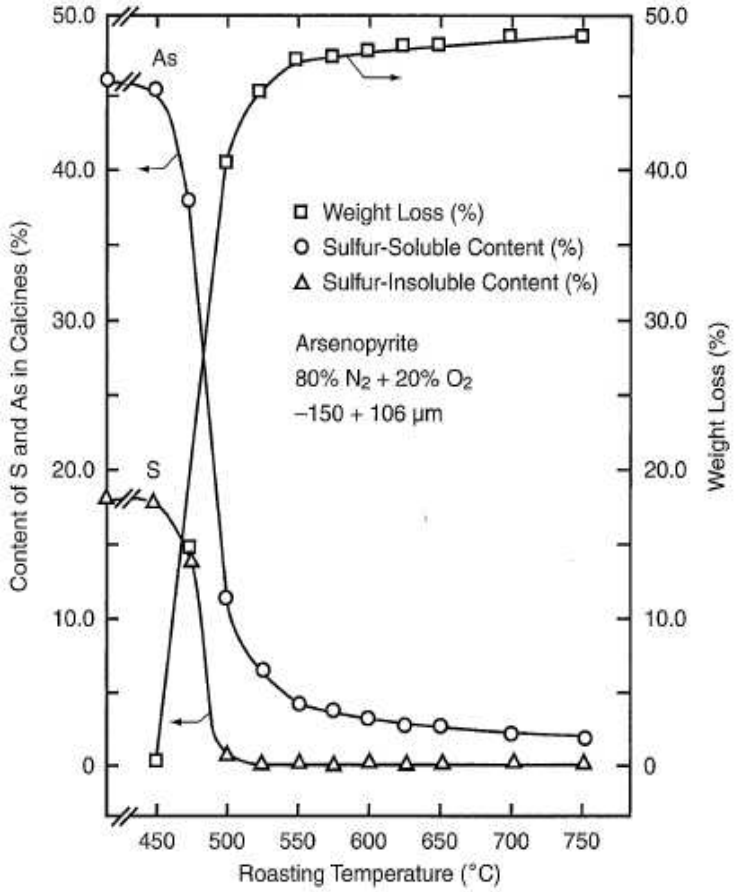

Figure 2.16 Content of sulfur (soluble and insoluble) in the calcines and weight losses in the roasting of arsenopyrite at different temperatures [2]

The effect of temperature of roasting on subsequent gold recovery [2] is shown in Figure 2.17. According to Marsden and House [2] “At high temperatures and under strongly oxidizing conditions, sulfur and arsenic may have insufficient time to diffuse to the mineral surface before extensive oxidation and recrystallization of the mineral structure occurs, prohibiting further pore development.”

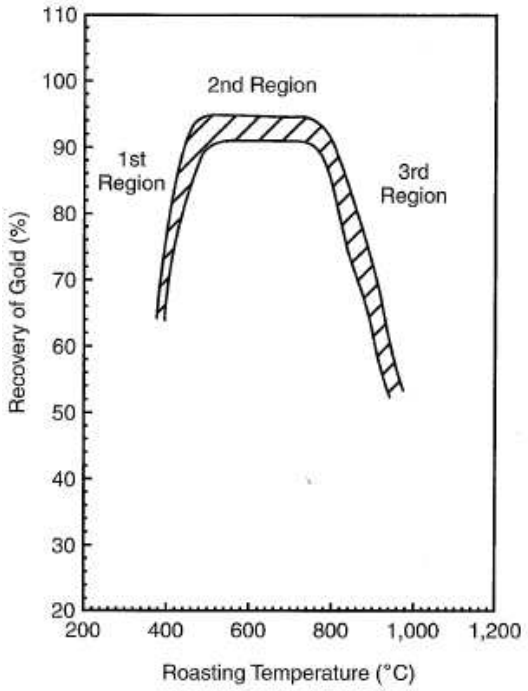

Figure 2.17 Recovery of gold as a function of roasting temperature for several gold ores and concentrates [2]

2.7.2 Particle Size Distribution

The kinetics of sulfide roasting is better with decreasing particle size [2]. According to Marsden and House [2] “For a given roaster system, particles coarser than the optimal particle size may be incompletely oxidized, whereas finer particles may be overroasted and possibly sintered. Sintering is a potentially serious problem because it can cause gold to become occluded and

inaccessible to leach solutions." The effect of temperature on product surface area, an indicator of porosity, is illustrated in Figure 2.18.

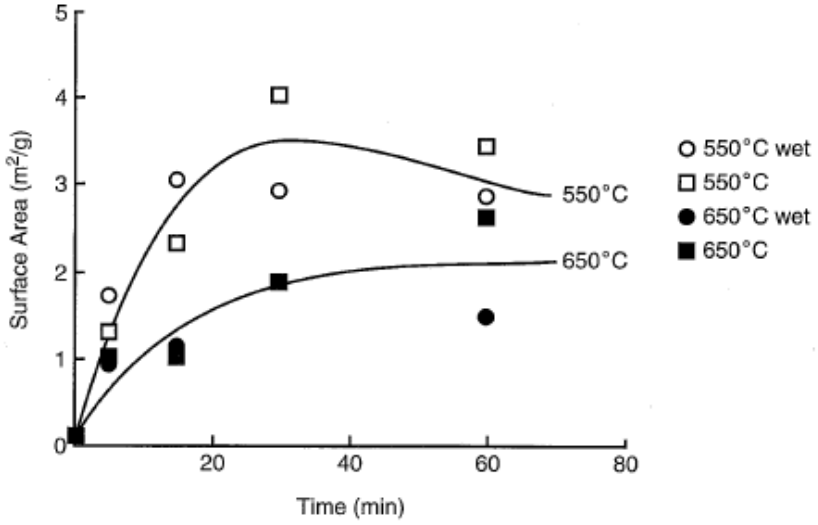

Figure 2.18 Effect of temperature on calcine surface area [2]

The roaster feed particle size distribution should be kept as narrow as possible, and the amount of fines and oversized material must be minimized [2]. According to Marsden and House [2] "Agglomeration or pelletization processes may be used to pretreat the roaster feed to produce a narrower and more even size distribution.

Particle sizes that are employed in practice depend on the material to be roasted and the roasting method. Sulfide ores can be successfully roasted at sizes as coarse as 12 mm, although this is rarely done. Typically ores and concentrates are ground to a size that gives optimum gold extraction in the recovery process that follows roasting, for example, 80% passing 75 to 150 µm. Gravity concentrates may be roasted at relatively coarse sizes (i.e., between 1 mm and 0.25 mm), with regrinding of the roasted calcine if necessary. Alternatively, they may be ground to a finer size at the outset for faster roasting kinetics."

2.7.3 Retention Time

The residence time of each particle in the roaster influences the efficiency of oxidation of that particle [2, 7]. According to Marsden and House [2] “If the retention time is too short, either due to overfeeding of the roaster or due to bypassing within the roaster, then incomplete oxidation can occur. This may result in high cyanide consumptions downstream, and the calcine produced may still be refractory in nature, causing high gold losses. Long retention times can cause overroasting or sintering of calcined material, especially of fine particles.”

2.7.4 Oxidation Efficiency

Marsden and House [2] noted that “Between 80% and 100% of the sulfide components and 60% to 70% of the carbonaceous components of materials treated by roasting are typically oxidized.” However, the preferred optimum roaster calcine is one containing 75% to 85% hematite and 15% to 25% magnetite [2, 8, 10]. “This indicates that complete, or close to complete, sulfide oxidation has been achieved, but that secondary oxidation of magnetite to hematite is incomplete.” concluded Marsden and House [2].

The incomplete oxidation of maghemite to hematite helps to minimize overroasting of hematite particles that remain in the roaster after oxidation has been completed [2]. According to Marsden and House [2] “The color of the calcine provides a useful indication of the degree of oxidation achieved in the roaster: a bright red color indicates a product that is essentially hematite (i.e., very little magnetite), caused by overroasting. This may be due to high temperatures, high oxygen content, or excessively long retention time in the roaster. On the other hand, a very dark brown or black coloration is characteristic of a magnetite rich product, resulting from too-low temperatures in the roaster, insufficient oxygen, or short particle-retention time.

2.8 Roaster Reaction Chemistry and Products

According to Aylmore and de Klerk [5] "The efficiency of roasting is strongly dependent on the roasting kinetics, which are largely a function of temperature, partial pressure of oxidising gas and particle size. The rate of volatilisation and oxidation of sulfur and arsenic minerals increases with increasing temperature and increasing partial pressure of oxygen in the gas phase."

The phase-stability diagram for the As-Fe-S-O system at 600°C is shown in Figure 2.19 below. The figure shows that, under oxidizing conditions (i.e., low sulfur dioxide content in the gas phase), pyrite, marcasite, and pyrrhotite are directly oxidized to magnetite and then further to hematite. The reactions are as follows:

$$3FeS_2 + 8O_2 \rightarrow Fe_3O_4 + 6SO_2 \quad (2.26)$$

$$3FeS + 5O_2 \rightarrow Fe_3O_4 + 3SO_2 \quad (2.27)$$

$$4Fe_3O_4 + O_2 \rightarrow 6Fe_2O_3 \quad (2.28)$$

With excess air, at low temperatures (450 - 500°C) pyrite and arsenic-bearing sulfides are converted directly to hematite [1-3, 8, 9]. Aylmore and de Klerk [5] found that there was a 37 per cent volume reduction in going from pyrite to hematite. However, they noted that the surface oxide layer is still not permeable to gas and thus a series of concentric shells tends to form [5].

According to Aylmore and de Klerk [5] "When pyrite is roasted in excess air at temperatures above 500°C an oxide rim forms initially, but once a localised sulfur dioxide atmosphere develops (>5 per cent SO_2), pyrite converts to pyrrhotite (21 per cent volume reduction) with the loss of half of its sulfur and adsorbs heat. The pyrrhotite has a porous sponge-like structure if pyrite decomposition is slow (lower temperatures), or has a radial structure if formed more rapidly at higher temperatures."

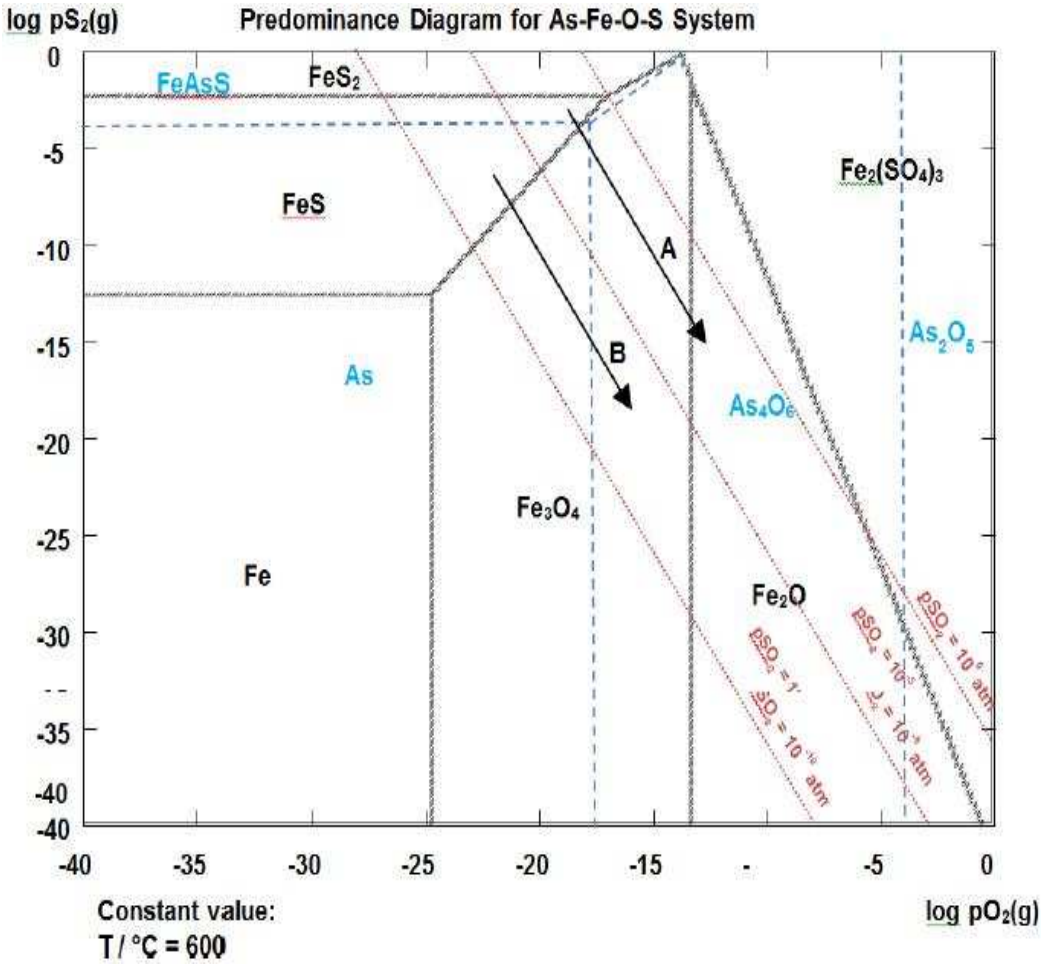

Figure 2.19 Phase stability diagram for As-Fe-S-O system at 600°C. Routes A and B show the sequence of mineralogical changes at different partial pressures of SO_2 gas for fine and coarse particles respectively [5]

The mechanism of oxidation of arsenopyrite (FeAsS) and pyrite (FeS_2) grains deduced from the results of small-scale tests, XRD, SEM, optical microscopy, and chemical analysis of roaster feed and products is summarized in Figure 2.20 [2] below.

Arsenopyrite and arsenian pyrites decompose with volatilisation of arsenic which absorbs heat and leaves pyrrhotite [2, 5, 8]. “The arsenic vapour then diffuses to the outer perimeter, where it reacts with oxygen to form $As_4O_6(g)$ and releases heat.” According to Aylmore and de Klerk [5]. The consumption of arsenic at the perimeter drives the diffusion process and the endothermic

decomposition is maintained by the transfer of combustion heat back into the particle towards the cooler centre. The arsenic is then oxidised at the particle surface. The pyrite and arsenopyrite decomposition reactions follow the simplified endothermic reactions:

$$FeS_2 \rightarrow FeS + S \tag{2.29}$$

$$4FeAsS \rightarrow 4FeS + As_4 \tag{2.30}$$

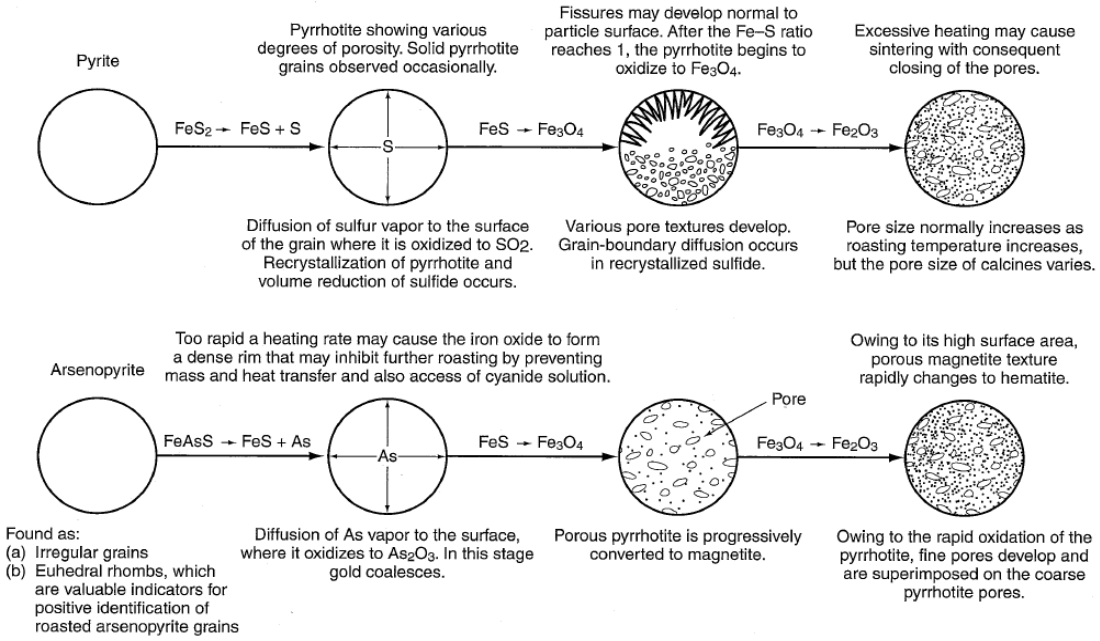

Figure 2.20 The mechanism of oxidation of arsenopyrite (FeAsS) and pyrite (FeS_2) grains [2]

According to Aylmore and de Klerk [5], Arsenic and sulfur are liberated by exothermic reactions from the decomposition oxides on the outer perimeter of the grains. The reactions [5] are as below:

$$As_4 + 3O_2 \rightarrow As_4O_6(g) \tag{2.31}$$

$$S + O_2 \rightarrow SO_2(g) \tag{2.32}$$

Upon the completion of pyrrhotite conversion, further oxidation to magnetite and hematite occurs under oxidising conditions [2, 5, 8]. According to Aylmore and de Klerk [5], "The iron oxide formed at temperatures below 650°C is very fine, but it recrystallises if heated above 750°C and may encapsulate gold. Hence roasting at too high a temperature or the presence of hot spots in the roaster can be even more detrimental to gold recovery than incomplete reaction." Figure 2.21 shows an example of the mineralogical transformations involved in the two-stage roasting of pyrite clearly demonstrating the intermediate formation of pyrrhotite [2].

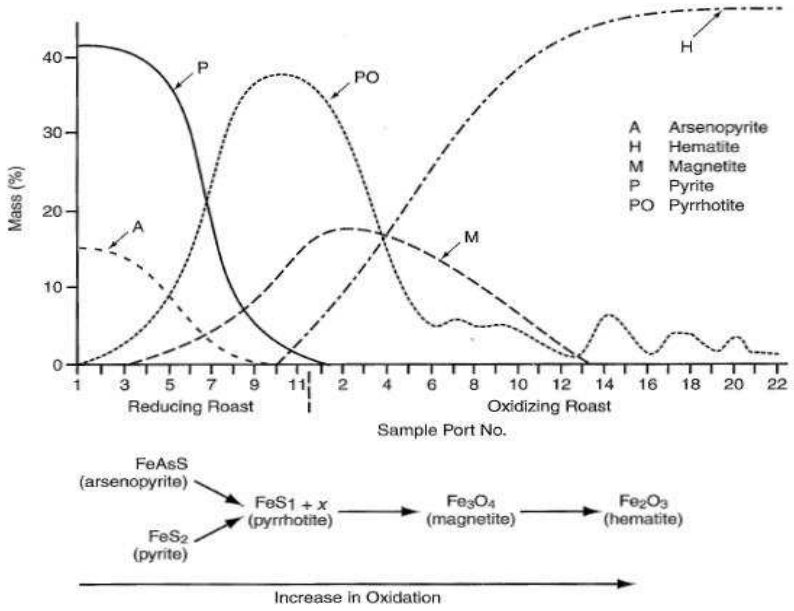

Figure 2.21 Mineralogical transformations observed in the Fairview roaster [2]

Though maaximum porosity is achieved at the pyrrhotite stage, pyrrhotite itself can be dissolved by cyanide solution and consumes available cyanide reagent [5]. "Consequently, complete conversion to an inert iron oxide calcine is required." According to Aylmore and de Klerk [5].

Ideally, the pyrrhotite is oxidised to magnetite and the magnetite further oxidised to hematite [5] following the reactions:

$$3FeS \rightarrow 5O_2(g) + Fe_3O_4 + 3SO_2(g) \quad (2.33)$$

$$4Fe_3O_4 + O_2(g) \rightarrow 6Fe_2O_3 \quad (2.34)$$

According to Aylmore and de Klerk [5], "Carbon as a carbonate or organic carbon oxidises within the roaster fluid beds to carbon monoxide and carbon dioxide. Sulfur dioxide can be fixed by reactions with minerals in the ore (carbonates and hematite)." The reactions [2, 4, 5] are as follows:

$$2CaCO3(s) + 2SO2(g) + O2(g) \rightarrow 2CaSO4(s) + 2CO2(g) \quad (2.35)$$

$$2Fe_2O_3(s) + 4SO_2(g) + O_2(g) \rightarrow 2Fe_2(SO_4)_2(s) \quad (2.36)$$

and with the lime added to the ore [4, 5]:

$$2CaO(s) + 2SO_2(g) + O_2(g) \rightarrow 2CaSO_4(s) \quad (2.37)$$

According to Marsden and House [2], "If carbonates are present in sufficient quantity (i.e. >2% $CaCO_3$), the evolved carbon dioxide can form an unreactive blanket over the roaster bed, preventing mineral oxidation."

Charitos et al [19] reported that Hedstrom et al (2012) prepared a comprehensive summary with regards to the fate of typical elements contained in gold ores during roasting. This is summarized on Table 2.6 below. According to Charitos et al [19] reported that Hedstrom et al (2012) concluded that:

- elements like copper and zinc are sometimes recovered as pure metals
- mercury is of particular importance since it will contaminate the sulfuric acid
- if selenium is present it will to a large extent react with mercury to form highly stable mercury selenide and report to the wet gas cleaning sludge
- when arsenic is present it will form the largest flow of volatile compounds since it will form gaseous arsenic trioxide As_4O_6 (g).

Table 2.6 Simplified summary of element distribution during roasting [19]

Element	Distributes mainly to	Recovered by/in	Recovered as	Special process needed to stabilise element
Fe	Calcine as Fe_2O_3	Remains in leach residue	-	No
Cu	Calcine as $CuSO_4$	Acid leach before cyanide leach	Copper precipitate or metallic copper	No
Zn	Calcine as $ZnSO_4$	Acid leach before cyanide leach	Zinc precipitate or metallic zinc	No
Pb	Calcine as $PbSO_4$	Remains in calcine residue	-	No
Ag	Calcine as Ag	Cyanide leach	with gold in bullion	No
As	Calcine as As_4O_6	Bag filter or by wet gas cleaning	Crude As_2O_3 or scorodite or calcium arsenite	Yes Bag filter or precipitation process
Sb	Gas as Sb_4O_6	Bag filter or by wet gas cleaning	Together with As	No Will follow arsenic
Se	Gas as SeO_2	Bag filter or by wet gas cleaning	In wet gas cleaning sludge	No
Hg	Gas as Hg	Wet gas cleaning and by B/N (see dedicated section in this paper)	Calomel an in wet gas cleaning sludge	Yes Boliden/Norzink mercury removal
Cl	Gas as HCl	Wet gas cleaning	In cleaned effluent water	No
F	Gas as HF	Special fluoride tower	As Fluorosilicic acid	Yes
S	Gas as SO_2	Acid plant	Sulfuric acid	Yes acid plant
C	Gas as CO_2	-	-	No

2.9 Desirable Qualities of Roaster Products

Aylmore and de Klerk [5] found out that "The structural properties of the final hematite product are dependent on the particular mechanism of transformation and on the structural changes associated with each of the intermediate steps." "These in turn are affected by the temperature, gaseous composition and pressure and the presence of reaction retardants (eg sulfates, arsenates)." They added. The most favourable roaster product for cyanidation is one in which [2, 5]:

- gold is fully liberated and agglomerated
- a porous inert hematite calcine (see Figure 2.22) is produced where cyanide solution is readily accessible to the gold
- compounds such as cyanicides and gold-coating materials (eg lead, antimony) are not present which consume reagents and reduce gold recovery at the subsequent cyanidation stage.

Douglas and Semenyna [10] noted that "The complete oxidation of pyrite to hematite is preferred as the texture of hematite is porous allowing for the penetration of cyanide. The porous texture of the hematite also allows for the escape of arsenic during roasting; and from dynamic secondary ion mass spectroscopy (D-SIMS) studies, the porosity promotes the formation of colloidal gold."

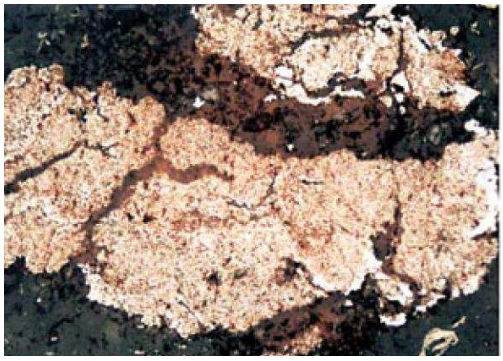

Figure 2.22 Reflected-light photomicrographs illustrating iron oxide particles deemed to be desirable calcine (Modified after [8])

According to Marsden and house [2] “The efficiency of conversion of magnetite to hematite is important because magnetite tends to retain arsenic, sulfur, and gold in the matrix. Recrystallization to hematite helps to remove these products and to expose contained gold.”

2.10 Gold Losses in Roaster Products

The roaster product known as calcine could have trace amount of gold still encapsulated such that there is reduced cyanide to gold contact during leaching thereby leading to reduced overall gold recovery. The gold losses are identified mainly as:

- surface-bound (preg-robbed) [5, 10]
- submicroscopic gold in solid solution residual in unoxidised sulfide and maghemite [10]
- as cluster (colloidal <0.2 µm) particles in hematite formed during the roasting process.

2.10.1 Maghemite

Ideally, the oxidation transformation from pyrite to pyrrhotite should be followed by conversion to magnetite and the magnetite further oxidised to hematite [5, 8]. However, in reality, an intermediate phase known as maghemite is usually formed during the transformation from magnetite to hematite [5, 8, 10-12]. Figure 2.23 below illustrates the various phases formed during the roasting of pyrite to hematite.

According to Douglas and Semenyna [10] “Maghemite, an intermediate oxidation phase between magnetite and hematite, is identified to be the main gold carrier, occurring as both liberated particles and as small (10 µm) inclusions in gangue minerals.”

Douglas and Semenyna [10] demonstrated that “Maghemite is massive and impervious to cyanidation. Gold in maghemite tends to remain in solid solution, and correlates to an elevated

arsenic concentration. Incomplete oxidation, demonstrated by the remnant ore texture of the pyrite inclusions in gangue, also contributes to the remaining solid solution gold in pyrite, as the pyrite has not fully oxidised within the gangue particle."

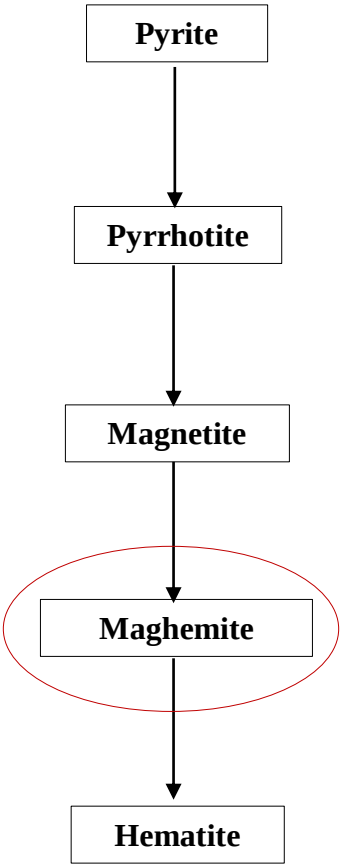

Figure 2.23 Mode of pyrite to hematite transformation by roasting (Modified after [2, 5, 10])

According to Paktunc et al [8] "Iron oxides particles resulting from high-temperature oxidation of pyrite during roasting consist of maghemite and hematite in alternating concentric bands. Hematite is highly porous, whereas maghemite is massive, with no evidence of permeability. Maghemite may contain significant amounts of As (*i.e.*, up to 18.6 wt%), whereas hematite contains minor or negligible As (*i.e.*, <2.9 wt%). Residual concentrations of gold in iron

oxides following cyanide leaching range from 30 ppb to 260 ppm. High concentrations of gold appear to be confined to impervious bands of maghemite within iron oxides.' Figure 2.24 below illustrates a photomicrograph based on reflected-light for a typical maghemite calcine.

Figure 2.24 Reflected-light photomicrographs illustrating iron oxide particles deemed to be undesirable calcine (Modified after [8])

Reaction between escaping arsenic gaseous phase an iron oxide interfaces to form a nonporous ferric arsenate or ferrous arsenite product [5]. From roasting studies on typical roaster product leach tailing at Barrick's Goldstrike, Douglas and Semenyna [10] concluded that "Under a highly oxidising environment, the arsenic can potentially be locked up as a nonporous ferric arsenate (FeAsO4) or ferrous pyroarsenite (Fe2AsO5) product." This is further illustrated on Figure 2.25 below [10].

Aylmore and de Klerk [5] noted that arsenic potentially forms arsenic pentoxide (As_2O_5) and reacts with hematite to yield arsenate according to the following reactions:

$$As_4O_6(s) + 2O_2(g) \rightarrow 2As_2O_5(s) \quad (2.38)$$

$$Fe_2O_3 + As_2O_5(s) \rightarrow 2FeAsO_4(s) \quad (2.39)$$

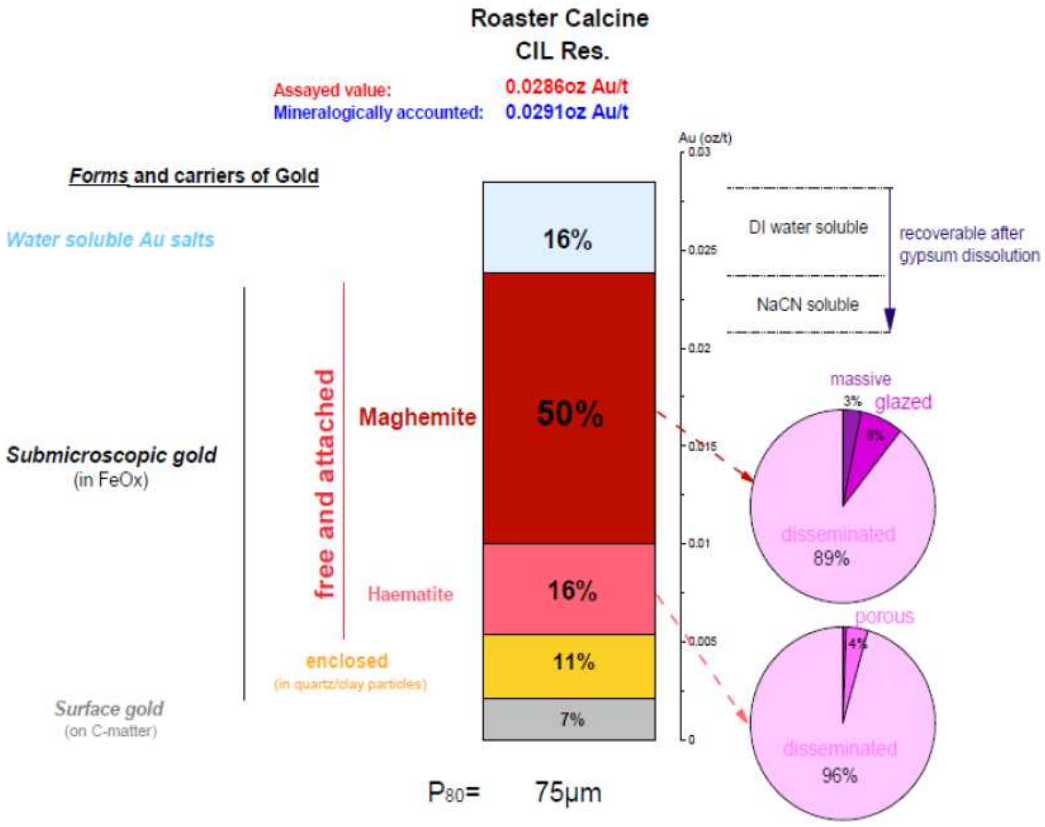

Figure 2.25 Gold deportment of a typical roaster product leach tailing from Barrick Goldstrike [10]

Aylmore and de Klerk [5] added that 'The formation of arsenic pentoxide by aerial oxidation of $As_4O_6(g)$ cannot be commercially produced without the system being pressurised." Hence the formation of arsenic pentoxide may proceed through the following reactions [5]:

$$1.5As_4(g) + 3SO_2 \rightarrow As_4O_6(g) + As_2S_3(g) \quad (2.40)$$

$$As_2S_3(g) + 5.5O_2 \rightarrow As_2O_5(s) + SO_2(g) \quad (2.41)$$

2.11 Roasting Equipment

According to several authors [2, 9, 12, 17] a number of different types of roasting equipment are available for oxidation of refractory gold ores. The ones used commercially are;

- Rotary kiln and multiple hearths (e.g. Edwards)
- Fluidized bed roaster (e.g. DORR-Oliver)
- Circulating fluidized bed roaster (CFB) (e.g. Inco and Lurgi)
- Oxygenated fluidized bed (e.g. Independence and Goldstrike)

According to Thomas and Cole [12] "The early roasters were installed with the minimum of gas cleaning. As time progressed, units such as Cottrell precipitators, to remove dust, baghouses, to remove arsenic trioxide, and the capturing of sulfur dioxide gas by neutralization with lime or the production of sulfuric acid were also integrated into roaster plants."

According to marsden and House [2] "The type of roaster used has an effect on the reaction chemistry and performance.' Table 2.7 shows a comparison of the four commercial roaster types.

Table 2.7 Roaster performance comparison [12]

Parameter	Edwards	Fluids	CFB	Oxygenated
Relative throughput per unit area	Very low	Moderate	High	High
Gas/solids mixing	Poor	Good	Very good	Good
Bed temperature control	Poor	Good	Very good	Good
Control of gas composition	Limited	Good	Very good	Very good
Solids retention time	Fixed	Fixed	Variable	Fixed
Feed type (wet or dry)	Dry	Both	Both	Both
Roast whole ore	No	Possible	Yes	Yes
Treat arsenic ore	Concentrate	Yes	Not yet	Not yet
Development	Pre-1910	1940s	1960s	1980s

A detailed description of the roaster equipment is provided in the ensuing section.

2.11.1 Multiple Hearth Furnace

Before the mid-nineties, rotary kilns and multiple-hearth roasters were used for the treatment of refractory ores [12, 17, 34]. According to Thomas and Cole [12] "The most common

in the gold industry was the single Edwards roaster as it provided better bed temperature control." A cross-section of a of a rabbled hearth roaster [12] is shown in Figure 2.26. The roaster consists of a bricked line floor in an enclosed hearth, and up to 40m long and 3.6m wide [12]. The rotating rabble arms advances concentrates down the hearth.

According to Thomas and Cole [12] "There are several examples of the successful application of the Edwards roaster to gold extraction: to name a few, Giant Yellowknife Mines Limited, Ashanti Goldfields Corporation (Ghana) Limited and the Government Roasting Plant in Zimbabwe."

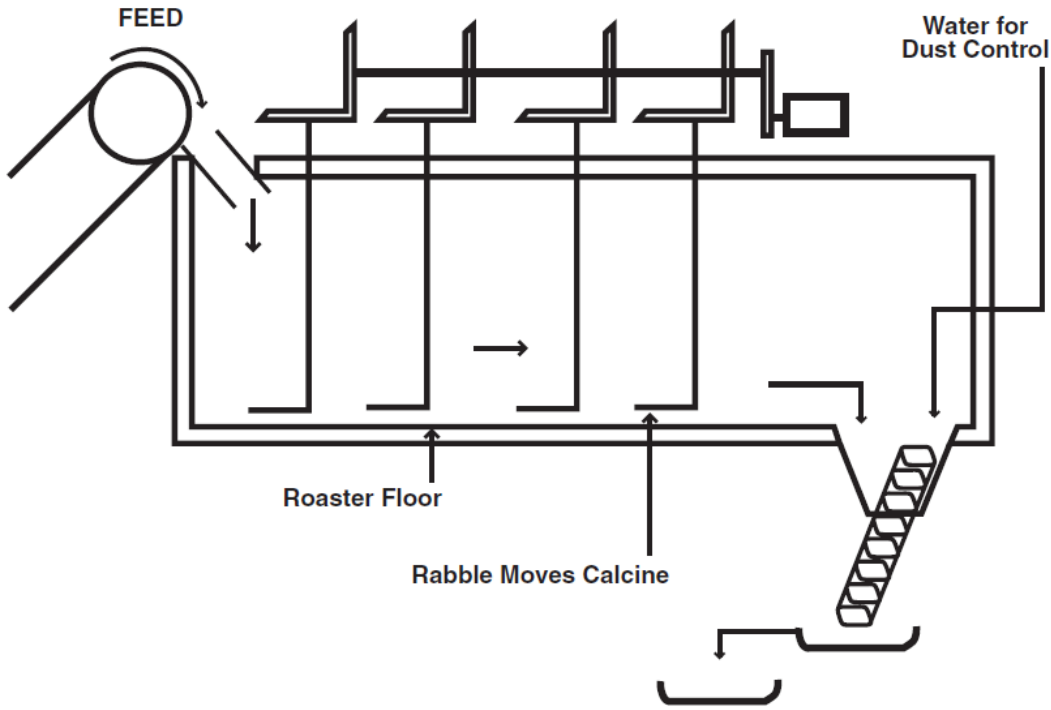

Figure 2.26 Diagrammatic view of a rabbled hearth roaster [12]

According to Carina [35] "Ores that can be roasted only with great difficulty, such as molybdenum disulfide, are still treated in multiple-hearth furnaces. Because roasting reactions are exothermic, the furnace usually has to be heated only at the start of the process. The material fed

to the topmost hearth is distributed by the teeth on the rabble arms, slowly transported to the center of the hearth, and dried. Then the ore falls into the first roasting zone, where it is heated in contact with hot roasting gas until it ignites. The reaction goes to completion as the charge is transported further over the hearths. On the last hearths, roasting air drawn or blown into the furnace from the bottom is preheated by cooling the residue. The progress of the reaction is monitored by measuring the temperature on the individual hearths."

2.11.2 Rotary Kiln

According to Carina [35] "A rotary kiln is an inclined, rotating cylindrical reactor through which a charge moves continuously. The rotary kiln is used when thermal processing of solids that is more severe than drying is required." The furnace walls (normally lined) make intermittent contact with the flue gas and the charge [2, 34, 35]. "Heat required for the various physical and chemical processes is delivered to the charge by lifting and overturning the charge as it moves through the interior of the rotary kiln." Carina [35] added.

According to Carina [35] "Rotary kilns were employed for the exothermic roasting of sulfidic ores and for the endothermic removal of water of hydration and carbon dioxide from fine-grained materials such as ores, phosphates, alumina, ilmenite, and titanium dioxide."

According to Heydenrych [34] Rotary kilns are found in many processes that involve solids processing. These include drying, incineration, mixing, heating, cooling, humidification, calcination, reducing, sintering and gas-solid reactions (Jauhari et. al. The most common and industrially important application of rotary kilns is in cement production; all major producers use the rotary kiln as their equipment of choice."

Particle characteristics, kiln size, rotation speed and bed fill affect the nature of the solids flow in rotary kilns [34]. Figure 2.27 illustrates the bed behavior in a rotary kiln.

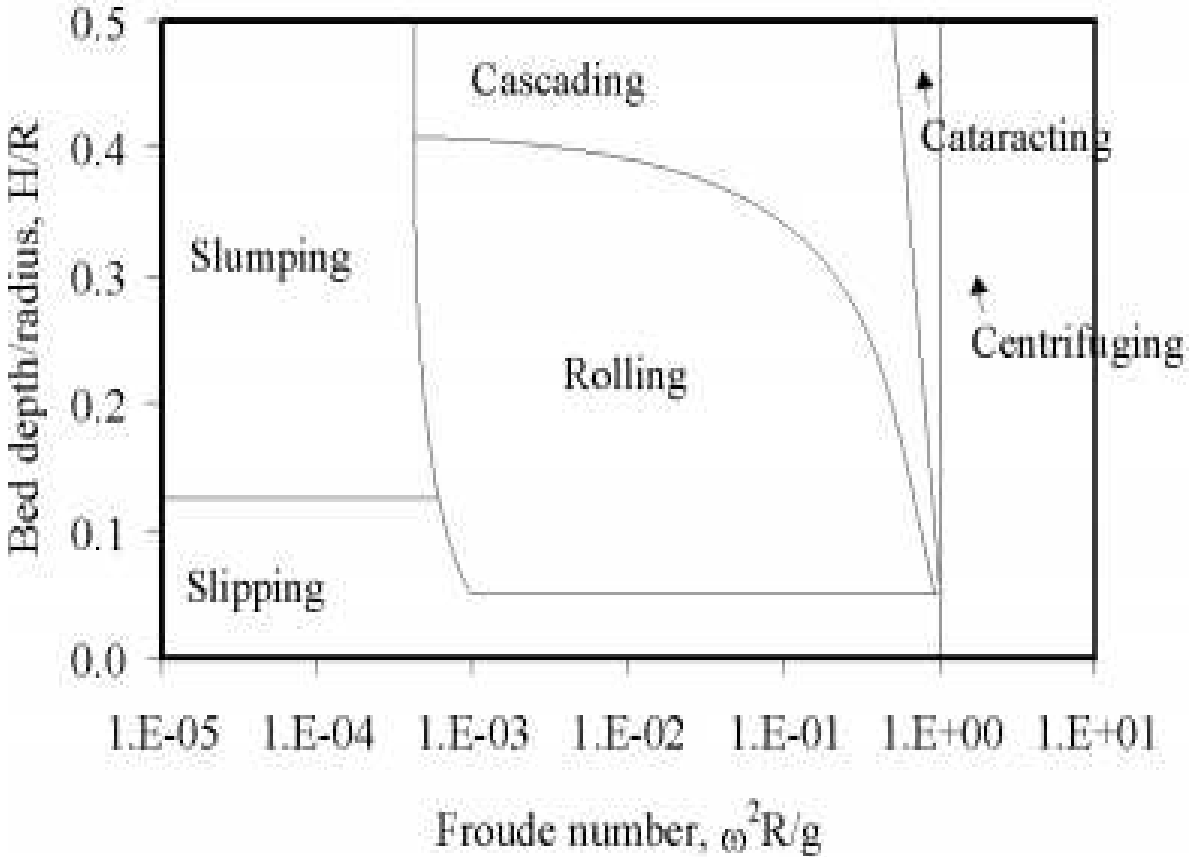

Figure 2.27 Bed behavior in a Rotary Kiln roaster [34]

According to Heydenrych [34] "For rotary kilns with shallow beds in particular, the bed is prone to slippage between the wall of the kiln and the bed. For deeper beds, the motion is either rolling or at lower rotation speeds, slumping. In slumping mode, the angle of repose of the material increases as the static bed rotates, until a segment of material shears off and comes to rest in the bottom half of the kiln. This process occurs repeatedly, and is less desirable than rolling mode for

heat and mass transfer. In rolling mode, the bed surface is continuously renewed, while in slumping mode, the renewal occurs at fixed intervals."

Movement of Material

The rotary kiln is a device for conveying, mixing, heat transfer, and reactions; making it a device that carries out several functions simultaneously [35]: For effective operations, all these functions must be in harmony [35]. The charge in the kiln moves both radially and axially [35]. According to Carina [35] 'Radial motion is determined by the degree of filling (percentage of cross-sectional area occupied by the charge) and the rotational speed." Dust production is often be limited by pelletizing the feed [34, 35].

Heat Transfer

According to Carina [35] "Heat transfer occurs principally from the combustion gas (generated by a burner usually installed at the discharge end of the kiln) to the charge. The driving force is generally the temperature difference. The gas can move co- or countercurrent to the longitudinal motion of the charge. Cocurrent gas flow is advantageous only when the charge temperature does not have to exceed a certain value. The countercurrent arrangement is preferred because it involves an increased total energy consumption." The different types of heat transfer in a rotary kiln are shown in Figure 2.28.

Today refractory ore roasting is performed almost exclusively in fluidized-bed reactors which offer better heat- and mass-transport conditions [2, 34, 35]. However, for applications where softening, sticking, or even partial melting of the material cannot be avoided, rotary kilns are preferred [35].

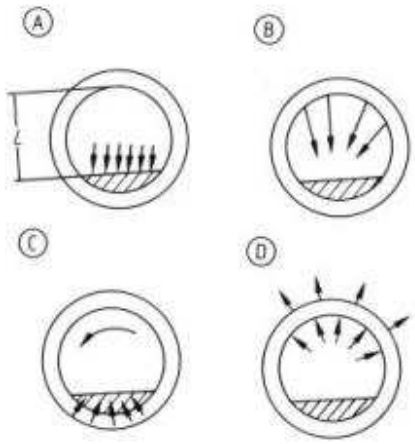

Figure 2.28 Various heat transfer scenarios in a rotary kiln [34]

A) Heat transfer to material by gas radiation and convection; B) Heat transfer to material by brick radiation; C) Conductive heat transfer to material from brick; D) Heat transfer to brick by radiation, convection, and heat loss by shell radiation and convection

2.11.3 Fluidized-Bed Roasters

Fluidized-bed reactors (FBR) are of several large scale industrial applications [12]. FBR operations have been successful at the Giant Yellowknife Mines Ltd., Yellowknife, Northwest Territories, Canada, Barrick's Goldstrike in Nevada, USA and Newmont's Carlin Mine in Nevada, USA [2, 8, 10, 12]. A cross-section of a fluidized-bed roaster is shown in Fig. 2.29. According to Thomas and Cole [12] "Off-gases are cleaned of goldbearing dust in an electrostatic precipitator; thereafter the gold is recovered by carbon-in-pulp. The cleaned arsenic-trioxide fume is cooled and the relatively pure dust collected in baghouses at 1051ºC for shipment to wood-preservative manufacturers or stored in underground vaults within the permafrost. Gold recovery is typically between 87 and 92%. Two-stage roasters are used for arsenopyrite ores and one-stage roasters for

pyritic ores. The reason for the two-stage roasters can be understood by studying the process chemistry. Ideally, the calcine product from roasters should be chocolate brown in colour."

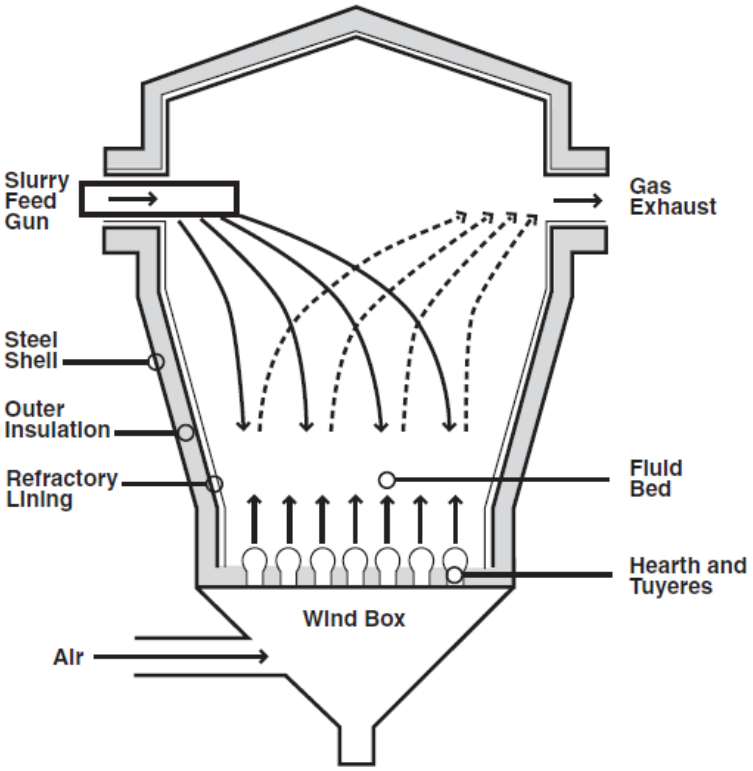

Figure 2.29 Diagrammatic view of a fluidized bed roaster [12]

2.11.4 Stationary Fluid Bed Furnace (SFB)

The SFB roaster was developed for dry pyrite feeding [31] and has been designed to recover the maximum amount of heat for steam production [31, 35]. According to Runkel and Sturm [31] "The temperature of the fluid bed is kept constant by indirect cooling; the surplus heat is removed in the fluid bed by immersed cooling elements which form part of a waste heat system for the production of high-pressure steam. Pyrite grain size is usually s up to 6 mm in diameter. The coarser the grain, the higher the gas velocity must be to maintain the bed in a fluidized state.

Even flotation pyrites with a grain size less than 70 µm can be processed in the fluid bed roaster. Gas velocity in the fluid bed ranges from 0.4 – 1.5 m/s at 1 bar and 850°C." The principle of operation of the SFB roaster is illustrated on Figure 2.30 below.

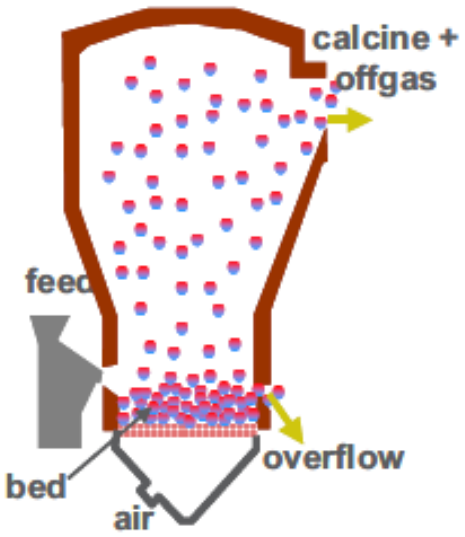

Figure 2.30 Illustration of operation of the SFB roaster [31]

2.11.5 Circulating Fluid Bed Roasting (CFB)

"A further step towards more efficient roasting in terms of higher throughput rates and process controllability is the the CFB process." According to Runkel and Sturm [31]. This CFB technology was originally applied in the calcination of hydrated alumina or clay and combustion of coal [31, 35], and was later adapted for the roasting gold-bearing minerals [2, 10, 31, 36]. Contrary to a the stationary fluid bed, circulating fluid bed roasters are operated at higher gas velocities in the range of 3 – 6 m/s [31]. "According to Runkel and Sturm [31]. Due to the velocity, the fine solids are entrained with the gas and partly recycled to the roaster via a cyclone." A section of the CFB roaster is shown in Figure 2.31.

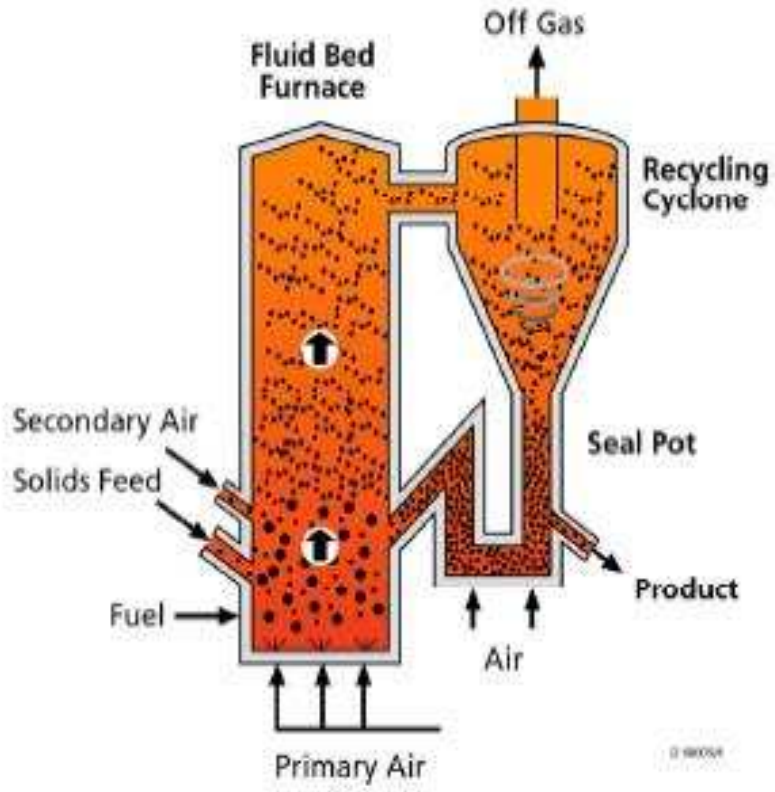

Figure 2.31 Illustration of operation of the CFB roaster [31]

According to Maycock et al [30] The main advantages of the circulating fluid bed are:

- High heat and mass transfer rates [2]
- Uniform temperature profile over the whole roaster system
- reduced capital and operating costs [12]
- excellent sulfur and carbon burnout [12]
- Accurate temperature control inside the fluid bed roaster
- Stable oxygen partial pressure throughout the system.
- Turn down capability to 50%.

CHAPTER 3

ANALYTICAL TECHNIQUES, MATERIALS AND EXPERIMENTAL METHODS

This chapter summarizes the analytical techniques and experimental methods utilized in this project.

3.1 Analytical Techniques

The main analytical techniques utilized in experiments for this research were:

1. Brunauer Emmett and Teller (BET)
2. X-Ray Diffraction (XRD)
3. LECO Analyzer
4. Microtrac Particle Size Analyzer
5. Mossbauer

3.1.1 Brunauer, Emmett and Teller (BET)

BET analysis is the most common method used to describe specific surface area. BET analysis provides precise specific surface area evaluation of materials by nitrogen multilayer adsorption measured as a function of relative pressure using a fully automated analyzer. The technique encompasses external area and pore area evaluations to determine the total specific surface area in m^2/g yielding important information in studying the effects of surface porosity and particle size in many applications.

Specific surface area a_{BET} is defined as the ratio A / ms (unit: m^2/g) between the absolute surface area A of a solid and its mass ms (sample weight). The surface area includes all parts of accessible inner surfaces (mainly pore wall surfaces).

The concept of the BET theory is an extension of the Langmuir isotherm, which is a theory for monolayer molecular adsorption, to multilayer adsorption with the following hypotheses:

- gas molecules physically adsorb on a solid in layers infinitely;
- there is no interaction between each adsorption layer; and
- the Langmuir theory can be applied to each layer.

The resulting BET equation is expressed by:

$$\frac{1}{v\left[(P_0/P)-1\right]} = \frac{c-1}{v_m c}\left(\frac{P}{P_0}\right) + \frac{1}{v_m c} \tag{3.1}$$

P and P_0 are the equilibrium and the saturation pressure of adsorbates at the temperature of adsorption, v is the adsorbed gas quantity, and v_m is the monolayer adsorbed gas quantity. *C* is the BET constant, which is expressed as;

$$c = \exp\left(\frac{E_1 - E_L}{RT}\right) \tag{3.2}$$

E_1 is the heat of adsorption for the first layer, and E_L is that for the second and higher layers and is equal to the heat of liquefaction.

Principle of the Method

According to Franziska [37] "The BET method involves the determination of the amount of the adsorbate or adsorptive gas required to cover the external and the accessible internal pore surfaces of a solid with a complete monolayer of adsorbate."

The monolayer capacity is calculated from the adsorption isotherm by means of the BET equation [37]. The gases used as adsorptives have to be only physically adsorbed by weak bonds at the

surface of the solid (van der-Waals forces) and can be desorbed by a decrease of pressure at the same temperature. The most common gas used is nitrogen at its boiling temperature (77.3 K).

According to Franziska [37] "In the case of a very small surface area (below 1 m^2/g), the sensitivity of the instruments using nitrogen is insufficient and krypton at 77.3 K should be used. In order to determine the adsorption isotherm volumetrically, known amounts of adsorptive are admitted stepwise into the sample cell containing the sample previously dried and outgassed by heating under vacuum. The amount of gas adsorbed is the difference of gas admitted and the amount of gas filling the dead volume (free space in the sample cell including connections). The adsorption isotherm is the plot of the amount gas adsorbed (in mmol/g) as a function of the relative pressure p/p_0."

For the multipoint determination, a BET diagram is plotted with

$$y_{BET} = \frac{p/p_0}{n_a(1-p/p_0)} = \frac{C_{BET}-1}{n_{mono}\cdot C_{BET}}\cdot(p/p_0) + \frac{1}{n_{mono}\cdot C_{BET}} = f(x) = i + kx \qquad (3.3)$$

As can be seen from Figure 3.1 below, BET analysis has a wide range of particle size analysis. The pore sizes are either classified as macropores, mesopores, and micropores.

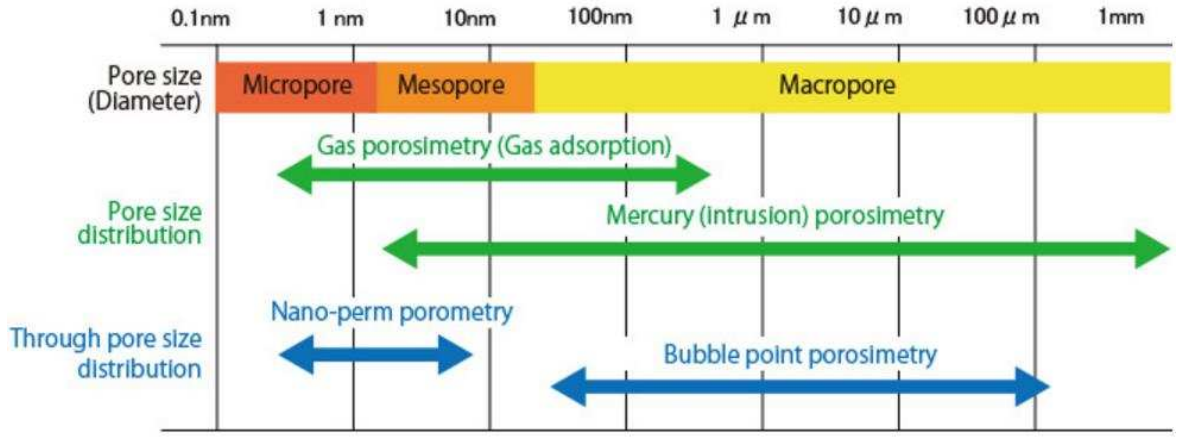

Figure 3.1 Various size ranges for BET measurements

Pore Volume

Total pore volume is derived from the amount of vapor adsorbed at a relative temperature close to unity (assuming pores are filled with liquid adsorbate).

$$V_{liq} = \frac{P_a \; V_{ads} \; V_m}{R\,T} \tag{3.4}$$

V_{ads} = volume of gas adsorbed

V_{liq} = volume of liquid N_2 in pores

V_m = molar vol. of liquid adsorbate (N 2=34.7cm 3/mol)

P_a = ambient pressure

T = ambient temperature

Pore Radius

Average pore size is estimated from the pore volume. Assuming cylindrical pore geometry average pore radius (r_p) can be expressed as:

$$r_p = \frac{2V_{liq}}{S} \tag{3.5}$$

Other pore geometry models may require further information on the isotherm hysteresis before applying appropriate model.

3.1.2 X-Ray Diffraction (XRD) Analysis

An X-ray diffraction pattern is a plot of the intensity of X-rays scattered at different angles by a sample. In XRD, X-rays with a relatively low wavelength of up to 0.1 Å, which are

comparable to the size of an atom, are used to probe the crystal structure of materials or minerals. The x-rays are produced using X-ray tubes or synchrotron radiations and the interaction of the X-rays with the electrons in the sample generates an analysis of crystal structure as well as the phases present [38].

When in operation, the detector moves in a circle around the sample. The detector position is recorded as the angle 2 theta (2θ). The detector records the number of X-rays observed at each angle 2θ. The X-ray intensity is usually recorded as "counts" or as "counts per second." To keep the X-ray beam properly focused, the sample will also rotate. On some instruments, the X-ray tube may rotate instead of the sample.

Single crystal Powder X-rays are passed through a crystalline material and the patterns produced give information of size and shape of the unit cell X-rays passing through a crystal will be bent at various angles: this process is called diffraction X-rays interact with electrons in matter, i.e. are scattered by the electron clouds of atoms. The angles at which x-rays are diffracted depends on the distance between adjacent layers of atoms or ions. This is illustrated in Figure 3.2 below. X-rays that hit adjacent layers can add their energies constructively when they are "in phase". This produces dark dots on a detector plate.

When an X-ray beam is made incident on an atom, the constituting x-ray photons may either be deflected elastically without a change in wavelength (Thompson Scattering) or in-elastically with a change in wavelength due to loss of energy (Compton Scattering). These diffracted beams interact with each other, which produces a resultant intensity modulation. By measuring the diffraction pattern, the user can evaluate the distribution of atoms in the crystal, as the diffracted beam will contain sharp interference peaks with same symmetry as the atomic distribution. This relationship is governed by Bragg's Law, which establishes a relationship

between scattering of an X-ray beam with respect to inter-atomic spacing and the angle of incidence:

$$\lambda = 2\ d \sin \theta \tag{3.6}$$

where 'd' is the inter-atomic distance in the crystal lattice, λ is the X-ray wavelength, and 2θ is the angle between incident and scattered beam.

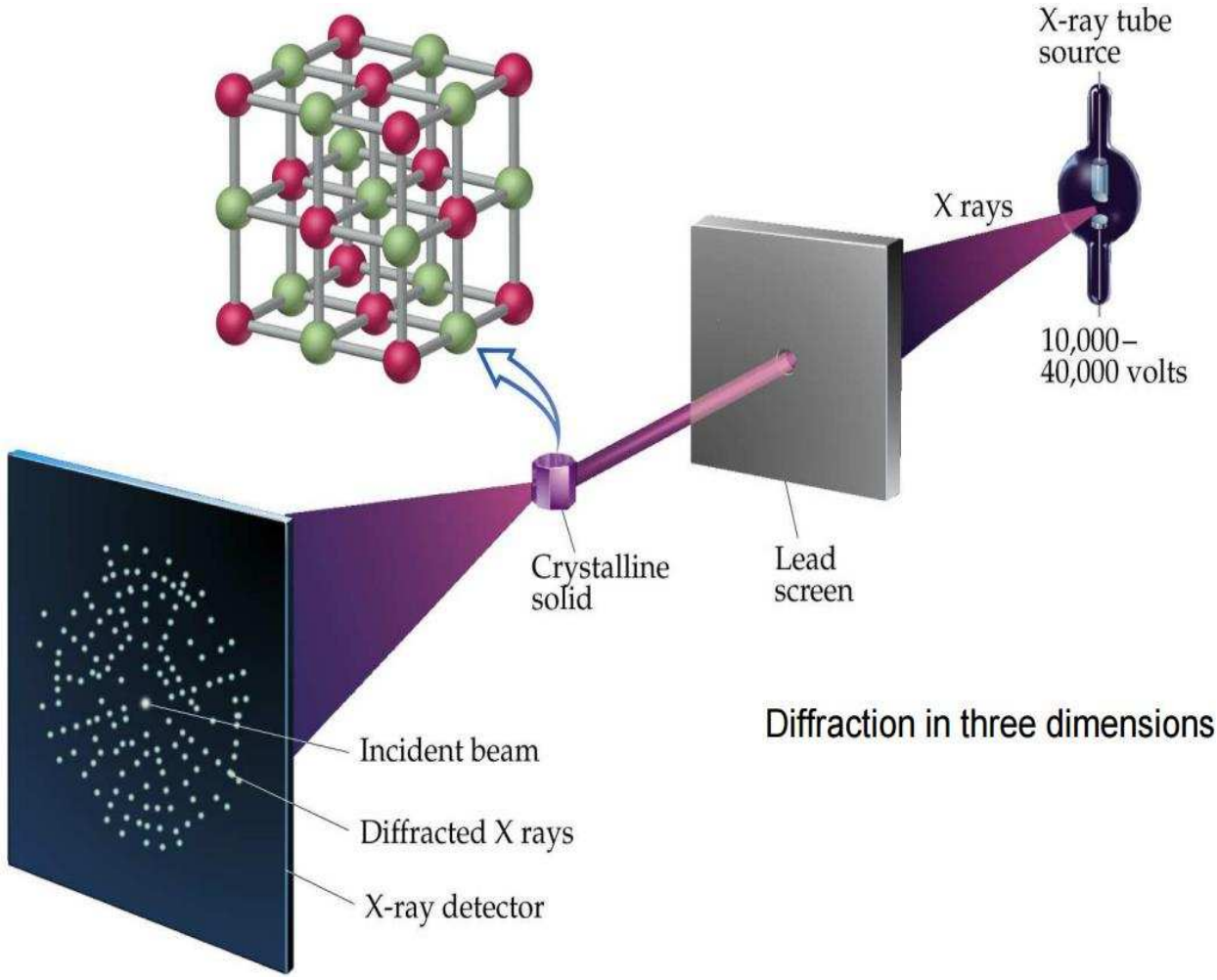

Figure 3.2 Diffraction of an X-ray beam

The incident angle and scattered angle are varied throughout the analysis as the X-ray source and detector are rotated about a fixed axis as shown in the Figure 3.3.

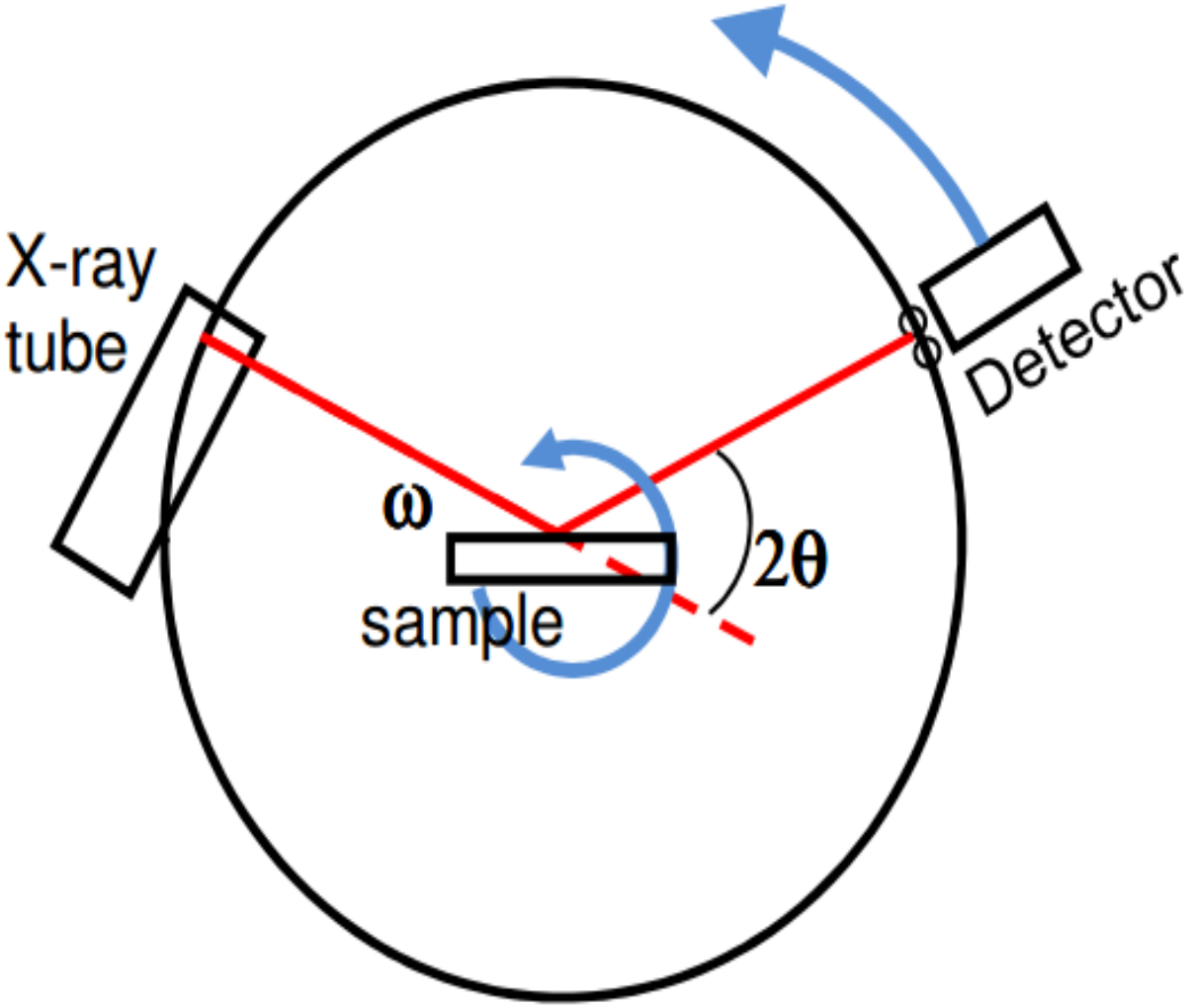

Figure 3.3 A schematic diagram showing the operation of XRD

The following can be determined from an XRD pattern, what crystalline phases are in a mixture, how much of each crystalline phase is in the mixture, and if any amorphous material is present in the mixture.

Figure 3.4 below shows a photograph of the X-ray diffraction facility available at the Colorado School of Mines (CSM). X-ray diffraction was used to characterize the incoming feed material, the leach residue and the precipitation product.

Figure 3.4: Photograph shows the inside chamber of XRD machine at CSM

3.1.3 LECO Analysis

The LECO method of estimating total organic carbon (TOC) and sulfide sulfur (TSS) uses an instrument known as a LECO carbon analyzer to measure TOC and TSS values by combusting the organic carbon and measuring the resulting carbon dioxide produced.

Samples are powdered, weighed, and chemically treated prior to analysis to remove the inorganic carbon (carbonate) from the rock. The sample is then combusted in the presence of excess oxygen, allowing carbon dioxide to form from the free (organic) carbon in the rock. The amount of carbon dioxide is directly proportional to the amount of organic carbon or the TOC of the rock. As the sample gas flows into a carrier stream, the sulfur content is measured as SO_2.

3.1.4 Microtrac Particle Size Analyzer

The Microtrac particle size analyzer gives a precise understanding of the particle size distribution in samples. The system consists of three lasers and two detector arrays that are used to take a measurement of scattered light over a 180-degree spectrum. The resultant scattered light

information from all three lasers is combined to generate the particle size distribution. Brownian motion is an effect that develops as a result of fluid molecules colliding with particles and causing their movement. According to the Stoke-Einstein formula shown below, the particles are treated as point objects have no mass or density. The movement of particles gives rise to diffusion through the suspension where the rate of diffusion is more rapid for small particle [39].

3.1.5 Mössbauer Effect Spectroscopy (MES)

The technique of Mössbauer spectroscopy is widely used in mineralogy to examine the valence state of iron, which is found in nature as Fe^0 (metal), Fe^{2+}, and Fe^{3+}, as well as the type of coordination polyhedron occupied by iron atoms (trigonal, tetrahedral, octahedral, etc.). It is sometimes used to determine redox ratios in glasses and (less successfully) in rocks. Mössbauer spectroscopy is also used to assist in the identification of Fe oxide phases on the basis of their magnetic properties.

Klingelhöfer et al [40] noted that "Iron Mössbauer spectroscopy makes use of the resonance absorption of 14.4 kev γ-rays (the Mössbauer effect) by ^{57}Fe nuclei (2.2% natural abundance) in a solid to investigate the splitting of its nuclear energy levels that is produced by interaction with the surrounding electronic environment. ^{57}Co, which decays to the proper excited state of ^{57}Fe, is normally employed as the source of the γ-rays. In general, the nuclear energy level structure of the absorber will be different from that of the ^{57}Co source (because of different oxidation states, chemical environments, and/or magnetic order), which requires modulation of the energy of the source γ-rays to achieve resonance. This is done using the Doppler Effect, by mounting the ^{57}Co source on a velocity transducer and moving it with respect to the absorber."

The basic elements of a Mössbauer spectrometer are a source, sample, detector, and a drive to move the source or absorber. Most commonly, this is done by moving the source toward and away from the sample, while varying velocity linearly with time. For example, for ^{57}Fe, moving the source at a velocity of 1 mm/sec toward the sample increases the energy of the emitted photons by about ten natural linewidths. For simplicity, "mm/sec" is the conventional "energy" unit in Mössbauer spectroscopy. It is also possible to leave the source stationary and oscillate the sample, as is done with synchrotron Mössbauer. The location of the detector relative to the source and the sample defines the geometry of the experiment (Figure 3.5); most commonly, either transmission or backscatter modes are used.

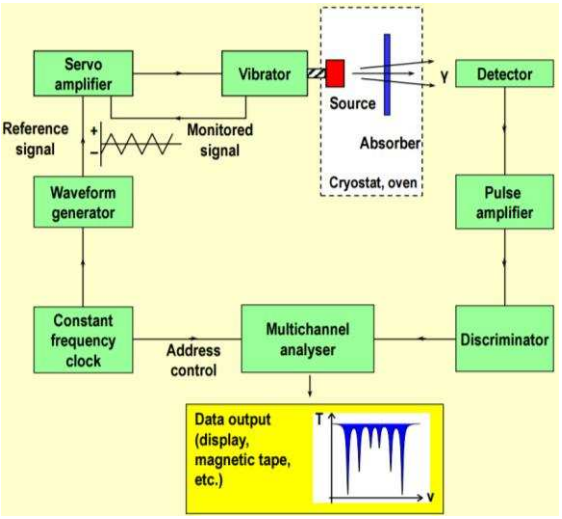

Figure 3.5 Schematic view of a Mössbauer Spectrometer

3.2 Materials

Samples used in this roasting studies were obtained from Newmont Carlin, Nevada. The samples were:

1. Magnetic Separation Feed (Mag Sep Feed),
2. Magnetic Separation Concentrate (Mag Sep Con), and

3. Magnetic Separation Tails (Mag Sep Tails)

All these samples were products from the roasters. The sampling points for these samples (per their positions in Newmont Carlin's flowsheet) are shown in Figure 3.6.

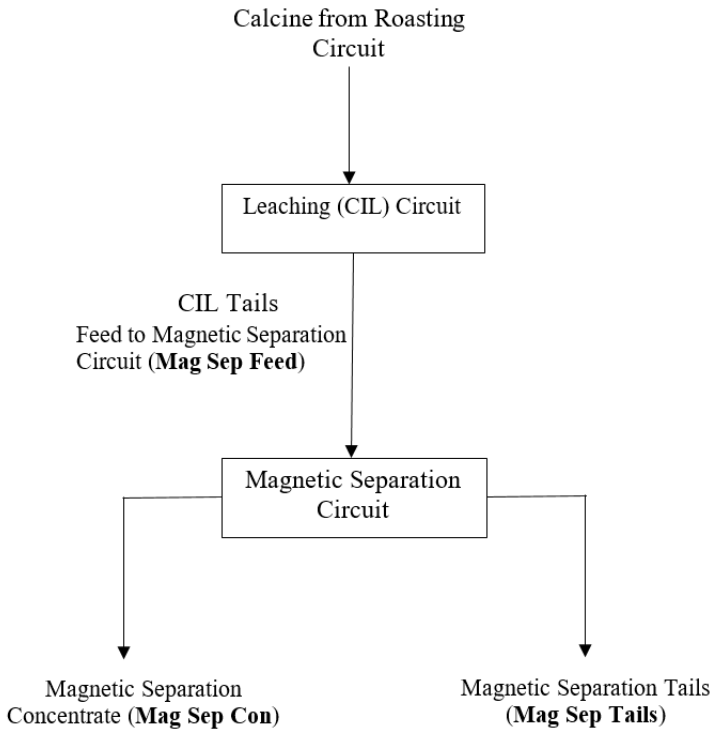

Figure 3.6 Samples obtained from Newmont Carlin (highlighted)

To better assess the optimum roasting parameters required for conversion of maghemite to hematite, pure standard samples of Maghemite and Hematite were purchased. Laser size diffraction (Microtrac) was performed on the standard pure samples. The respective particle size distributions for each mineral size fraction can be found in Figure 4.2 in Chapter 4. X-Ray diffraction was also performed on all samples to illustrate the phases present (see Appendix C).

3.3 Experimental Methods

A brief description of the various experimental methods used in this project is presented in this section.

3.3.1 Sizing

The As-received Magnetic Separation Feed (Mag Sep Feed), Magnetic Separation Concentrate (Mag Sep Con), and Magnetic Separation Tails (Mag Sep Tails) from Newmont, Carlin had a cut-size of 80% passing 200 mesh (74 µm). Wet sieving was done initially to find out the size distribution of the particles in the Mag Sep Feed, Mag Sep Con, and Mag Sep Tails samples. The method consists of placing the desired sieves in order of decreasing mesh opening and using wash water and a vibrating motor to aid the particles to pass through the mesh. The fraction of feed passing 200 Tyler Mesh (P_{200}), with mesh opening of 74 µm, was used for further roasting tests.

The standard maghemite and hematite samples had average particle size of P_{80} = 31 µm. Particle size distributions of the standard maghemite and hematite samples were obtained using Microtrac Size Analyzer.

3.3.2 Roasting

Batch roasting experiments were conducted on the standard maghemite sample mainly in a tube furnace (see Figure 3.7) to establish operating conditions for the roasting experiments. The roasting parameters or variables tested were temperature, time, and oxygen enrichment.

Two thermocouples were installed to record the temperature of the sample being roasted and the other for tracking the temperature in the furnace. Roast temperature data were captured with an Omega® DP1001AM Automatic Temperature Scanner. A Bacharach Oxor® III Oxygen Meter was also attached to off gas line to measure the oxygen consumption in the system.

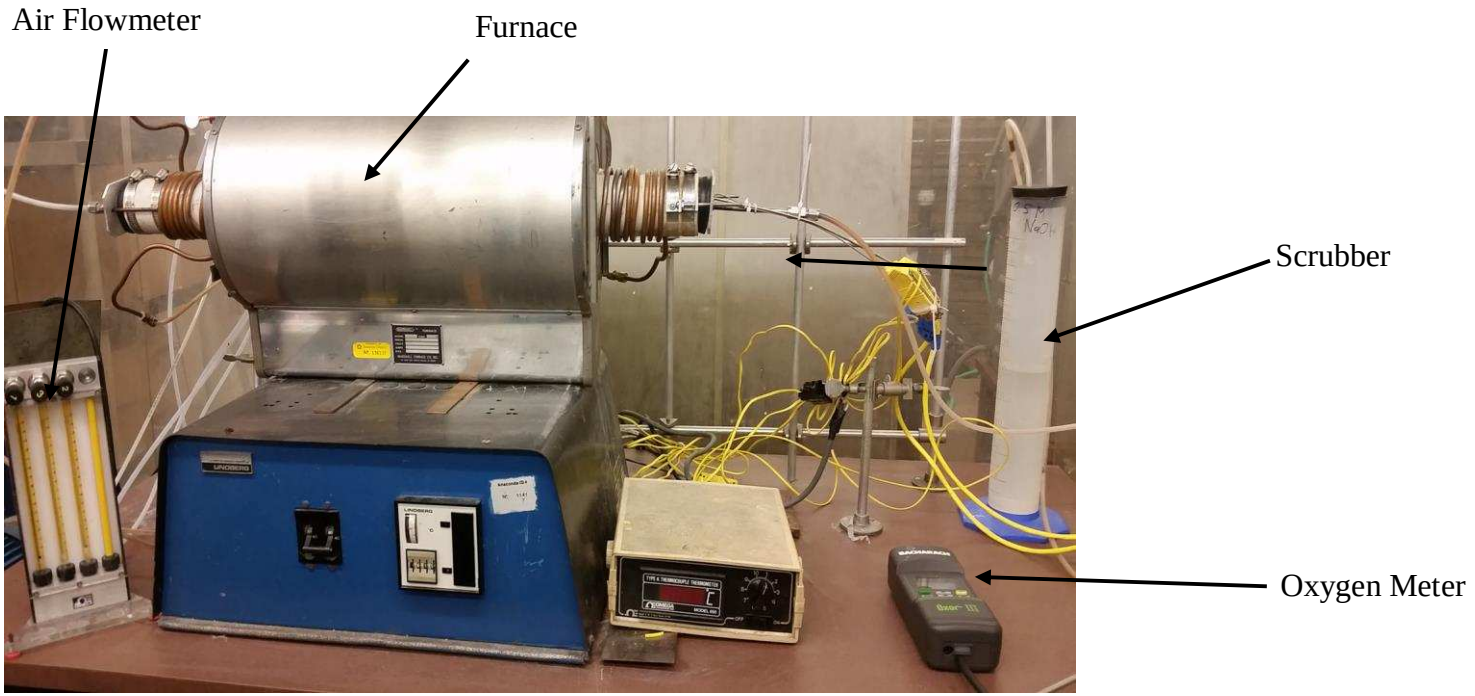

Figure 3.7 Setup for tube furnace

Pure Maghemite Roasting

The pure maghemite (γ-Fe_2O_3) sample was roasted at varying temperatures to establish the optimum temperature at which maximum transformation to hematite occurs. Maghemite is ferromagnetic and has its Néel point close to 650°C [41]. This means that beyond 650°C, the ferromagnetic maghemite could be altered to its antiferromagnetic iron oxide (hematite) [41]. Tronc et al [41] investigated the conversion of γ-Fe_2O_3 (maghemite) into α-Fe_2O_3 (hematite) and concluded that at a temperature of 475°C, conversion of about 80% was obtained within two days.

The pure maghemite sample was roasted at a starting temperature of 450°C, and in incremental temperatures of 50°C up to 750°C. Complete roasting was determined from oxygen consumption. Furnace and ore tempearture was recorded at 10 s intervals and the results are shown in Appendix A.

The established roasting parameters were then tested on Mag Con samples to determine the optimum roasting parameters required for the conversion of maghemite to hematite. The resulting calcine from each roast test was analyzed by XRD and BET measurements. At each temperature of roasting, oxygen consumption was tracked (see Appendix B). Since roasting is an oxidation process, the reaction was deemed complete at the time when there was no further oxygen consumption.

3.3.3 Leaching

The efficiency of gold ore roasting can be assessed based on the amount of gold that can be recovered from the calcine by leaching [8, 42]. To this end, the roasted calcines were leached with NaCN (≥98% purity), obtained from VWR International, to assess whether roasting of the

Mag Con at various temperatures had resulted in relevant increase in gold recovery. Figure 3.8 below shows the setup used for leaching.

Figure 3.8 Setup for leaching

The leaching parameters are summarized in Table 3.1 below.

Table 3.1 Leaching parameters

Pulp Density (% solids)	40%
NaCN Concentration	0.33 g/L
pH	10.5 – 11.0
Leaching time	12 hr
Magnetic Stirrer agitation speed	600 rpm

CHAPTER 4

MATERIAL CHARACTERIZATION AND SIZE BASED SEPARATION

This chapter presents the characterization and size based separation tests that were conducted.

4.1 XRD Analysis

X-ray diffraction was carried out to determine the phases of the minerals present in the Mag Feed, Mag Con and Mag Tails samples as was previously determined for the pure hematite and maghemite samples. X-ray-diffraction (XRD) analyses were performed on each roast calcine with Cu-Ka radiation in a conventional h/2h diffractometer in the symmetric Bragg–Brentano mode [43]. The graphite monochromator was on the detector side of the sample [43]. The ore samples were ground to 80% passing 74 μm and the standard maghemite (γFe_2O_3) to 20-40 μm and packed on Teflon covered aluminum sample holders for X-ray powder-diffraction analysis. Micro-XRD analyses were performed on polished sections in areas of about 50 mm. In this technique, the polished section is rotated within all possible geometrical angles to expose the grain or grains in the area of interest to the incident X-ray beam.

Data were collected in a step-scan mode with a step size of 0.05° 2θ and time per step of 10–100 s. Peak fits were performed with a non-linear least-squares fitting routine and the Pearson VII function.

For the Mag Feed, Mag Con and Mag Tails samples, The XRD quantities were determined by Rietveld refinement and whole pattern fitting, where XRD spectra are calculated from crystallographic parameters of the minerals identified, and mineral quantities are adjusted so that the calculated spectra compare with the sample spectra. Some of the gangue minerals present were

illite, kaolinite, and quartz. The results is shown on Table 4.1. All the samples were micronized to minus 25 microns for XRD, for improved quantification. The XRD plots for all the samples are shown in Appendix C.

Table 4.1 Semi-quantitative XRD Analyses of Magnetic samples - Wt. %

Mineral	Formula	Mag Feed	Mag Con	Mag Tails
Bassanite	$CaSO_4 \cdot 0.5H_2O$	6	1.4	6
Calcite	$CaCO_3$	5	-	6
Barite	$BaSO_4$	1.2	-	1.1
Dolomite	$CaMg(CO_3)_2$	13	7	13
Hematite	Fe_2O_3	0.5	20	-
Maghemite	γ-Fe_2O_3	0.4	32	-
Illite	$(K,H_3O)Al_2(Si_3Al)O_{10}(H_2O,OH)_2$	10	9	11
Kaolinite	$Al_2Si_2O_5(OH)_4$	3	1.7	3
Quartz	SiO_2	61	30	61

The major phases identified in the pure maghemite sample were Fe_2O_3 (both alpha and gamma) see Figure 4.1. The constituents of the pure maghemite and hematite samples as obtained from the Certificate of analysis are presented in Table 4.2.

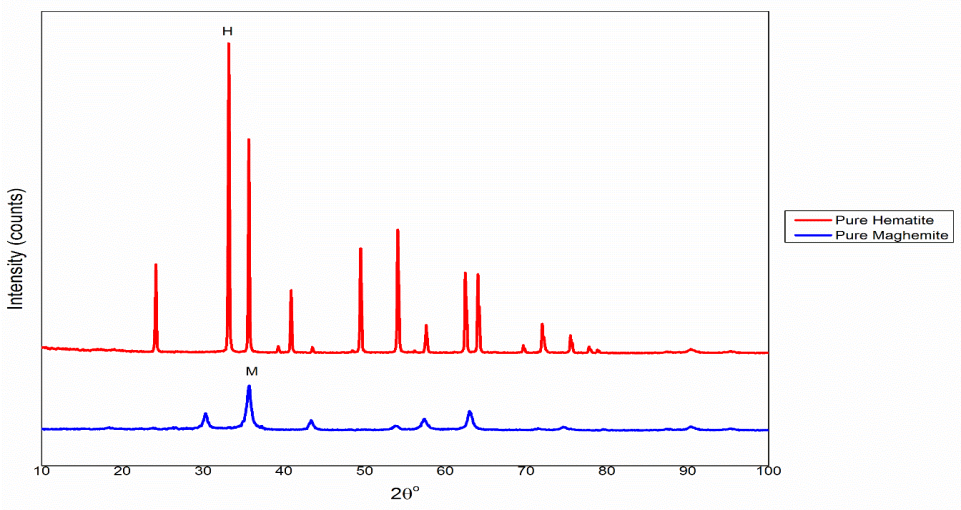

Figure 4.1 XRD results for phases present in pure maghemite and hematite samples

Table 4.2 Properties and contents of pure maghemite and hematite samples

	Pure Maghemite	Pure Hematite
Purity (%)	99+	99+
Average Particle Size (nm)	20 – 40	20 – 40
Specific Surface Area (m^2g^{-1})	40 – 60	40 – 60
Contents (%)		
Fe_2O_3	99.15	99.15
CuO	<0.00001	<0.00001
SO_3	0.31	0.31
CaO	0.04	0.04
SiO_2	0.13	0.13
MnO	0.173	0.173
P_2O_5	-	-
Cr_2O_3	0.03	0.03
V_2O_5	0.009	0.009

4.2 ICP - MS

The chemical composition of each sample was measured using Inductively Couple Plasma Mass Spectrometry (ICP-MS). ICP results for the Mag Feed, Mag Con and Mag Tails samples are presented on Table 4.3.

Table 4.3 Elemental analysis of the Mag Feed, Mag Con and Mag Tails.

Element	**Mag Feed (ppm)**	**Mag Con (ppm)**	**Mag Tails (ppm)**
Ag	<0.5	5.2	<0.5
Al	33400	18600	35000
As	1400	12800	1200
Be	<2	<2	<2
Ca	4.12	1.29	4.92
Cd	2.4	9.1	2.3
Co	10	165	8
Cr	90	279	88
Cu	177	576	173
Fe	26900	411400	19000
Li	34	30	32
K	9900	4600	10100
Mg	19200	0.55	2.01
Mn	376	931	360
Mo	11	83	8
Na	734	512	711
Ni	86	746	71
Pb	41	237	34
Sb	109	596	101
Se	<10	<10	<10
Sr	51	41	61
Ti	0.18	0.16	0.18
V	151	176	152
Zn	482	1016	463

4.3 Sieving and Microtrac Particle Size Analysis

About 150 g each of Mag Feed, Mag Con and Mag Tails samples was wet screened with a bucket vibrating screen using a Tyler screen arrangement of 212 µm, 150 µm, 106 µm, 75 µm, 53 µm, and 38 µm, in that order. The material was fed onto the212 µm sieve and washed with running water. The undersize (- 212 µm) material was collected in a bucket and then transferred over to the 150 µm sieve and the sequence was followed using the stated sieving configuration. The undersize of the last sieve (- 38 µm) was collected in the pan. The material retained on each sieve was collected and weighed after drying.

The particle size distribution and cumulative percentage passing value for each of the three samples is shown on Figure 4.2. From the particle size distribution analysis, it was confirmed that 80% of each of the three samples passed 74 µm (200 mesh).

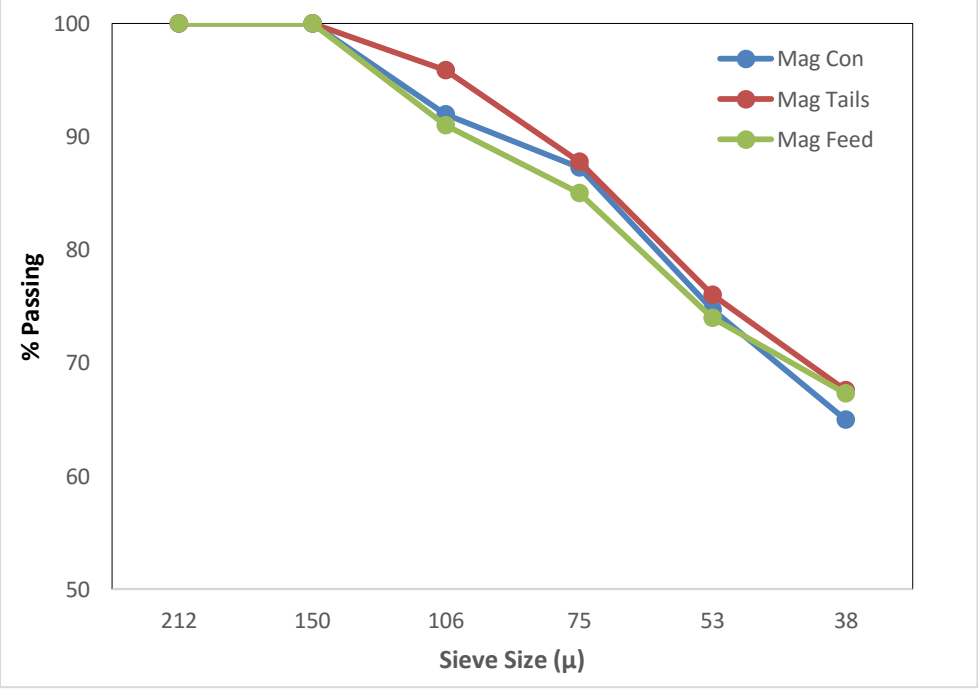

Figure 4.2 Particle Size analysis for the three magnetic separation samples

The pure maghemite and hematite samples were analysed for particle size distribution using the microtrac particle size analyser. A comparison of the size distribution of the pure samples is shown in Figure 4.3. Both pure maghemite and hematite samples have much finer particle sizes with their P_{80} at 31.5 µm and 30.9 µm respectively.

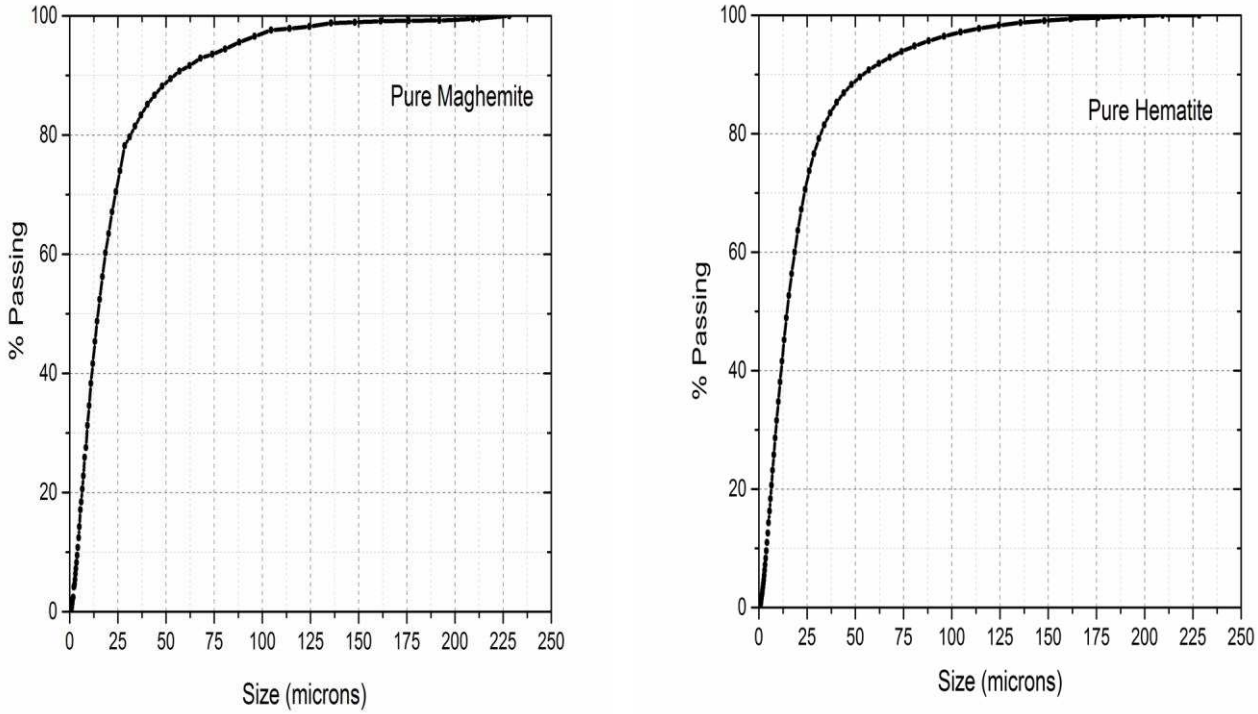

Figure 4.3 Particle size analysis for pure maghemite and hematite sample

4.4 Brunauer, Emmett and Teller (BET) Analysis

BET surface and porosity measurements were carried with a BELSORP-MR6 shown in Figure 4.4 below. The BELSORP surface analyzer has a capability of pretreating the sample and simultaneously conduct a measurements. Samples were pretreated at a temperature of 300°C for 90 mins. Nitrogen gas was used as the adsorption gas at an adsorption temperature of -196.15°C (77K).

Figure 4.4 BET instrument

4.5 Mössbauer Effect Spectroscopy (MES)

Maghemite, γ-Fe_2O_3 is ferrimagnetic and has its Néel point close to 650°C [41]. This means that beyond 650°C, the ferromagnetic maghemite could be altered to its antiferromagnetic iron oxide (hematite) [41]. Tronc et al [41] investigated the conversion of γ-Fe_2O_3 (maghemite) into α-Fe_2O_3 (hematite) and concluded that at a temperature of 475°C, conversion of about 80% was obtained within two days.

CHAPTER 5

PURE MAGHEMITE ROASTING RESULTS AND DISCUSSIONS

The results obtained from roasting of pure maghemite and the analysis of the resulting roast products have been discussed in this chapter.

5.1 Mössbauer Results

The calcine from each roast test was analysed for maghemite and hematite content by XRD analysis and the pore volume and area of pores generated in each calcine was determined by BET measurements. About 50 mg each of the pure maghemite sample, as well as its calcine from the 450°C and 600°C were first analysed in the Mössbauer Effect Spectroscope. This was to establish the basis for semiquantification of the maghemite and hematite contents in each calcine as determined from the XRD measurements.

Mossbauer spectra for pure hematite, maghemite and the calcines at 450°C and 600°C are stacked on Figure 5.1 below. It can be seen from the absorptrion spectra that the Mossbauer spectra for the pure maghemite standard is broad whereas that for the pure hematite standard is narrow. From Figure 5.1, the 450^{o}C maghemite calcine has a similar absorption spectra as the standard maghemite suggesting virtually no hematite conversion upon roasting at 450^{o}C. The spectra for the 600^{o}C calcine on the other hand tends to assume the narrow spectra observed in the pure hematite. This suggests an evidence of hematite conversion when the pure maghemite is roasted at 600^{o}C. The detailed absorption spectra are presented in Appendix C.

The percentages of maghemite and hematite in each of the samples have been presented in Figure 5.2. The 25°C on the graph denotes the pure maghemite standard sample which is unroasted thus being at room temperature.

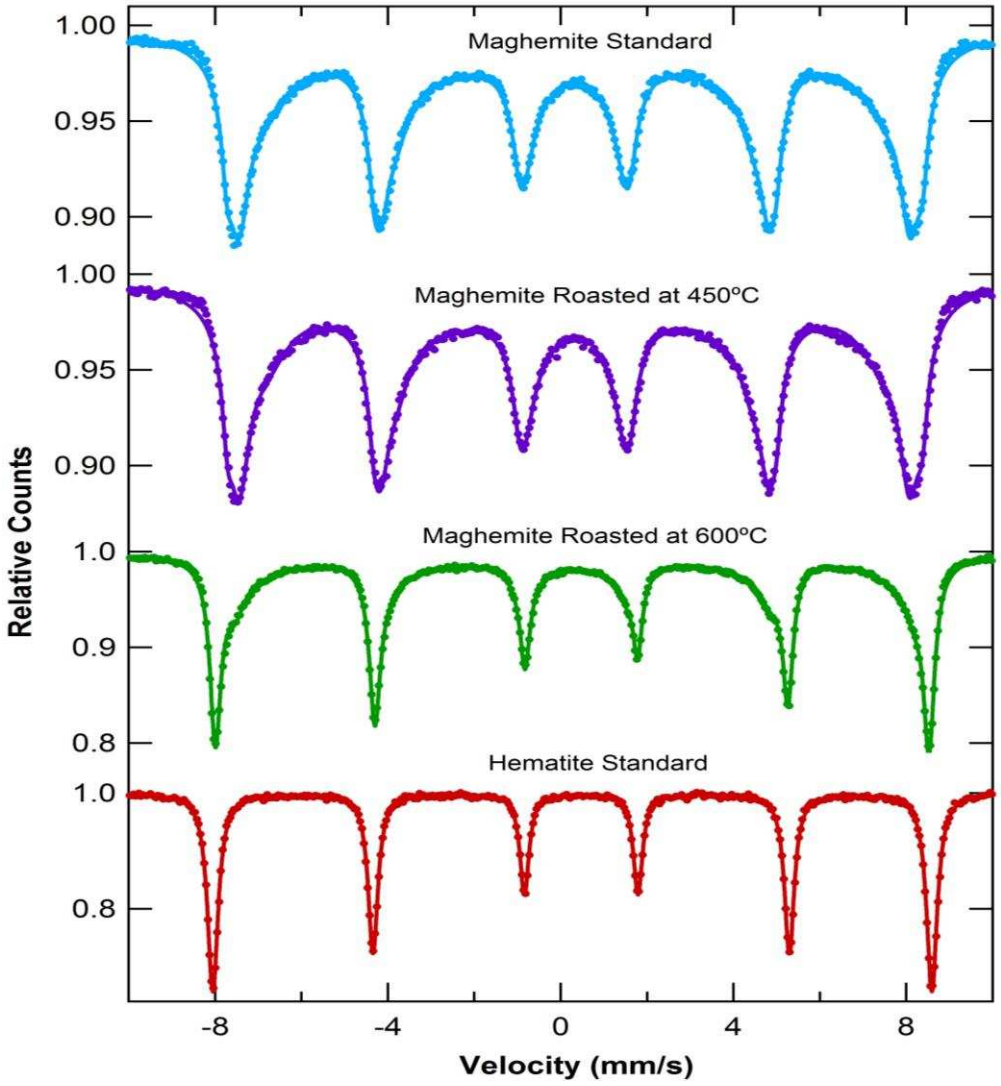

Figure 5.1 Mossbauer absorption spectra for standard maghemite sample and calcines

The percentage maghemite left in the 450°C and 600°C maghemite calcines were 98.5% and 64% respectively. This means that only 1.5% of maghemite was oxidized into hematite in the 450°C calcine whereas 36% hematite conversion was achieved after roasting the pure maghemite to 600°C. Mossbauer results indicating the percentage of maghemite and hematite in the respective samples are shown in Figure 5.2.

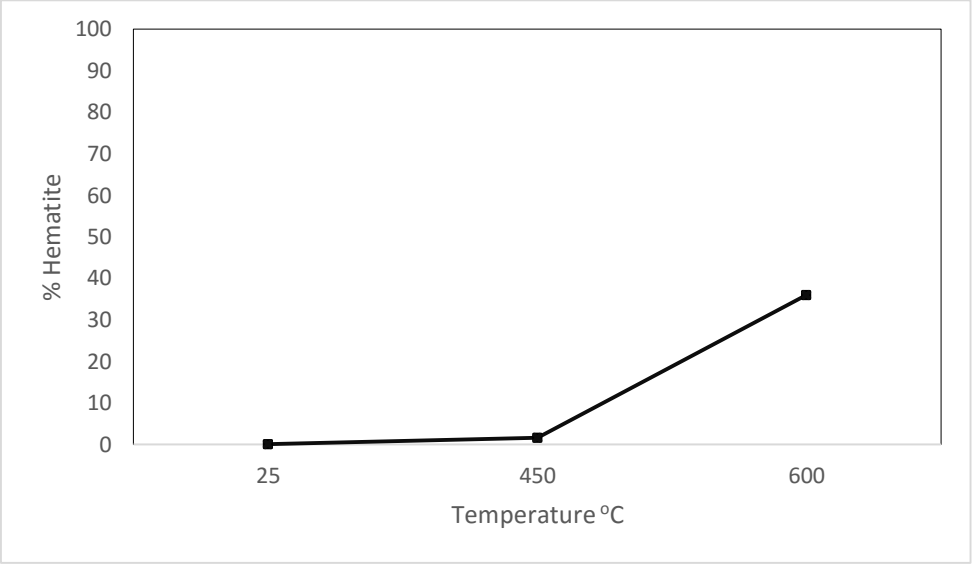

Figure 5.2 Mossbauer results indicating % hematite in pure and roasted maghemite

Since these Mossbauer results corresponded to the relative maghemite and hematite percentages based on the areas (A%) bounded by the maximum peaks of maghemite (2θ = ~35.659) and hematite (2θ = ~33.153) from the respective XRD runs. The areas bounded by the maximum peaks of maghemite and hematite were then used in calculating, semiquantatively, the percentages of maghemite relative to that of hematite in each calcine.

5.2 XRD Results

Figure 5.3 below shows the percentage of maghemite remaining in each roast calcine at the indicated temperatures. It can be seen that roasting of pure maghemite at temperatures up to 500°C did not yield in any appreciable hematite conversion. However, the conversion of maghemite to hematite occurred at temperatures above 500°C.

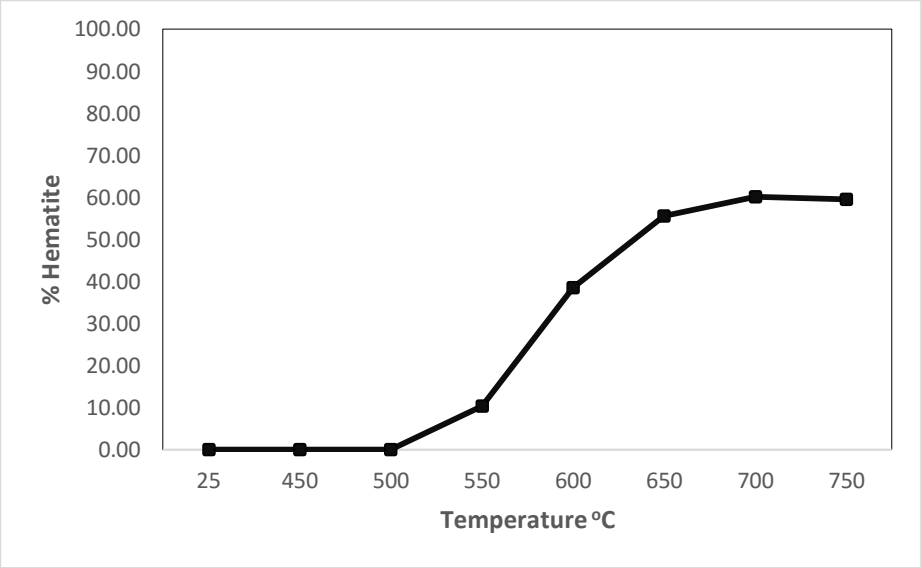

Figure 5.3 XRD based % hematite in pure and roasted maghemite

Only about 10% hematite conversion occurred at 550°C. According to Tronc et al [41], at lower temperatures (< 500°C), appreciable conversion of maghemite to hematite is only possible over prolonged reaction times. Tronc et al [41] concluded that at a temperature of 475°C, conversion of about 80% was achieved within two days. This probably explains the relatively poor hematite conversions recorded at temperatures below 550°C since these roasting experiments were all conducted at less than 90 mins.

From literature, maghemite, γ-Fe_2O_3 is ferromagnetic and has its Néel point close to 650°C [41]. This means that beyond 650°C, the ferromagnetic maghemite could be altered to its antiferromagnetic iron oxide (hematite) [41]. As can be seen from Figure 5.3 the hematite conversion rate increased quite steeply beyond 550°C with about 60% conversion occuring at 700°C. However, beyond 700°C, the rate of maghemite to hematite conversion tended to decrease. Maghemite to hematite conversion in the pure maghemite sample is therefore optimum at temperatures between 650°C and 700°C.

Paktunc et al [8] concluded that the efficiency of gold extraction is improved if the calcine has a high proportion of hematite to maghemite. Therefore from Figure 5.3, it can be inferred that roasting of Mag Con at temperatures above 600°C can enhance the efficiency of gold extraction.

5.3 Effect of Oxygen Enrichment on Hematite Conversion

From the XRD results for pure maghemite roasting, it was determined that hematite conversion was optimum between 650°C and 700°C. Samples of pure maghemite were roasted at these determined temperatures in an oxygen enriched atmosphere; at oxygen percentages of 50%, 75% and 100%. Again, since hematite conversion only occurred at temperatures above 500°C, the standard sample was also roasted at 500°C with the air enriched with oxygen to investigate if oxygen enrichment might enhance appreciable hematite conversion. The hematite conversions obtained at the various enriched oxygen percentages are shown in Figure 5.4. On the graph, the un-enriched air is marked as having 21% oxygen.

From Figure 5.4, it can be seen that enriching the air used for roasting with oxygen up to 100% does not result in any measurable maghemite to hematite conversion. This suggests that at temperatures up to 500°C, both temperature and oxygen does not yield any transformation of maghemite to hematite even over prolonged time.

It can also be seen that at 650°C, oxygen enrichment only slightly enhances hematite conversion, with maximum conversion occuring at 75% oxygen enriched air. However, enriching the air for roasting above 75% results in a decline in the hematite conversion rate. Even at the 75% oxygen enrichment, where the highest hematite conversion occurred, only an additional ~3% conversion was achieved.

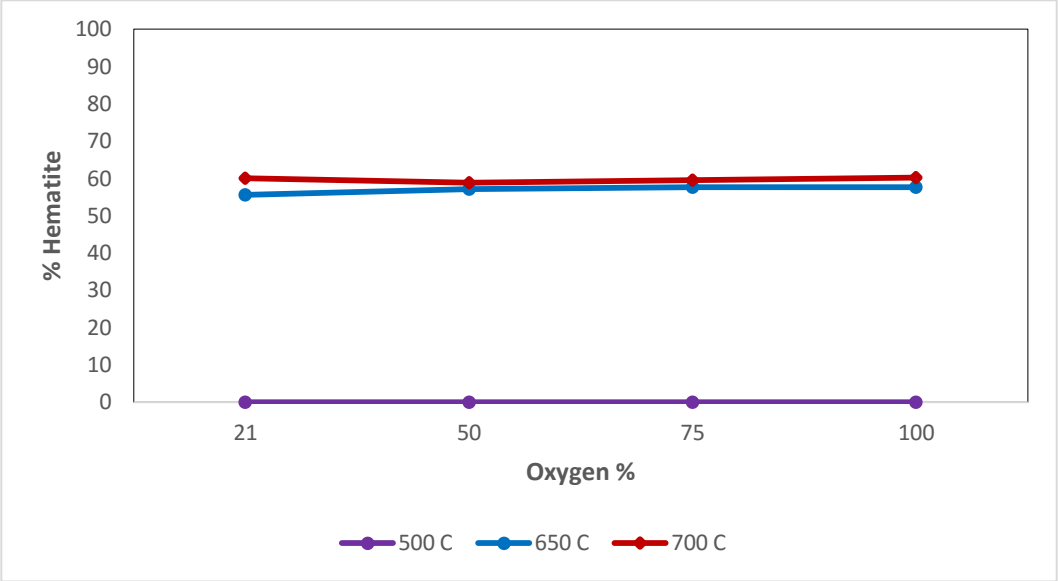

Figure 5.4 Effect of O_2 enrichment on hematite conversion

Conversely, at 700°C, oxygen enrichment rather leads to a decline in hematite conversion as can be seen from Figure 5.4. This suggests that it may not be worth enriching the air used for roasting with oxygen. From Figure 5.5 below, it can be inferred that hematite conversion depends largely on roasting temperature and immeasurably on O_2 enrichment.

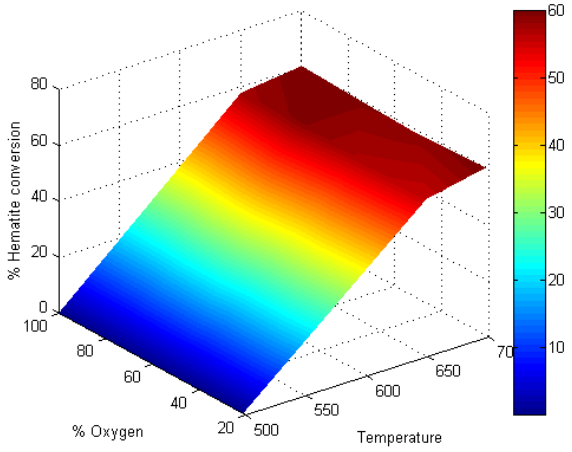

Figure 5.5 Plot of dependence of hematite conversion on roasting tempearture and O_2 enrichment

CHAPTER 6

MAGNETIC CONCENTRATE ROASTING RESULTS AND DISCUSSIONS

The results obtained from roasting of the magnetic concentrate sample and the analysis of the resulting roast products have been discussed in this chapter.

6.1 Introduction

The results obtained from the pure maghemite roasting tests (discussed in Chapter 5) were used as a basis for further roasting the Mag Con samples at temperature increments of 50°C starting from 550°C up to 750°C. This was to evaluate the posibility of recovering more gold from the maghemite-rich Mag Con.

From their studies on distribution of gold in pyrite and in its roasting products, Paktunc et al [8] concluded that the efficiency of gold extraction from maghemite roasting products is improved if:

- The calcine has a high proportion of hematite to maghemite,
- The calcine has high porosity with coarse pores,
- There exists good permeability aided by microfractures in the calcine.

On this basis, the roasted calcines were analyzed by XRD to semi-quantitatively measure the proportion of hematite to maghemite in the roast calcines. The pore areas and volumes generated in the calcines were also measured by BET followed by cyanide leaching to measure gold extraction. The calcines were also analyzed by LECO for organic carbon and sulfide sulfur remaining in the calcine as this gives an indication of the efficiency of roasting. The arsenic content in each calcine was also measured. The results obtained are discussed in the sections below.

6.2 XRD Results for Magnetic Concentrates

XRD results from roasting of the Mag Con sample are discussed below.

6.2.1 Effect of Temperature on Maghemite to Hematite Conversion

To investigate the effect of temperature on maghemite to hematite conversion, the proportion of hematite in each calcine (based on XRD) at the various roast temperatures have been compared. The % of hematite conversion recorded at each temperature roast for the Mag Con sample is presented in Figure 6.1. Conversion of maghemite in the Mag Con to hematite increased with increasing roasting temperature. The increase was quite rapid up to 650°C and only slightly beyond that until at 750°C where the maximum conversion (~69%) was recorded. At the least, about 50% of the maghemite in the Mag Con could be converted to hematite at roasting temperatures around 650°C.

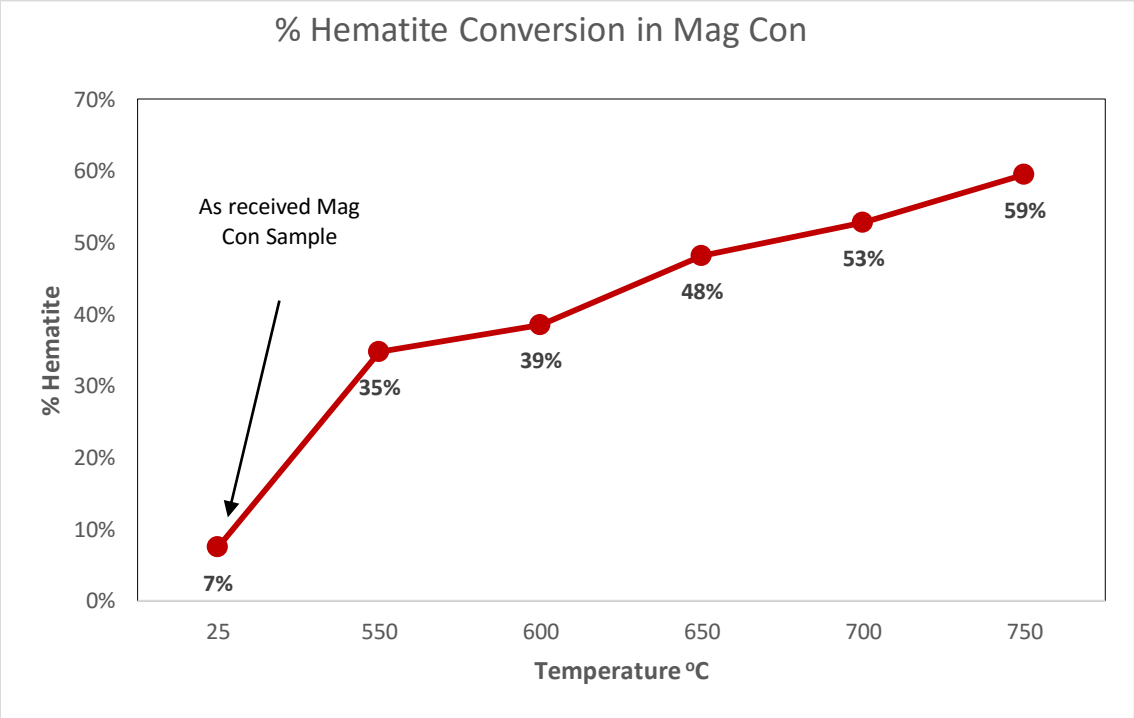

Figure 6.1 Hematite conversion in Mag Con at various roast temperatures based on XRD

Even though it appears roasting the Mag Con concentrates at higher temperatures results in appreciable conversion of a greater percentage of the maghemite to hematite, the cost incurred at operating a typical roasting plant at higher tempeartaures may not make this economically viable [17]. Again, on a large scale, roasting at very high tempeartures may result in handling of high volume of offgases which might impact on operations of the downstream gas cleaning and acid plants [5]. It is therefore important to explore whether enriching the roasting air with oxygen could result in optimized maghemite to hematite conversion at at relatively lower temperatures

6.2.2 Effect of Oxygen Enrichment on Maghemite to Hematite Conversion

Since higher hematite conversions were obtained at temperatures above 600°C, the Mag Con sample was roasted from 650°C to 750°C and the air enriched at various oxygen percentages up to 100% to investigate whether or not oxygen enrichment impacts maghemite to hematite conversion. The results based on XRD is shown on Figure 6.2.

It can also be seen that at 650°C, oxygen enrichment only slightly enhances hematite conversion, with maximum conversion occuring at 75% oxygen enriched air. Even at the 75% oxygen enrichment, where the highest hematite conversion occurred, only an additional ~3% conversion was achieved. However, enriching the air for roasting above 75% results in a decline in the hematite conversion rate.

Again, at 700°C, oxygen enrichment at 50% and 75% only increased maghemite to hematite conversion by about 1% and 3% respectively with 100% O_2 resulting in no increase (over 75% O_2 enriched air) in hematite conversion. As can also be seen from Figure 6.2 oxygen enrichment at 750°C resulted in no appreciable increase in hematite conversion with 100% O_2

enrichment actually decreasing hematite conversion by about ~1%.

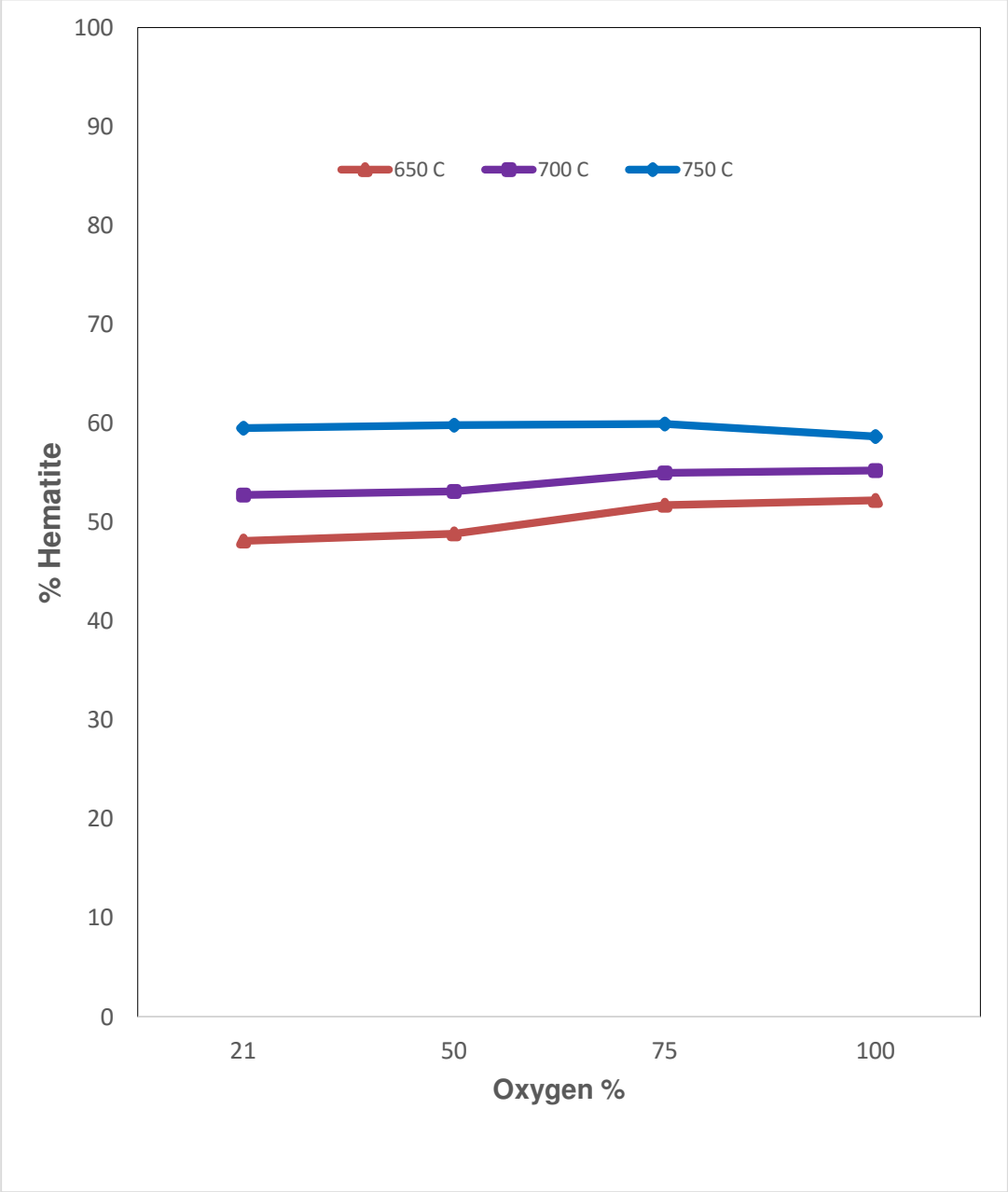

Figure 6.2 Hematite conversion in Mag Con at various O_2 enriched air based on XRD

The 3D plot on Figure 6.3 below depicts the dependence of hematite conversion on roasting temperature and O_2 enrichment.

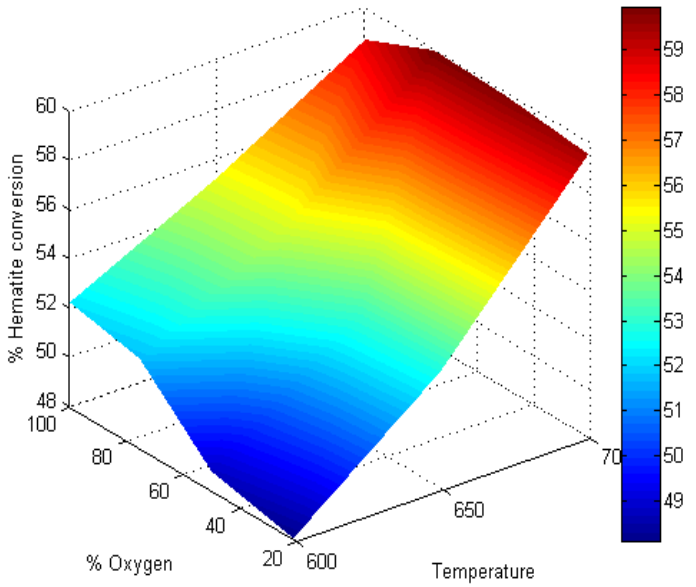

Figure 6.3 A 3D plot showing dependence of hematite conversion on % oxygen in roast air and temperature

This implies that the enriching the air for roasting the Mag Con sample with oxygen does not result in any appreciable hematite conversion beyond that obtained by roasting with normal air. In essence, at very high temperatures, above 700°C, high O_2 enriched roasting air actually slightly hinders the conversion of maghemite to hematite. Oxygen enrichment creates a highly oxidizing environment which can potentially cause the arsenic to be locked up as a nonporous ferric arsenate ($FeAsO_4$) or ferrous pyroarsenite (Fe_2AsO_5) product which is rich in maghemite [5]. Oxygen enrichment therefore has no correlation with maghemite to hematite conversion in Mag Con by roasting.

6.3 Effect of Pore Volume and Pore Area on Maghemite to Hematite Conversion

The primary objective of the Mag Con roasting process was to make the “invisible” gold locked in the maghemite accessible to the cyanide solution for effective leaching [2][5].

Amenability of the calcine to gold recovery was evaluated by the degree of the porosity and permeability shown by the iron oxide particles.

Results of the pore volume [$cm^3.g^{-1}$] and area of pores [$m^2.g^{-1}$] of each Mag Con calcine as measured by BET are shown in Figure 6.4. As can be seen from Figure 6.4, the pore volumes and pore areas in the resulting Mag Con calcines increased with increasing roasting temperatures. The BET results confirm the trend obtained from the XRD results.

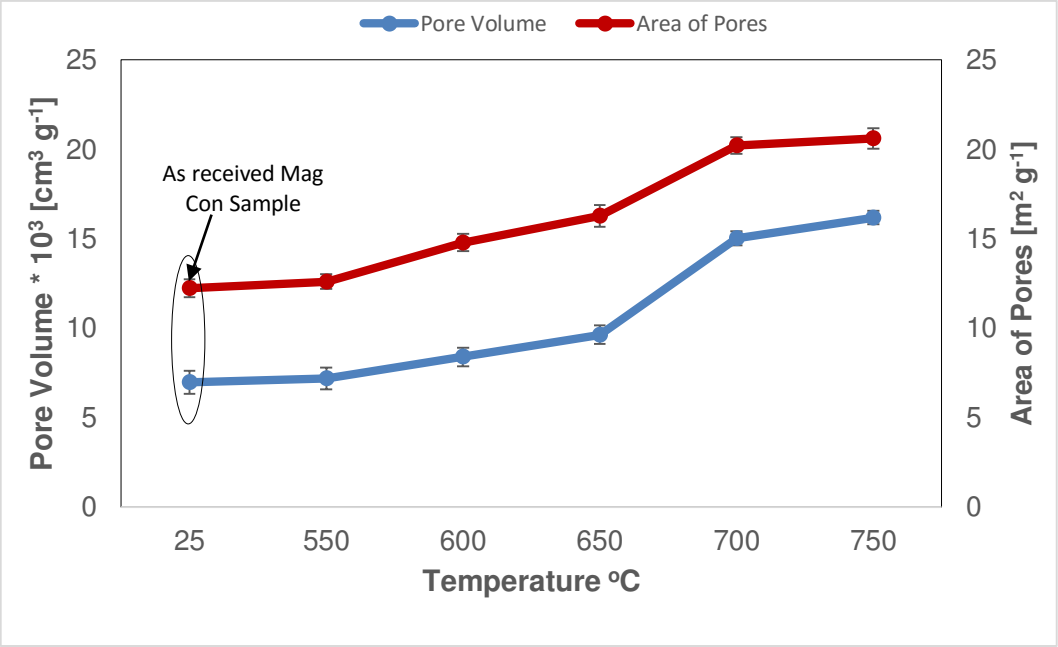

Figure 6.4 BET pore volume and pore area in in Mag Con calcines

Figure 6.5 below shows results of pore volume and pore area developed in the 650°C roast calcines at various O_2 enriched air percentages. It can be inferred that oxygen enrichment results in appreciable increase in both pore volume and pore area of the roast calcine with a 100% O_2 enrichment resulting in about 20% increase in pore area and a 40% increase in pore volume. The pore volumes were probably developed as a result of volume decreases during mineral transformation from maghemite to hematite [8].

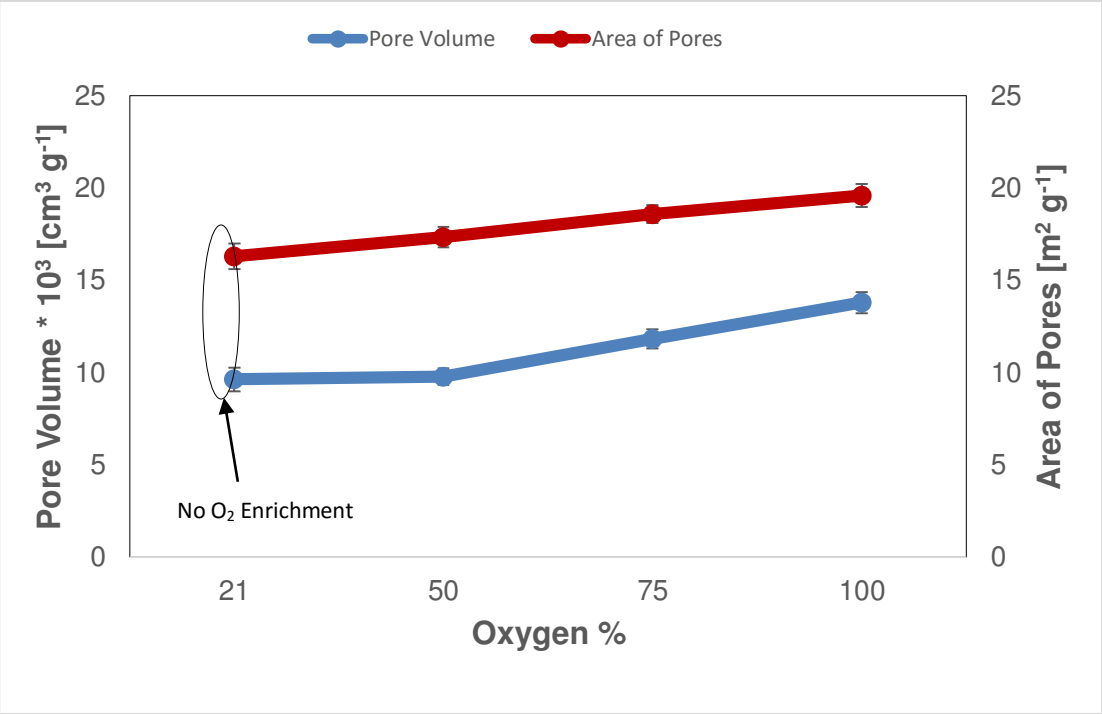

Figure 6.5 BET pore volume and pore area in 650°C Mag Con calcine in O_2 enriched air

6.4 Leaching Results

The BET and XRD results indicated that appreciable proportion of the non-porous maghemite in the Mag Con was transferred to porous hematite upon roasting the Mag Con at elevated temperatures. The roast calcines were therefore leached to assess if there was appreciable gold recovery following the indication of some maghemite to hematite conversion.

Gold recoveries from cyanide leaching of the Mag Con calcine (see Figure 6.6) indicates that at least 75% of gold can be recovered from the Mag Con upon roasting it at 550°C or above. The amount of gold recovered from the Mag Con increased with increasing roasting temperature with a maximum recovery of ~85% at 750°C. Above 550°C, there was a ~2% recovery increment at each temperature increase.

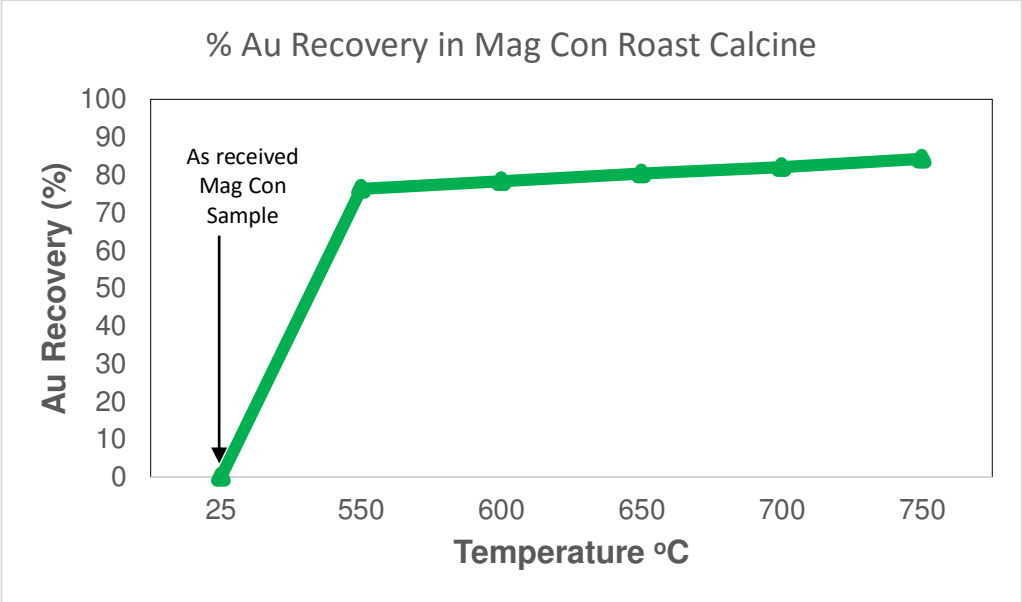

Figure 6.6 Gold recovery in Mag Con roast calcine

6.4.1 Effect of Organic Carbon and Sulfide Sulfur Burn on Gold Recovery

Several authors have submitted that the appreciable amount of organic carbon and sulfide sulfur remaining magnetic concentrates partly accounts for the poor gold extraction from the Mag Cons without any further pretreatment [2, 10, 17, 32, 42, 44]. The organic carbon pregrobbs dissolved gold during leaching thereby reducing the overall gold recovery. Efficiency of refractory ore roasting can therefore be tied to the extent at which the organic carbon and sulfide sulfur are oxidized [8].

As can be seen from Figure 6.7, the efficiency of total carbon oxidation in the Mag Con increases with increasing roasting temperature. Prior to roasting, the Mag Con had an organic carbon content of 0.73% but it can be inferred from Figure 6.7 that raising the roasting tempearture

above 600°C results in at least 50% of the organic carbon being oxidized; with complete carbon oxidation occuring at 750°C.

It can also be seen that gold recovery is enhanced as the organic carbon content is reduced. Maximum gold recovery occurred at a roasting temperature of 750°C where all the organic carbon in the Mag Con sample was burnt off.

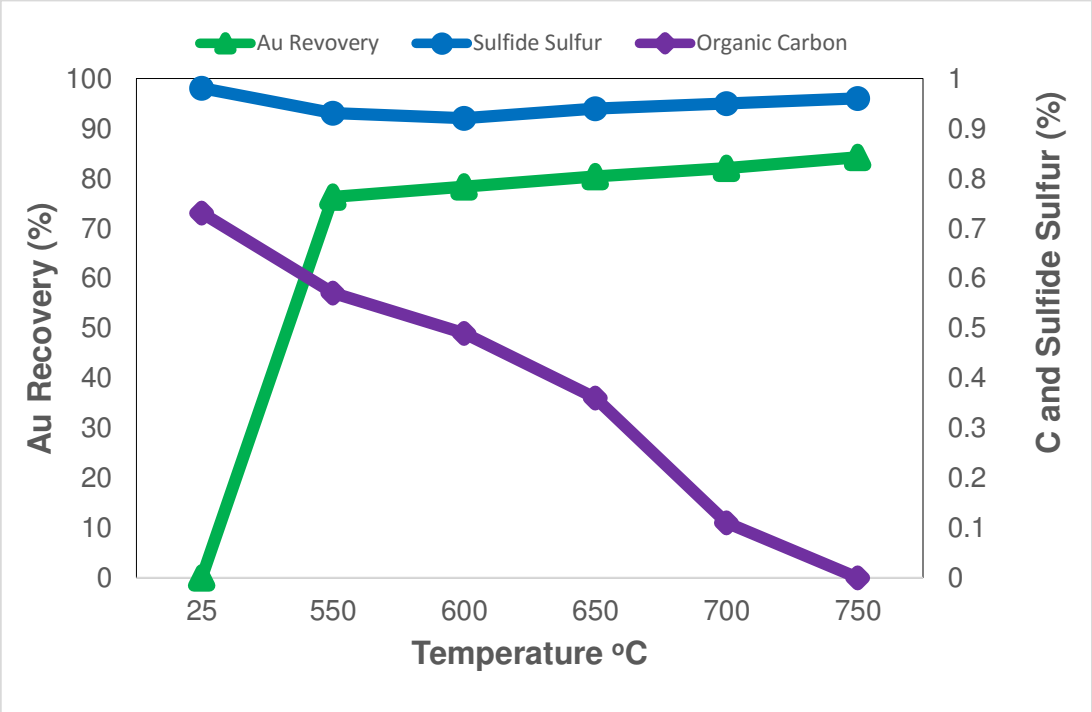

Figure 6.7 Effect of carbon and sulfur burning on gold recovery in Mag Con roast calcine

Also from Figure 6.7, it can be seen that increasing the roasting temperature resulted in further oxidation of the sulfur present in the Mag Con with the maximum, ~6%, occuring at 600°C. There seems to be a drop in the percentage of total sulfur burnt at roasting temperatures above 600°C. To further investigate the potential cause(s) for the poor oxidation of the remnant sulfide sulfur, sample of the Mag Con was ground finer and roasted longer. This has been presented in section 6.4.4.

6.4.2 Effect of Enhanced Calcine Pore Volume and Area on Gold Recovery

To further investigate whether or not enhanced calcine pore volume and pore area had an influence on gold recovery, the BET pore volumes and areas recorded in the calcines at each roast temperature has been juxtaposed on the leaching recoveries at the respective roast temperatures as can be seen on Figure 6.8 below.

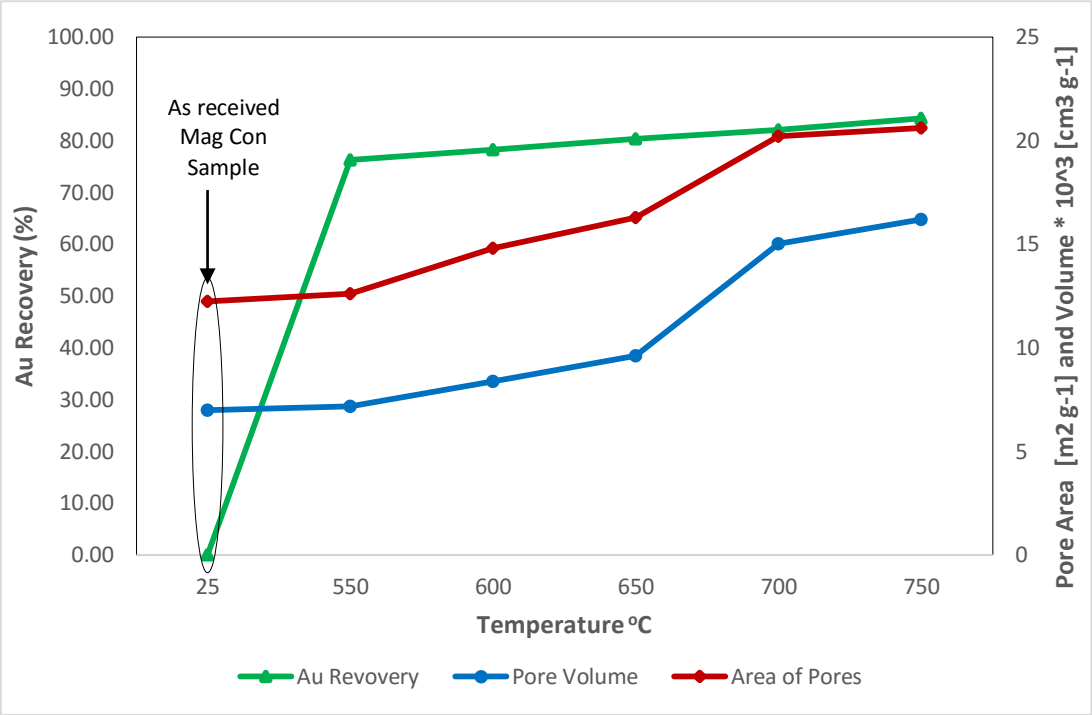

Figure 6.8 Effect of calcine pore volume and area on gold recovery from Mag Con roast calcine

From Figure 6.8, it can be seen that the roast calcines that had higher pore volumes resulted in higher gold recoveries.

6.4.3 Effect of Maghemite to Hematite Conversion on Gold Recovery

The Figure 6.9 below indicates the gold recoveries obtained at each roast temperature and the corresponding % hematite conversion at the respective temperatures. It can be seen that there

seems to be a correlation between the proportion of hematite to maghemite in the roast calcines and the resulting gold recovery obtained from leaching. This seems to confirm previous literature works that the higher the proportion of hematite to maghemite is in a roast calcine, the better the gold extraction by leaching. This is also partly because the 'dominant' hematite calcine is porous (see Figure 6.8) thus allowing effective contact of the cyanide-to-the 'exposed' gold in the calcine.

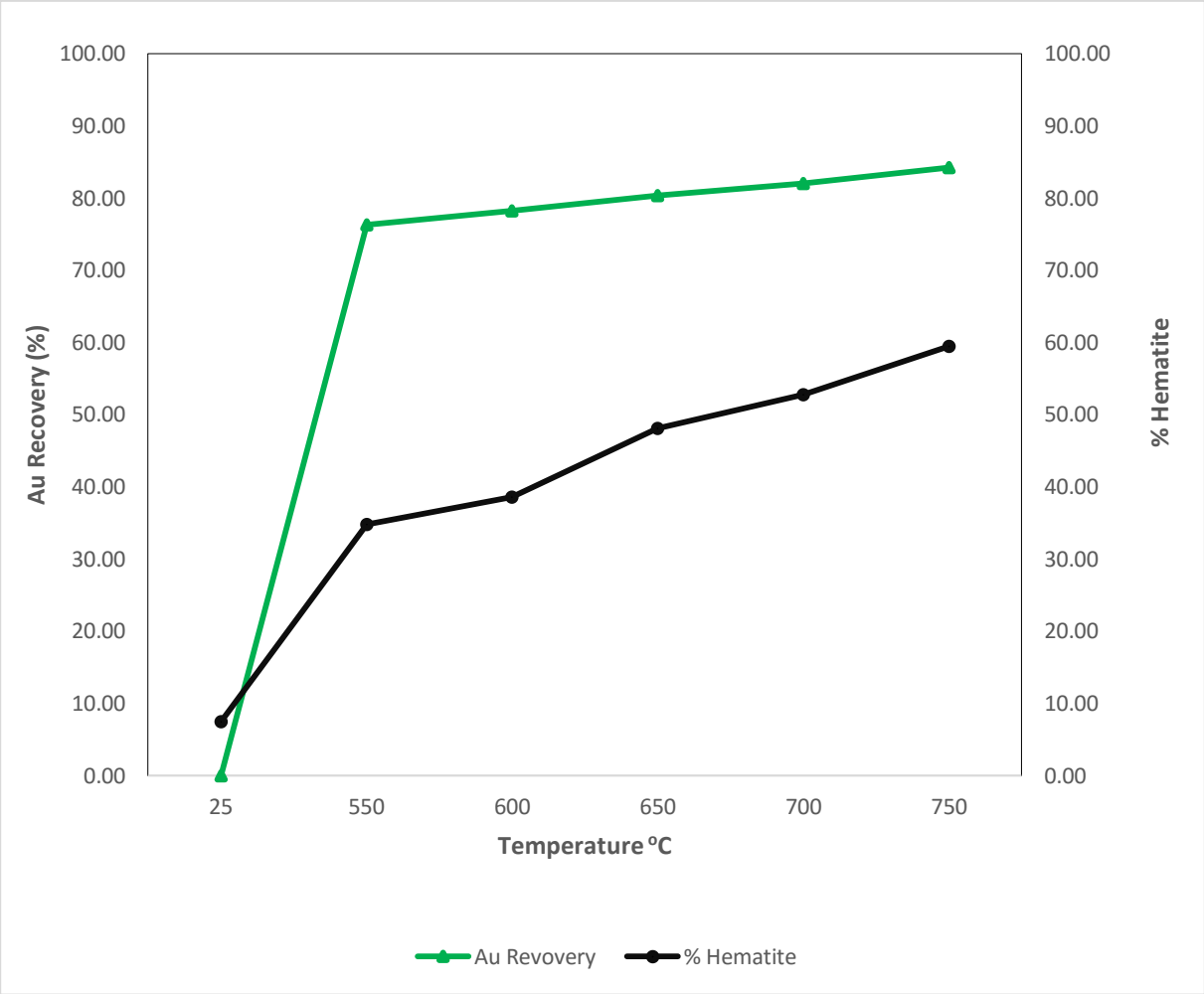

Figure 6.9 Effect of calcine hematite content on gold recovery from Mag Con roast calcine

In summary, both the roasting effect and the leaching effect are affected significantly by the roasting temperature. Under the conditions of up to 25 mins roasting time and ≥ 600°C roasting

temperature, about 80% of gold trapped in the dominantly maghemite magnetic concentrates can be recovered requiring no further size reduction of the magnetic concentrates.

The relatively high gold extractions at higher roasting temperatures is probably due to the success in oxidizing the remaining carbon in the magnetic concentrates. Oxidation of the sulfur and carbon in the maghemite probably led to the creation of microfractures in the resulting calcine thus opening up the pores and enhancing effective transfer of cyanide solution to the interior of the particles. This means that roasting the Mag Con resulted in transforming a majority of the maghemite into hematite and also opened up the pores in the resulting calcine thereby enhancing cyanide-to-gold contact.

6.5 Effect of Fine Grinding and Prolonged Roasting Time

To investigate whether fine grinding and extended roasting time could influence gold recovery from the magnetic concentrate, a sample of the Mag Con was further grounded to a P_{80} of 50 µm and roasting done at 30, 60 and 90 min. At a roasting temperature of 600°C, recoveries as well as arsenic contents in the roast calcines are shown in Figure 6.10.

It can be seen from Figure 6.9 that at each roasting time, there was a relatively appreciable increase in gold recovery from the 50 µm Mag Con calcines than in the 74 µm calcines. This is consistent with conclusions by several authors that fine grinding enhances gold recovery [2, 5, 10, 17, 24]. Even though fine grinding slightly increased gold recovery, prolonging the roasting time beyond 60 min does not really result in any appreciable increase in gold recovery. In essence, there was a reduction in gold recovery beyond roasting time of 60 min. This is probably due to sintering of the already opened pores thus consequently reducing cyanide-to-solution contact [10].

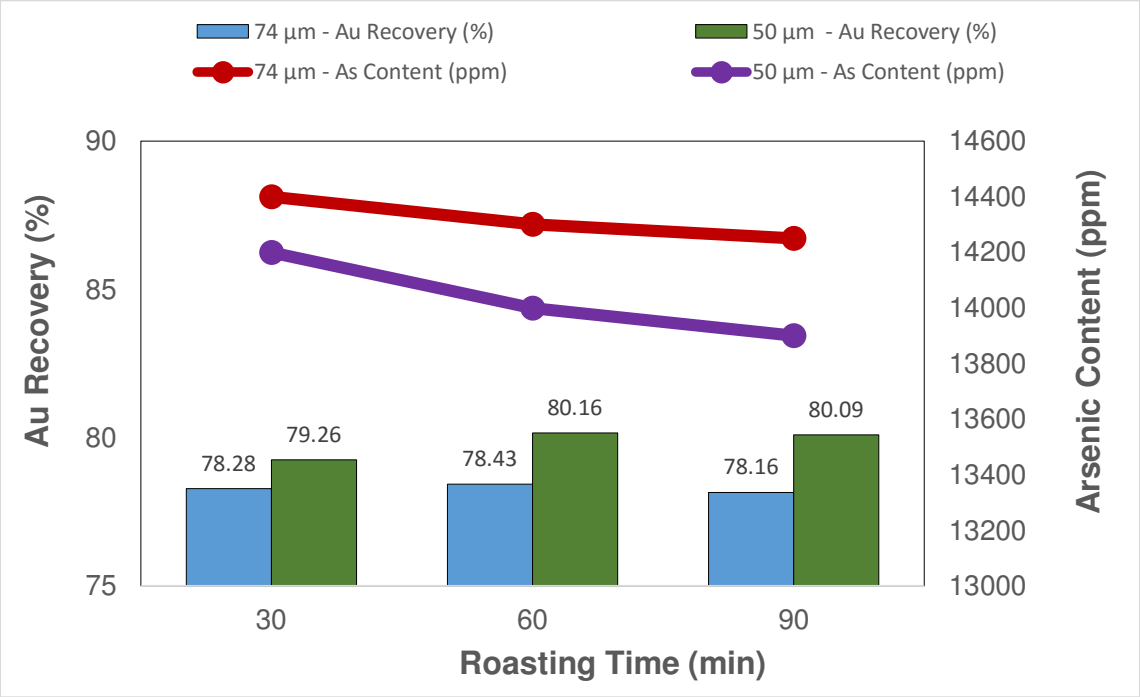

Figure 6.10 Effect of fine grinding and prolonged roasting on Au recovery and As content

Again, from Figure 6.9, it can be seen that for both the 74 µm and 50 µm samples, there is a slight increase in reduction of arsenic with roasting time. There was less arsenic in the finer Mag Con calcine (50 µm particles) than in the relatively coarser one, 74 µm particles. This is probably because fine grinding helps expose the arsenic bound maghemite and thus enhancing oxidation of As to As_2O_5 [8]. Aylmore and de Klerk [5] conducted mineralogical examinations on highly oxidised roasted samples and discovered that arsenic is locked at the magnetite-to-hematite transformation boundary where maghemite occurs.

Again, it can be seen from Figure 6.10 that gold recovery from each roast calcine slightly increased with lowering arsenic content in the calcine. This is probably explained by findings from Paktunc et al [8] that the nonporous fields within iron oxide particles represent maghemite and are enriched in As. They concluded that hematite compositions are characterized by low As totals

owing to the highly porous nature of the hematite bands. Arsenic levels are generally low in hematite than in maghemite. The extra reduction in arsenic content at prolonged roasting times therefore indicates a further conversion of maghemite to hematite.

Again, the effect of fine grinding and prolonged roasting time on residual organic carbon in the calcine and how that impacts gold recovery has been shown on Figure 6.11. It can be seen that grinding the Mag Con further from 74 µm to 50 µm only slightly enhances the oxidation of carbon during roasting with a ~9% increase in carbon oxidation from a roasting time of 30 min to 60 min. However, prolonging the roasting time from 30 min to 60 min resulted in a ~4% increase in carbon oxidation in the 74 µm particles. The slight increments in carbon oxidation that were recorded were too little and so it can be concluded that grinding the Mag Con finer and roasting it longer does not result in any appreciable increase in organic carbon reduction.

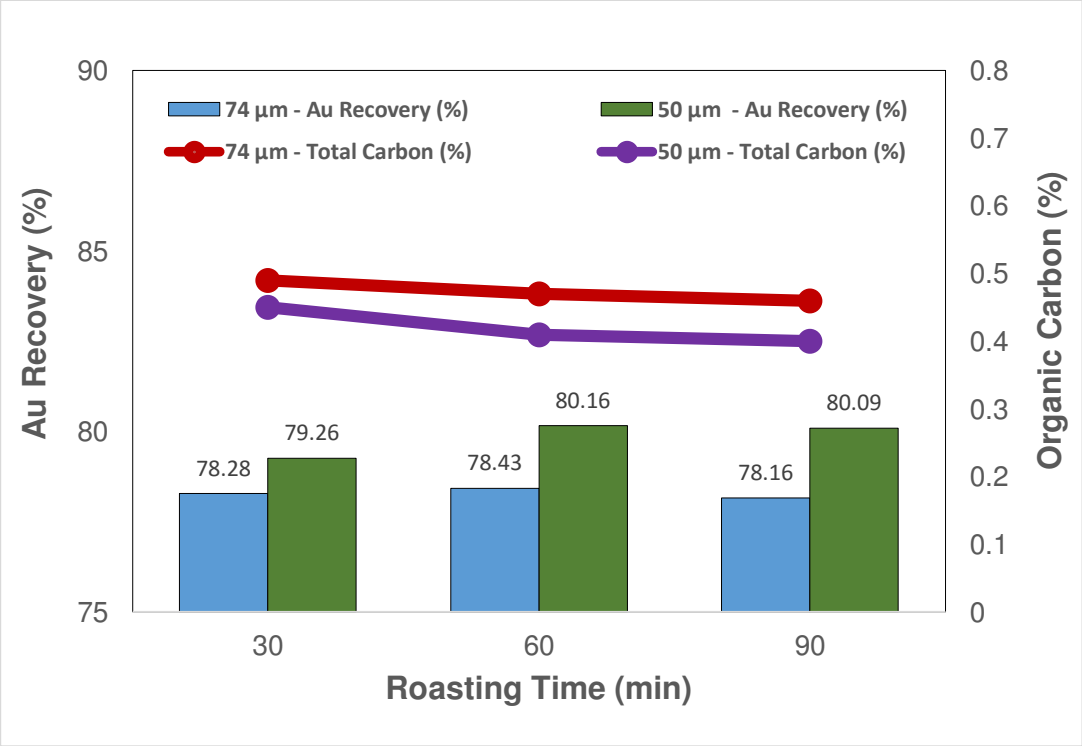

Figure 6.11 Effect of fine grinding and prolonged roasting on Au recovery and total carbon content

As can be seen from Figure 6.11, gold recovery is influenced by the amount of organic carbon in the calcine. The carbon preg-robbs the leached gold thereby reducing the free gold in solution and consequently reducing the gold recovery [2, 17]. Prolonging the roasting time beyond 60 min does not result in any appreciable oxidation of the organic carbon.

Figure 6.12 below illustrates the sulfide sulfur contained in both the relatively coarse (P_{80} of 74 µm) and fine (P_{80} of 50 µm) at the various roasting times at 600^{o}C. It can be seen that in the 74 µm particles, only a slight reduction of sulfur was recorded from the 30 min roast calcine beyond which there was no notable decrease in sulfur reduction. The results for the 50 µm were no different. In all cases, neither fine grinding nor prolonged roasting resulted in appreciable reduction of sulfur.

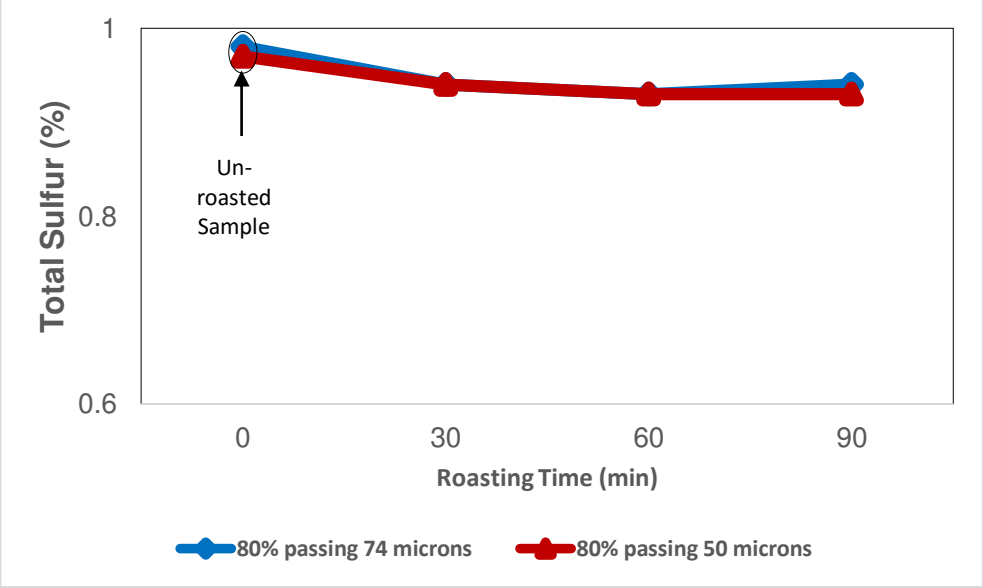

Figure 6.12 Effect of fine grinding and prolonged roasting on sulfur burning

The pronounced effect of prolonged roasting time and temperature on gold recovery is shown on Figure 6.13 below. It can be seen from Figure 6.13 below that prolonged roasting did not result in any appreciable increase in Au recovery.

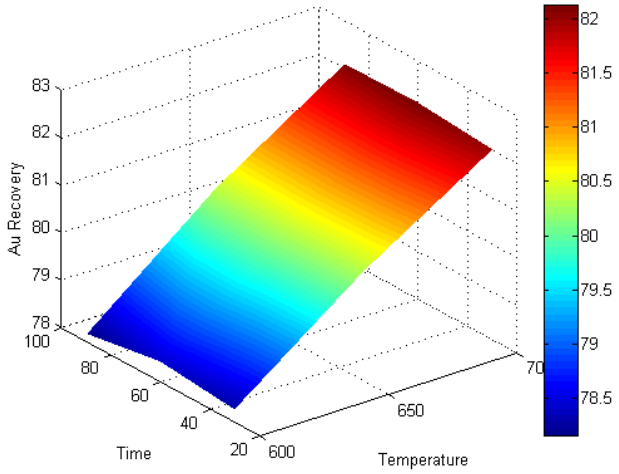

Figure 6.13 A 3D plot showing the effect of temperature and prolonged roasting time on Au recovery

In essence, fine grinding and prolonged roasting of the Mag Con sample did not result in any appreciable reduction in organic carbon and sulfide sulfur. Rather, the arsenic content was only slightly decreased as a result of grinding the Mag Con fine and roasting it longer. The virtually no reduction in organic carbon and sulfide sulfur in the Mag Con even after fine grinding and prolonged roasting could be due to the following reasons;

Even though about 80% of the gold in the Mag Con was recovered upon roasting at 600^{o}C, there still seems to be up to about 40% of unconverted maghemite present in the calcine. This maghemite component is rich is arsenic and could trap the organic carbon and sulfide sulfur within the calcine. The organic carbon and sulfide sulfur are probably not exposed for oxidation as they may be trapped within the maghemite.

It may also be that the roasting temperatures were not high enough to completely decompose components such as dolomite and kaolinite and other impurities in the Mag Con. The carbonates from the partial decomposition of dolomite, $CaMg(CO_3)_2$ may have been the source of the carbon still present in the calcine.

CHAPTER 7

CONCLUSIONS

X-ray Diffraction and BET measurement results indicated that appreciable proportion of the non-porous maghemite in the Mag Con was converted to porous hematite upon roasting the Mag Con at elevated temperatures. Roasting at temperatures up to 500°C does not yield any appreciable hematite conversion. The no reaction at lower temperatures was because the Mag Con sample is already a roast calcine, having been roasted to temperatures around 500°C, thus making roasting at or below 500°C redundant. However, the conversion of maghemite to hematite occurs when the Mag Con is roasted at higher temperatures, with a 35% conversion occuring at 550°C. The conversion of maghemite to hematite in the Mag Con increases with increasing temperature with at least 50% conversion at 650°C and a maximum conversion of ~70% occuring at 750°C.

Oxygen enrichment of the roast air at various temperatures was explored. Enriching the air for roasting the Mag Con sample with oxygen, even up to 100%, does not result in any appreciable hematite conversion beyond that obtained by roasting with normal air. In essence, at very high temperatures, above 700°C, high O_2 content in the air for roasting actually slightly hinders the conversion of maghemite to hematite. Oxygen enrichment therefore has no correlation with, and does not enhance maghemite to hematite conversion in Mag Con by roasting.

Cyanide leaching of the Mag Con roast calcines have shown that at least 75% of the gold can be recovered upon roasting at 550°C or above. The amount of gold recovered from the Mag Con increased with increasing roasting temperature with a maximum recovery of ~85% at 750°C. Above 550°C, there was a ~2% recovery increment at each temperature increase. LECO analysis showed that raising the roasting tempearture above 600°C results in at least 50% of the total carbon being oxidized; with complete carbon oxidation occuring at 750°C.

To explore the possibility of having a complete oxidation of the organic carbon, sulfide sulfur and arsenic in the Mag Con at a relatively lower roasting temperature, 600°C, prolonged roasting was done. The arsenic, carbon and sulfur content in the calcine only slightly reduced up to a roasting time of 60 min beyond which there was no appreciable reduction in their levels. In essence, prolonged roasting did not result in any appreciable reduction of the organic carbon and sulfide sulfur in the Mag Con. Leaching results showed that extending the roasting time beyond 60 min actually resulted in a somewhat reduced gold recovery. This is probably due to sintering of the calcine thus closing up the already opened pores and consequently reducing cyanide-to-solution contact.

The effect of fine grinding on overall gold recovery from the Mag Con was also briefly looked into. At the tested roasting temperature of 600°C, grinding the Mag Con further from a P_{80} of 74 µm to a P_{80} of 50 µm resulted only a minimal reduction in the As and organic carbon contents in the resulting Mag Con calcine; though a 1.25% increase in gold recovery was realized. In essence, grinding the Mag Con finer and roasting it longer does not result in any appreciable gain. The 1.25% gain in recovery by grinding finer from 74 µm to 50 µm may not justify the cost that may be incurred by the required fine grinding.

The seemingly no-reduction in arsenic, organic carbon and sulfide sulfur levels in the magnetic concentrate roast calcines is probably due to;

- Significant proportions of maghemite (up to 40% - relative to hematite) still present in the roast calcines. This unconverted maghemite provides a hotspot for arsenic [8].
- The presence of gangues such as dolomite in the calcine suggesting that entrapped organic matter and sulfide sulfur may not have been liberated and thus unavailable for oxidation.
- Possible sintering in the calcine – though BET results seem to suggest otherwise.

CHAPTER 8

SUGGESTIONS FOR FUTURE WORK

It is highly recommended that upon roasting of the maghemite-rich magnetic concentrates, a second stage magnetic separation be performed on the calcine to concentrate the remnant maghemite portions into magnetic concentrates and the dominant hematite portion into magnetic tails. The resulting magnetic tails will be mainly hematite and so leaching may result in a better gold recovery.

Future work should focus on roasting the magnetic concentrate in a continuous fluidized bed reactor for a detailed evaluation of the viability and feasibility of recovering gold from the maghemite-rich magnetic concentrates. This may produce a more reliable prediction of the conditions required for operation, provide some suggested changes for the operation, and/or provide some guidance for equipment changes to improve overall gold extraction.

Fine grinding of the magnetic concentrates to a P_{80} of 50 µm showed evidence of increased gold recoveries, though minimal, at a relatively low roasting temperatures. If the magnetic concentrates was ground even finer, perhaps the gold recovery could be greatly improved at a much reduced roasting temperatures ($\leq$ 600°C). Future work should thoroughly investigate the effect of fine grinding on gold recovery from magnetic concentrates.

Even though oxygen enrichment of the roast air suggested there was appreciably no improvement in gold recovery, the limitations on the Bacharach Oxor® III Oxygen meter probably

did not provide a good account of tracking oxygen consumption in the roast set-up. The meter had a maximum capacity of reading O_2 concentrations up to 20%. It was therefore difficult to track oxygen consumption during roasting at higher O_2 enriched ratios. For a better evaluation of the effect of oxygen enrichment on roasting of magnetic concentrates, a high capacity and more robust oxygen meter will be required.

Arsenic results from the roast products showed that the calcines had about 1.2% of As even after roasting at prolonged roasting times and at 600ºC. The residual arsenic content in the roast products suggests that arsenic rims were formed in the calcines which occluded the gold thus leading to the relatively low gold recoveries. Running a Back-Scattered Electron (BSE) microscopy test on the calcines will help in further investigating whether arsenic rims are formed or not.

It is recommended that further mineralogical studies be conducted on the magnetic concentrate calcines to better understand why the residual organic carbon and sulfide sulfur do not seem to be liberated.

Even though roasting has proven to be a technically feasible means of recovering gold from the maghemite-rich magnetic concentrates, it is highly recommended that a detailed economic analysis be conducted to assess the viability of this process before applying it on a large scale.

A process flowsheet is hereby proposed for consideration in Figures 8.1.

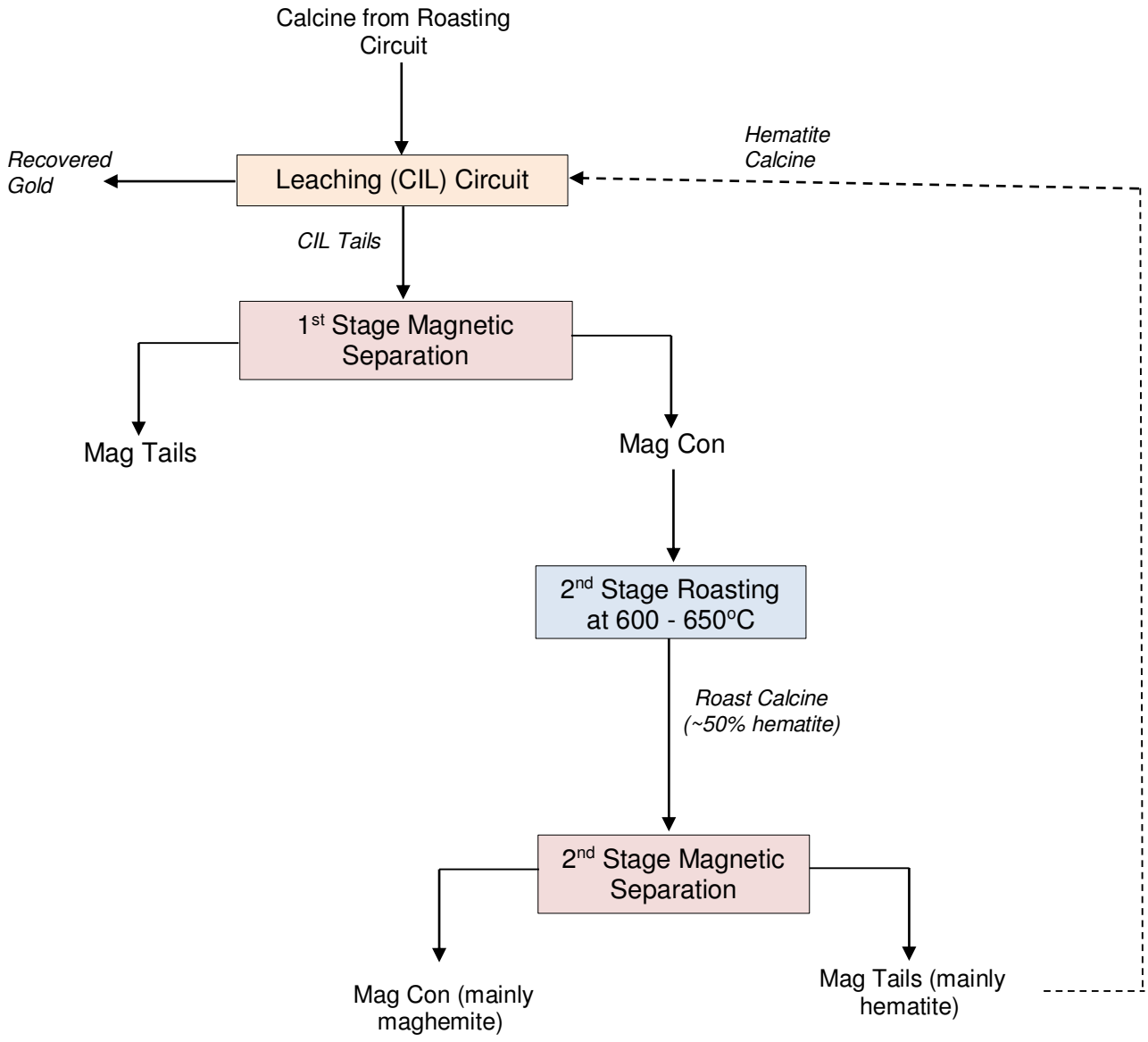

Figure 8.1 Proposed flowsheet for future work

CITED REFERENCES

[1] A. Taylor, “Developments in the Processing of Refractory & Complex Gold Ores," at *AusIMM Bendigo Technical Meeting,* August 2013.

[2] J. Marsden and I. House, “The Chemistry of Gold Extraction,” *Society for Mining, Metallurgy and Exploration,* 2nd ed. Littleton, CO, 2006, pp. 147-285.

[3] R. K. Amankwah, W. T. Yen, and J. A. Ramsay, “A Two-Stage Bacterial Pretreatment Process for Double Refractory Gold Ores,” *Minerals Engineering,* vol. 18, no. 1, 2005, pp. 103–108.

[4] P. R. Taylor, Z. Yin, S. L. Bell, and R. W. Bartlett, “Lime Roasting of Pyrite,” *Gold 90*, Society for Mining, Metallurgy and Exploration, Llttleton. CO, pp. 411-419.

[5] C. Paper and M. G. Aylmore, “Conditions and Design Considerations for Maximising Recoverable Gold in Roasting of Refractory Gold Ores,” *World Gold Conference*, Brisbane, Qld, 26 - 29 September 2013.

[6] P. M. Afenya, “Treatment of Carbonaceous Refractory Gold Ores,” *Minerals Engineering,* vol. 4, nos. 7–11, 1991, pp. 1043–1055.

[7] K. S. Fraser, R. H. Walton, and J. A. Wells, “Processing of Refractory Gold Ores,” *Minerals Engineering*, vol. 4, nos. 7–11, 1991, pp. 1029–1041.

[8] D. Paktunc, D. Kingston, A. Pratt, and J. McMullen, “Distribution of Gold in Pyrite and in Products of its Transformation Resulting from Roasting of Refractory Gold Ore,” *The Canadian Mineralogist,* vol. 44, no. 1, 2006, pp. 213–227.

[9] J. Hammerschmidt, J. Güntner, and B. Kerstiens, “Roasting of Gold Ore in the Circulating Fluidized-Bed Technology,” *Developments in Mineral Processing.*, vol. 15, No. 05, 2005, pp. 433–453.

[10] W. Douglas and L. Semenyna, “Magnetic Recovery of Gold-Bearing Iron Oxides at Barrick Goldstrike’s Roaster,” *World Gold Conference,* Brisbane, Qld, 26 - 29 September 2013, pp. 79-85.

[11] M. F. Hochella, B. M. Bakken and A. F. Marshall, “Transmission Electron Microscopy (Tem) of Partially Oxidized Gold Ore, Carlin Mine, Nevada,” pp. 153–155.

[12] K. G. Thomas and A. P. Cole, “Roasting Developments - Especially Oxygenated Roasting,” *Developments in Mineral Processing.*, vol. 15, no. 05, 2005, pp. 403–432.

[13] G. Mudd, D. Giurco, S. Mohr, and L. Mason, “Gold Resources and Production: Australia in a Global Context”, Cluster Research Report No. 1.11, October. 2012.

[14] R. S. Jones, “Gold in Meteorites and in the Earth’s Crust,” *Geological Survey Circular 603*, 1968, pp. 1–4.

[15] M. Neuvonen, “Pretreatment Processes in Gold Recovery By Thiosulphate Leaching,” *Masters Thesis Report,* Lappeenranta University of Technology, 2013, 62 pp.

[16] J. Robinson, "The Extraction of Gold from Sulphidic Concentrates by Roasting and Cyanidation," *Journal of the South African Institute of Mining and Metallurgy*, vol. 88, No. 4, pp. 1988, 117–130.

[17] S. R. La Brooy, H. G. Linge, and G. S. Walker, "Review of Gold Extraction from Ores," *Minerals Engineering.*, vol. 7, no. 10, 1994, pp. 1213–1241.

[18] B. Nanthakumar, C. A. Pickles, and S. Kelebek, "Microwave pretreatment of a double refractory gold ore," *Minerals Engineering*, vol. 20, no. 11, 2007, pp. 1109–1119.

[19] A. Charitos, M. Runkel, J. Güntner, A. Holmström, and J. Hammerschmidt, "Roasting – A Study on Environmental Aspects, Off-Gas, Effluents and Residue Treatment," *World Gold Conference*, Brisbane, Qld, 26 - 29 September 2013, pp. 26–29.

[20] N. Iglesias and F. Carranza, "Refractory Gold-Bearing Ores: A Review of Treatment Methods and Recent Advances in Biotechnological Techniques," *Hydrometallurgy*, vol. 34, no. 3, 1994, pp. 383–395.

[21] P. R. Taylor and Z. Yin, "Soda Ash Roasting of As-Sb-Precious Metal Concentrates," *Minerals and Metallurgical Processing*, November 1993, pp. 163-169.

[22] H. Yang, Q. Liu, X. Song, and J. Dong, "Research Status of Carbonaceous Matter in Carbonaceous Gold Ores and Bio-Oxidation Pretreatment," *Transactions of Nonferrous Metal Society of China*, vol. 23, no. 11, 2013, pp. 3405–3411.

[23] A. Barnes and N. Stubina "Roasting Renaissance-Triple Refractory Ores" *World Gold 2011*, Montreal, October 2011, 28 pp.

[24] S. Ellis, "Ultra Fine Grinding - A Practical Alternative to Oxidative Treatment of Refractory Gold Ores," 2001, 21 pp.

[25] J. R. Flatt and R. Woods, "Oxidation of Pyrite in Nitric Acid Solutions: Relation to Treatment of Refractory Gold Ores," 1995, pp. 852–856.

[26] M. Adams "Comparison of the MMS CN-D^{TM} Cyanide Destruction Process With Caro's Acid , SMBS/Air and Hydrogen Peroxide Options," pp. 1–7.

[27] C. Komnitsas and F. D. Pooley, "Mineralogical Characteristics and Treatment of Refractory Gold Ores," *Minerals Engineering*, vol. 2, no. 4, 1989, pp. 449–457.

[28] Z. Cui, Q. Liu, and T. H. Etsell, "Magnetic Properties Of Ilmenite, Hematite and Oilsand Minerals after Roasting," *Minerals Engineering*, vol. 15, 2002, pp. 1121–1129.

[29] P. J. Cleyle, W. F. Caley, L. Stewart, and S. G. Whiteway, "Decomposition of Pyrite and Trapping of Sulphur in a Coal Matrix During Pyrolysis of Coal," *Fuel*, vol. 63, no. 11, 1984, pp. 1579–1582.

[30] A. R. Maycock, W. Nahas and T.C. Watson "Review of the Design and Operation of Roasters for Refractory Gold Bearing Materials," *Gold '90*, vol. 12, 2007, pp. 45–53.

[31] M. Runkel and P. Sturm, "Pyrite Roasting, an Alternative to Sulphur Burning," *Journal of the South African Institute of Mining and Metallurgy*, vol. 109, no. 8, 2009, pp. 491–496.

[32] J. R. Goode, "Refractory Gold Ore Causes Processes, Testing and Plants," *Society for*

Mining, Metallurgy and Exploration, vol. 5002, no. 800, 1993, 22 pp.

[33] M. Brittan, "Oxygen Roasting of Refractory Gold Ores," *Minerals Engineering*, vol. 47, no. 2, 1995, pp. 145–148.

[34] M. Heydenrych, "Modelling of Rotary Kilns," 2001, 123 pp.

[35] K. Carina, "Metallurgical Furnaces," 1965, 46 pp.

[36] R. R. Fernandez, A. Collins, and E. Marczak, "Gold Recovery from High-Arsenic-Containing Ores at Newmont's Roasters," *Minerals & Metallurgical Processing*, vol. 27, no. 2, 2010, pp. 60–64.

[37] E. Franziska, "Precision Measurement of the Specific Surface Area of Solids by Gas Adsorption," vol. 1, no. 3, 2014, pp. 3–5.

[38] S. A. Speakman, "Introduction to X-Ray Powder Diffraction Data Analysis," 22 pp.

[39] P. M. Eduafo, "Experimental Investigation of Recycling Rare Earth Elements From Waste Fluorescent Lamp Phosphors," *Masters Thesis Report*, Colorado School of Mines, 2013, 95 pp.

[40] G. Klingelhöfer, R. V. Morris, P. A. de Souza, and B. Bernhardt, "The Miniaturized Mössbauer Spectrometer MIMOS II of the Athena Payload For The 2003 MER Missions," *Sixth International Conference on Mars*, vol. 5, 2003, pp. 3–5.

[41] E. Tronc, J. P. Jolivet, and J. Livage, "Mossbauer Investigation of the $\gamma \rightarrow \alpha$-$Fe_2O_3$ Transformation in Small Particles," *Hyperfine Interactions*, vol. 54, 1990, pp. 737–740.

[42] L. Bailong, Z. Zhaohui, L. Linbo, and W. Yujie, "Recovery of Gold and Iron from the Cyanide Tailings by Magnetic Roasting," *Rare Metal Materials and Engineering*, vol. 42, no. 9, 2013, pp. 1805–1809.

[43] D. T. Pierce, D. R. Coughlin, D. L. Williamson, K. D. Clarke, A. J. Clarke, and J. G. Speer, "Characterization of Transition Carbides in Quench and Partitioned Steel Microstructures by Mössbauer Spectroscopy and Complementary Techniques," *Acta Materialia.*, vol. 90, 2015, pp. 1–14.

[44] I. Alp, O. Celep, D. Paktunç, and Y. Thibault, "Influence of Potassium Hydroxide Pretreatment on the Extraction Of Gold And Silver From A Refractory Ore," *Hydrometallurgy*, vol. 146, 2005, pp. 64–71.

APPENDIX A

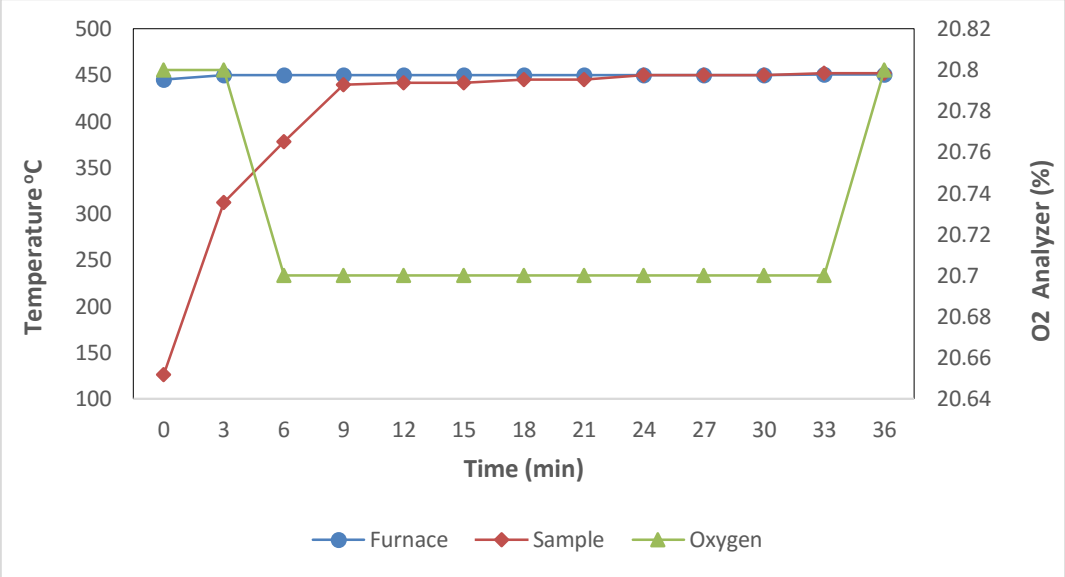

Figure A.1 Roast temperature and oxygen plot for pure maghemite at 450°C

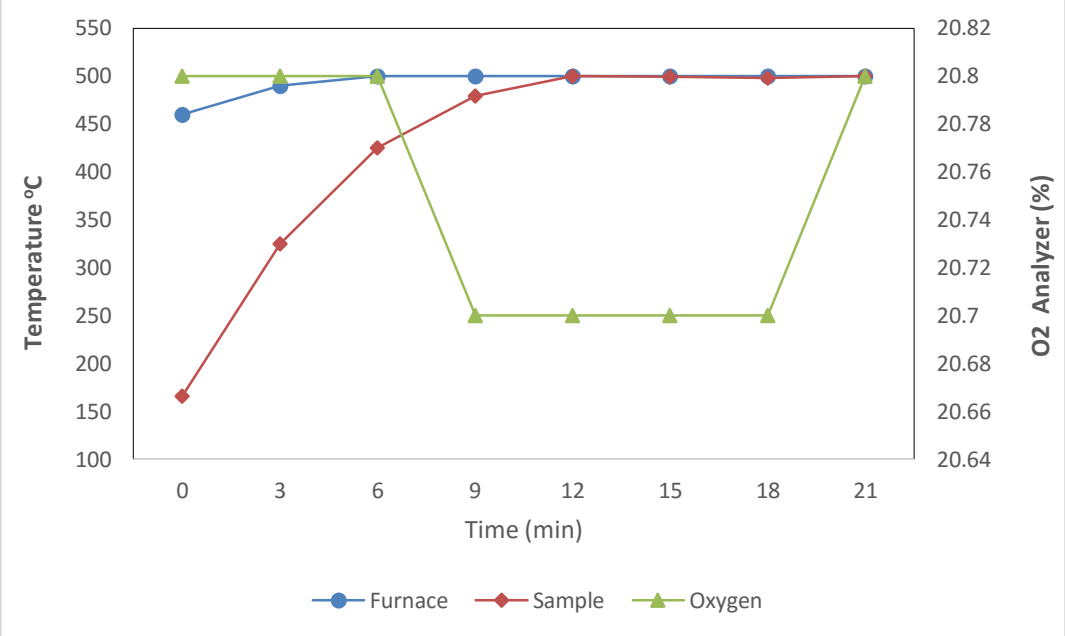

Figure A.2 Roast temperature and oxygen plot for pure maghemite at 500°C

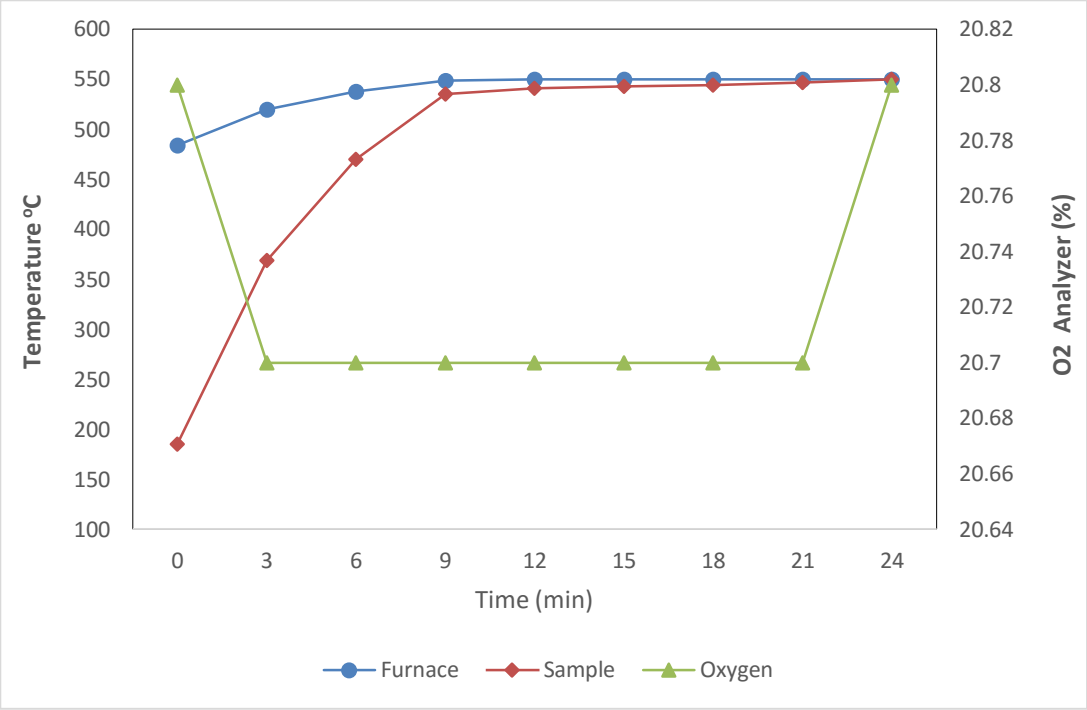

Figure A.3 Roast temperature and oxygen plot for pure maghemite at 550°C

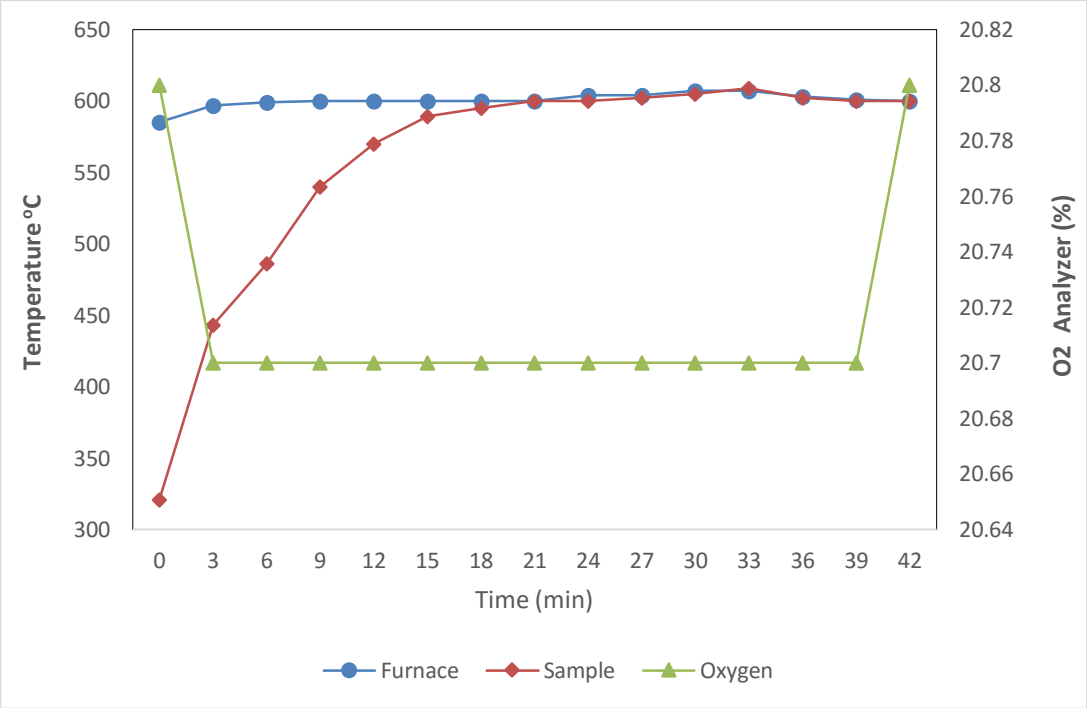

Figure A.4 Roast temperature and oxygen plot for pure maghemite at 600°C

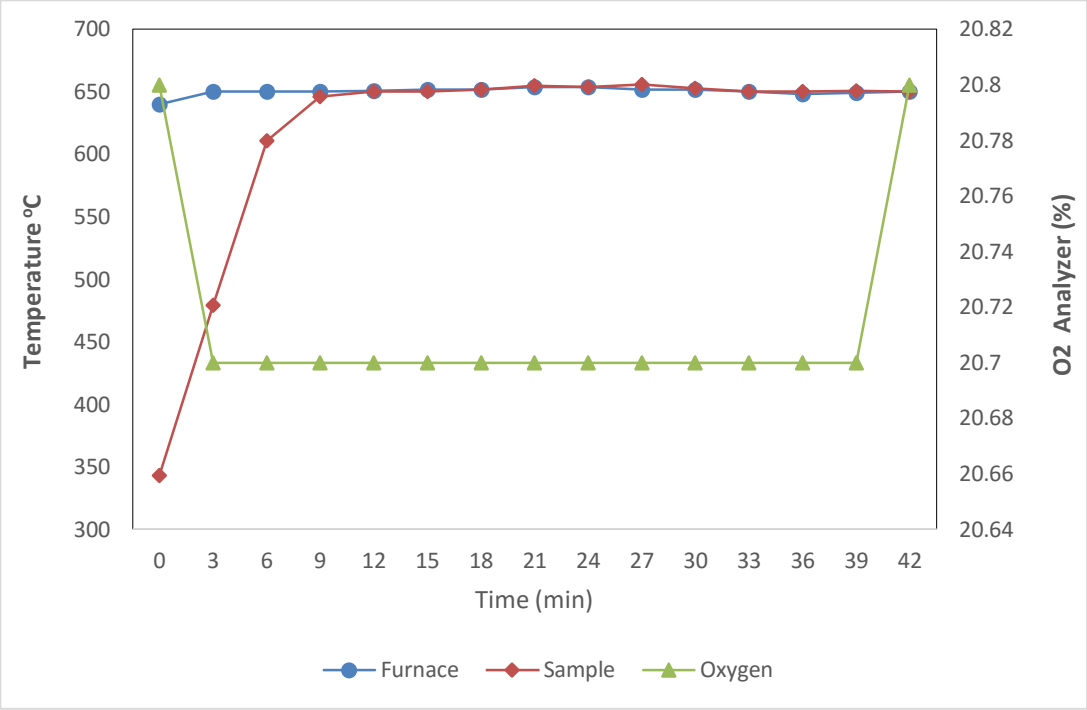

Figure A.5 Roast temperature and oxygen plot for pure maghemite at 650°C

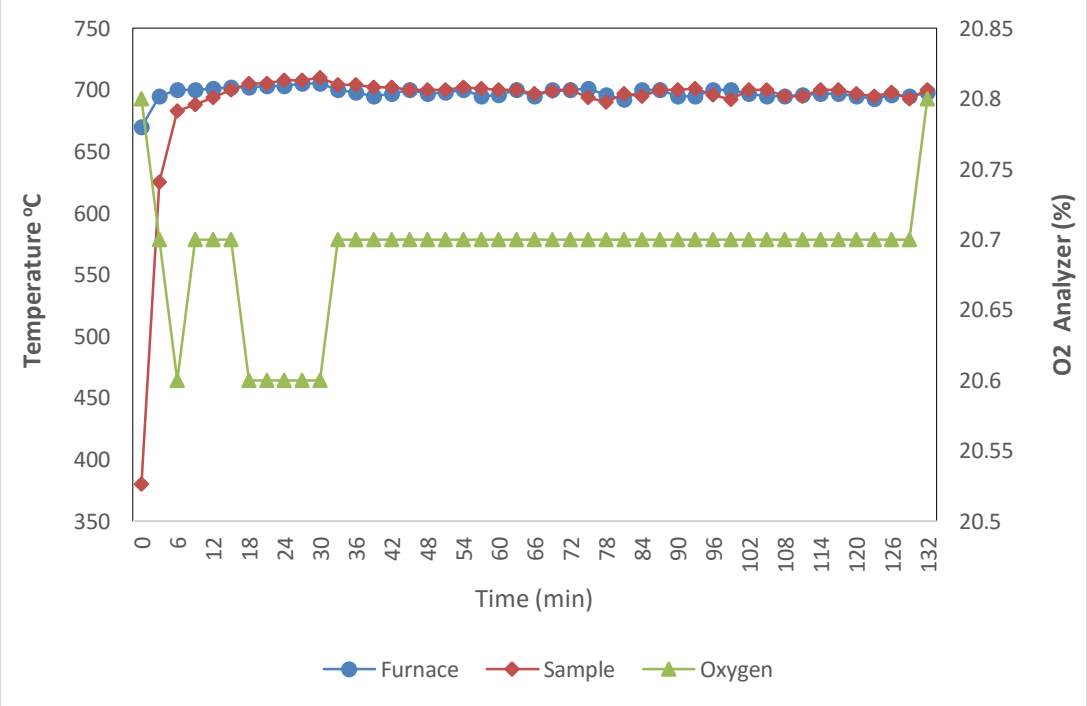

Figure A.6 Roast temperature and oxygen plot for pure maghemite at 700°C

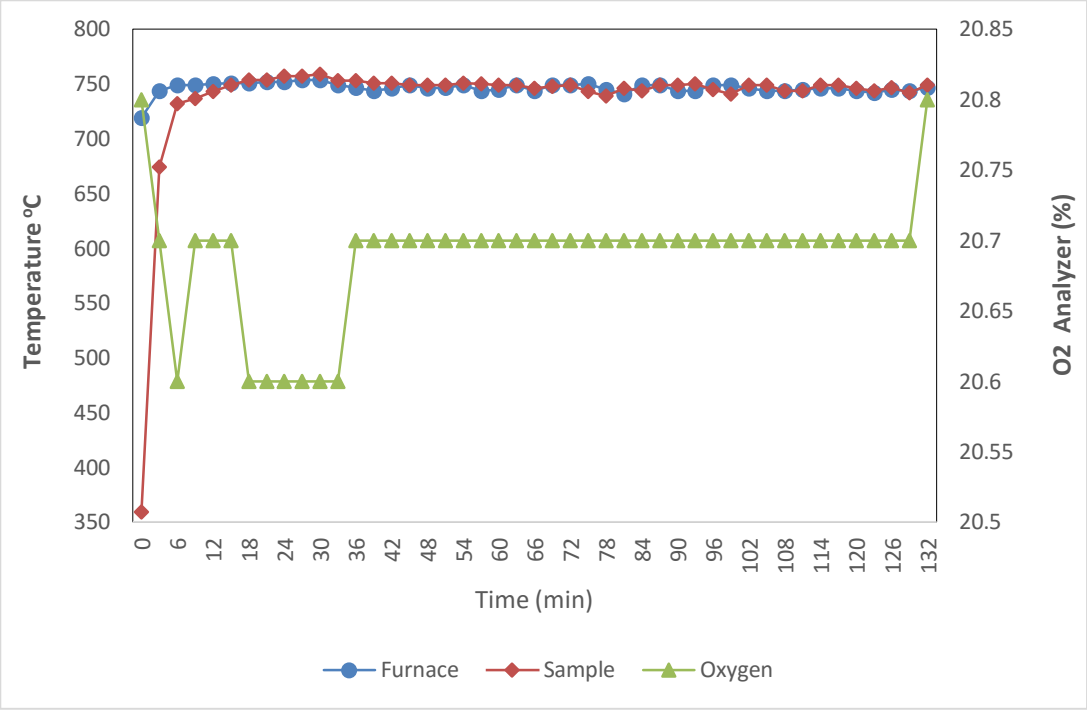

Figure A.7 Roast temperature and oxygen plot for pure maghemite at 750°C

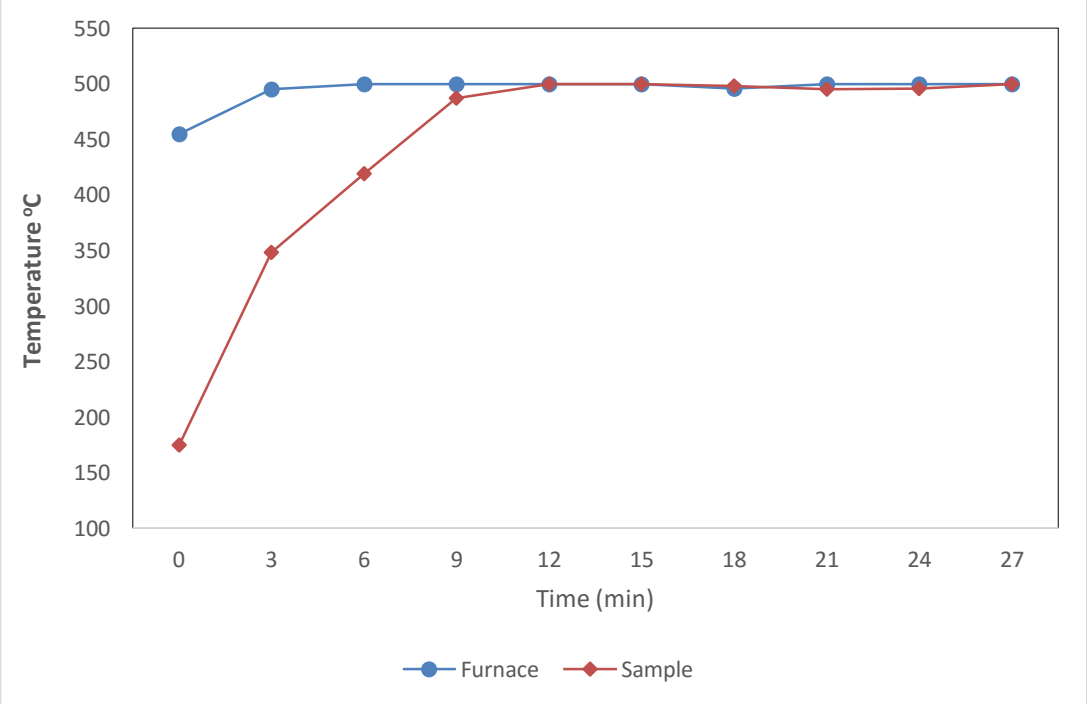

Figure A.8 Roast temperature plot for pure maghemite at 500°C and 50% O_2

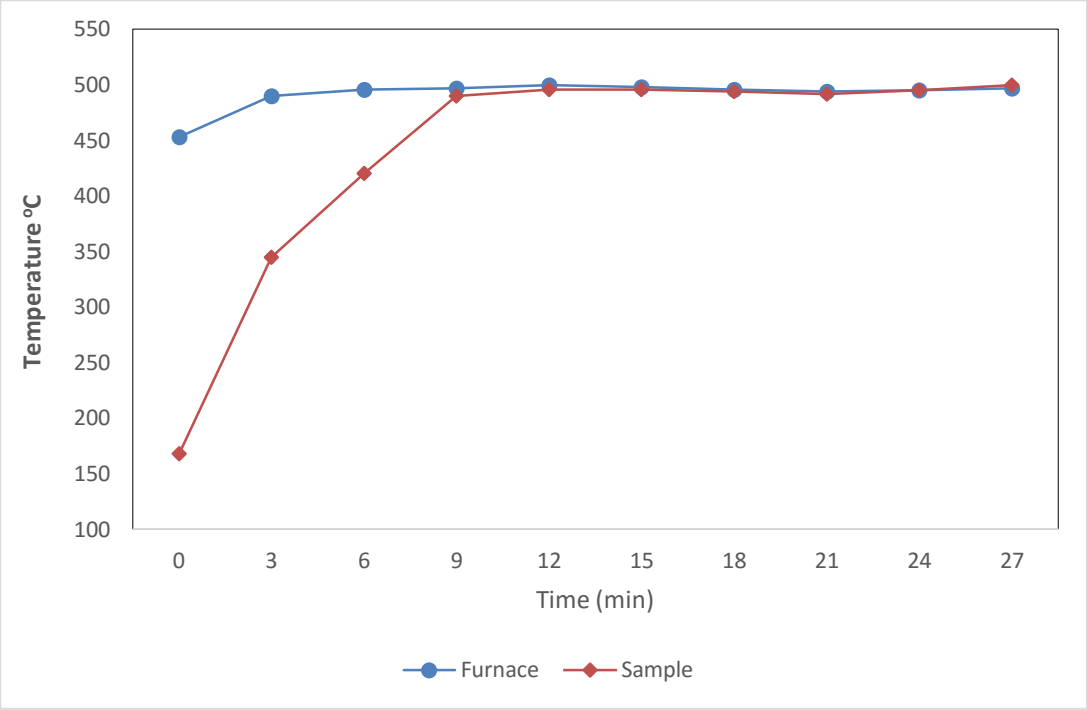

Figure A.9 Roast temperature plot for pure maghemite at 500°C and 75% O_2

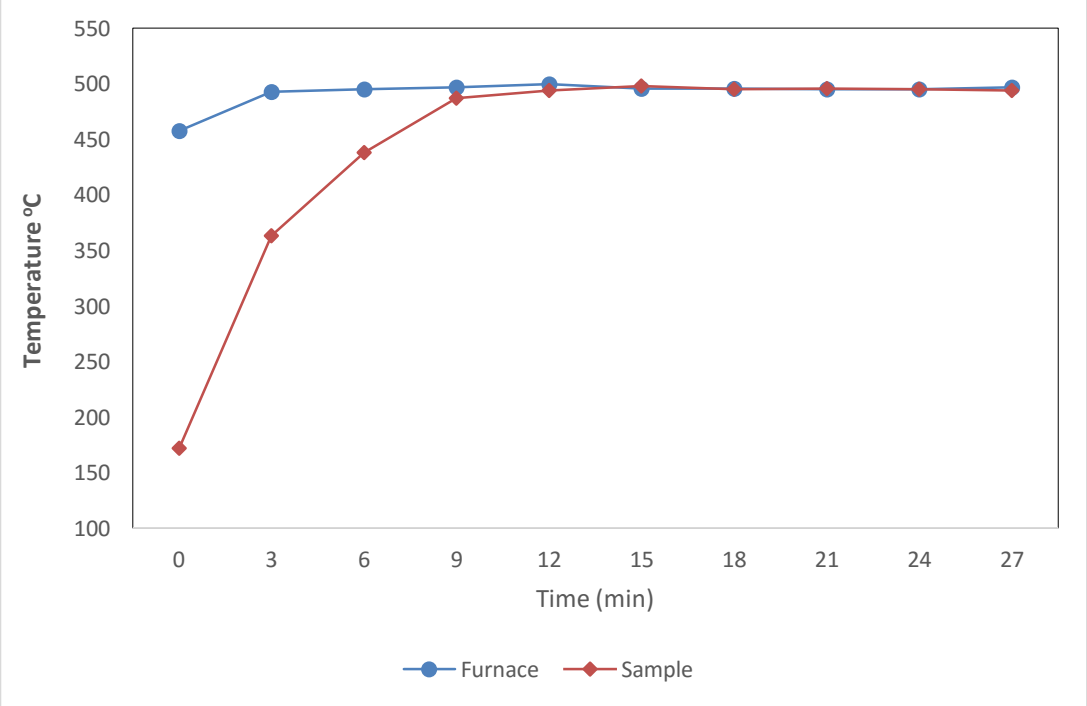

Figure A.10 Roast temperature plot for pure maghemite at 500°C and 100% O_2

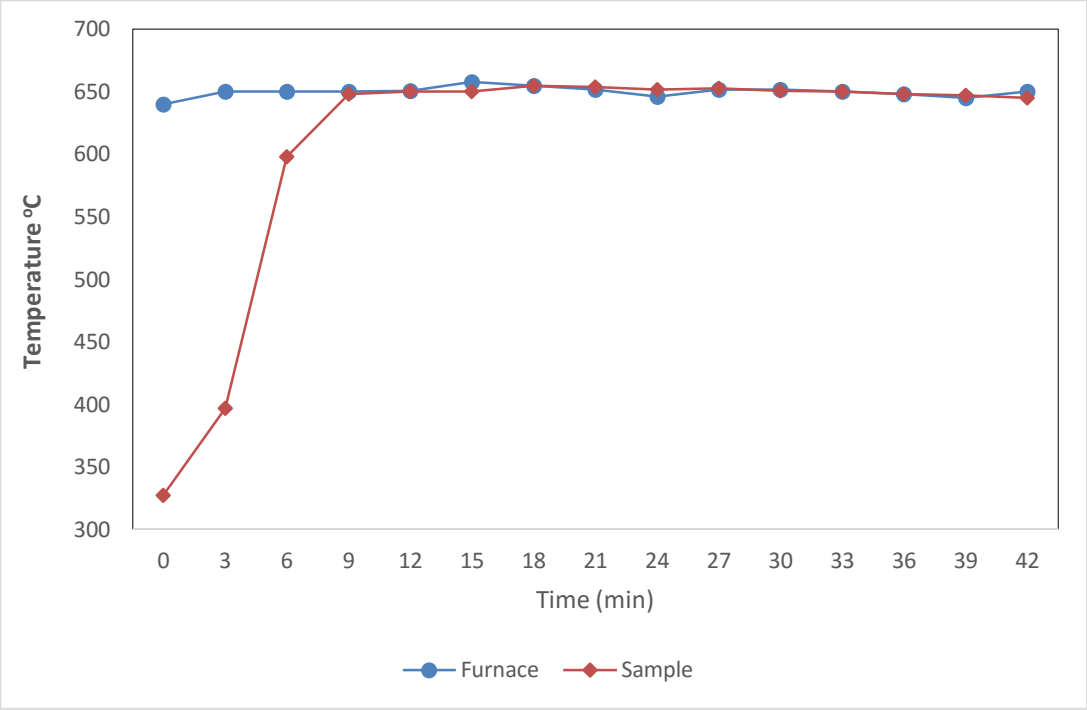

Figure A.11 Roast temperature plot for pure maghemite at 650°C and 50% O_2

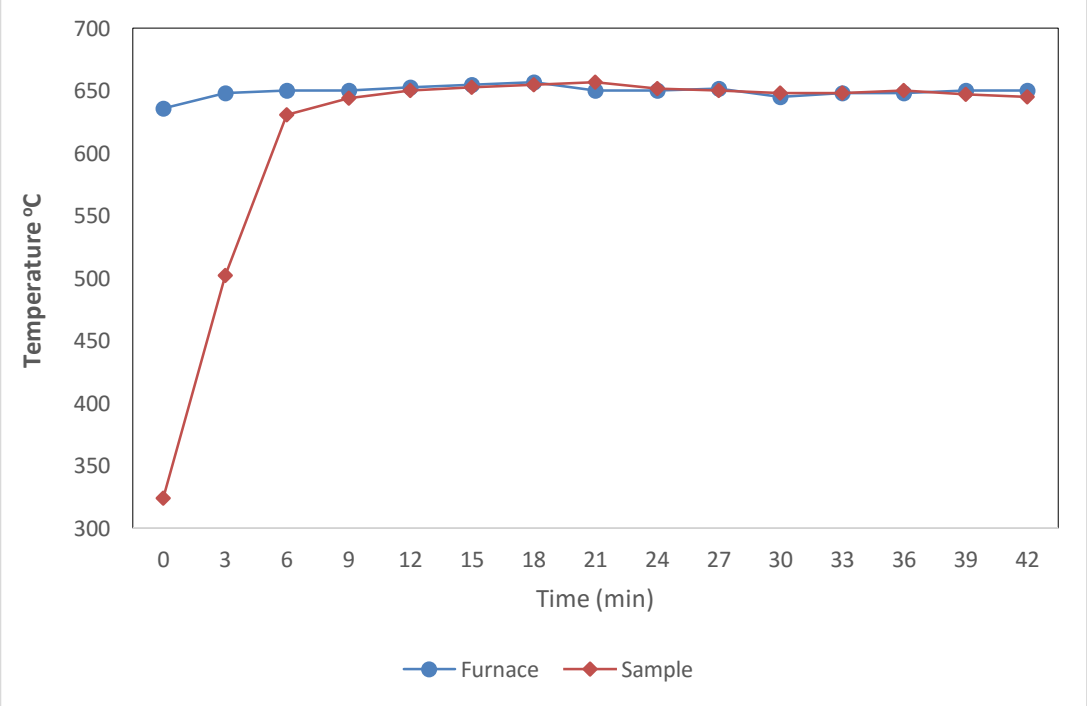

Figure A.12 Roast temperature plot for pure maghemite at 650°C and 75% O_2

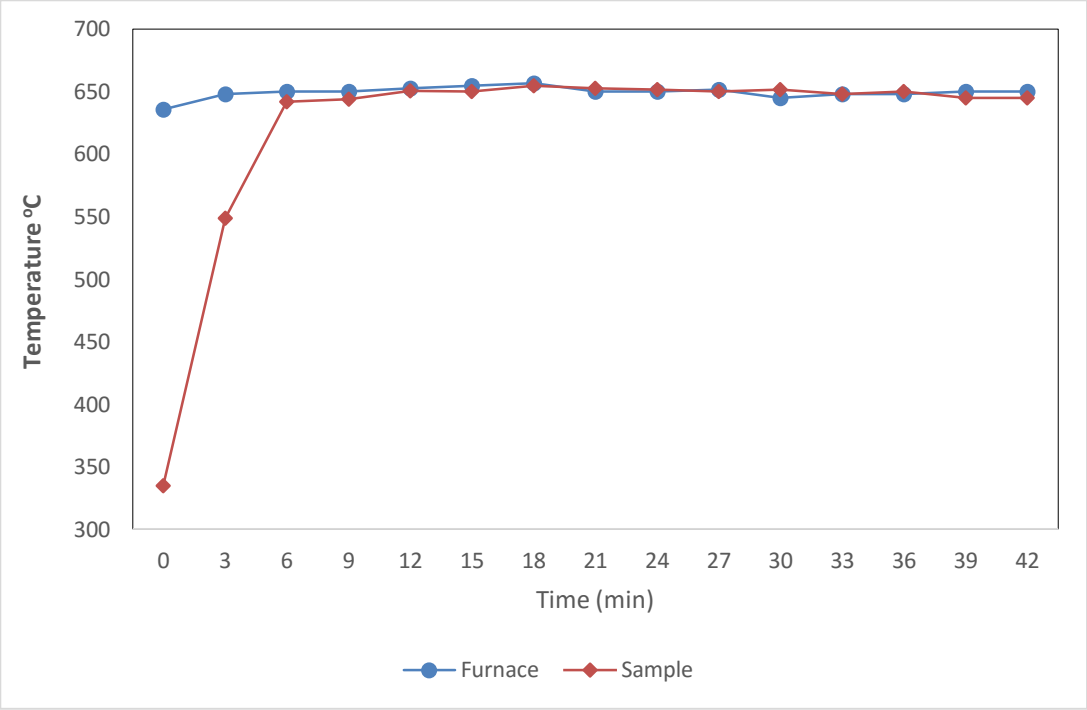

Figure A.13 Roast temperature plot for pure maghemite at 650°C and 100% O_2

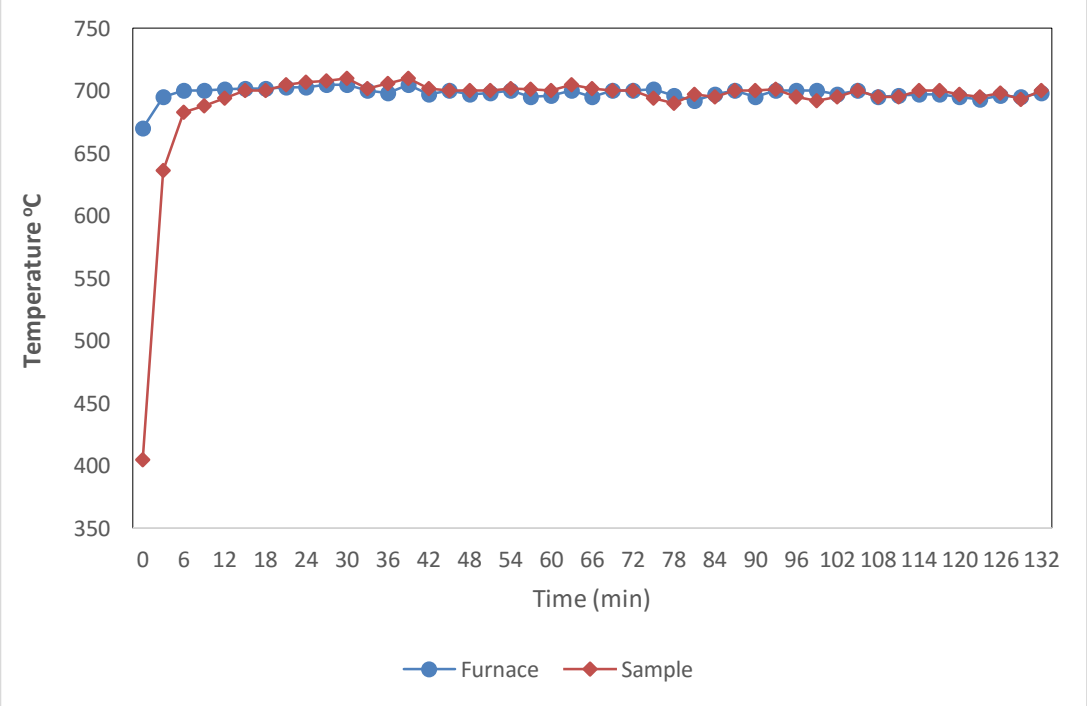

Figure A.14 Roast temperature plot for pure maghemite at 700°C and 50% O_2

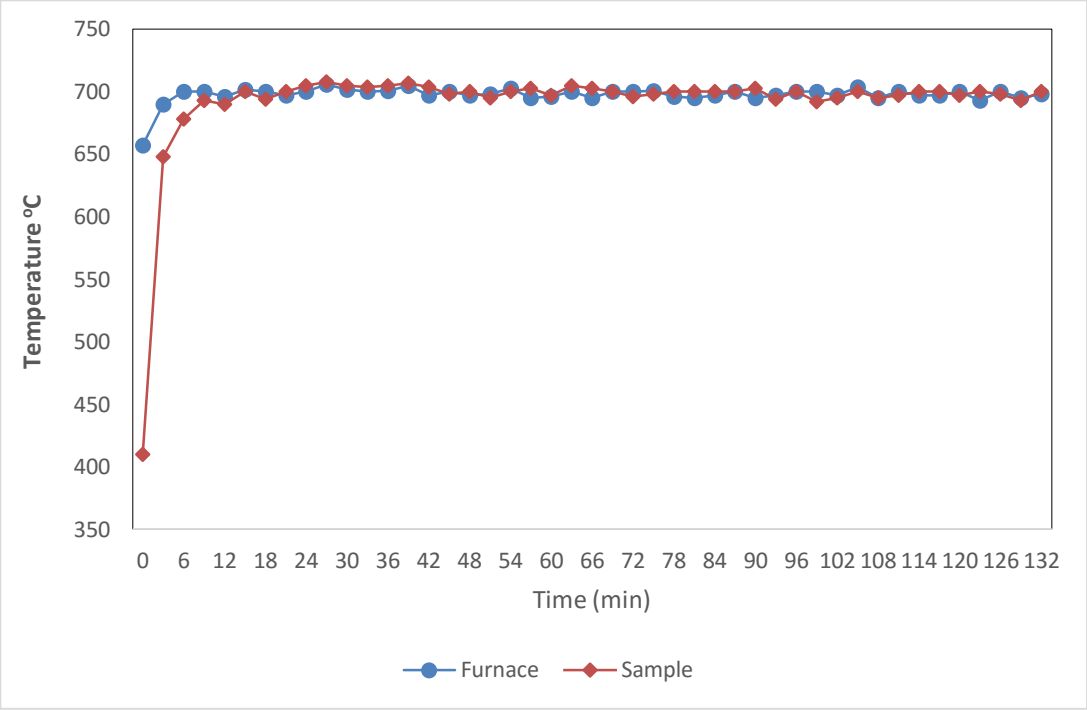

Figure A.15 Roast temperature plot for pure maghemite at 700°C and 75% O_2

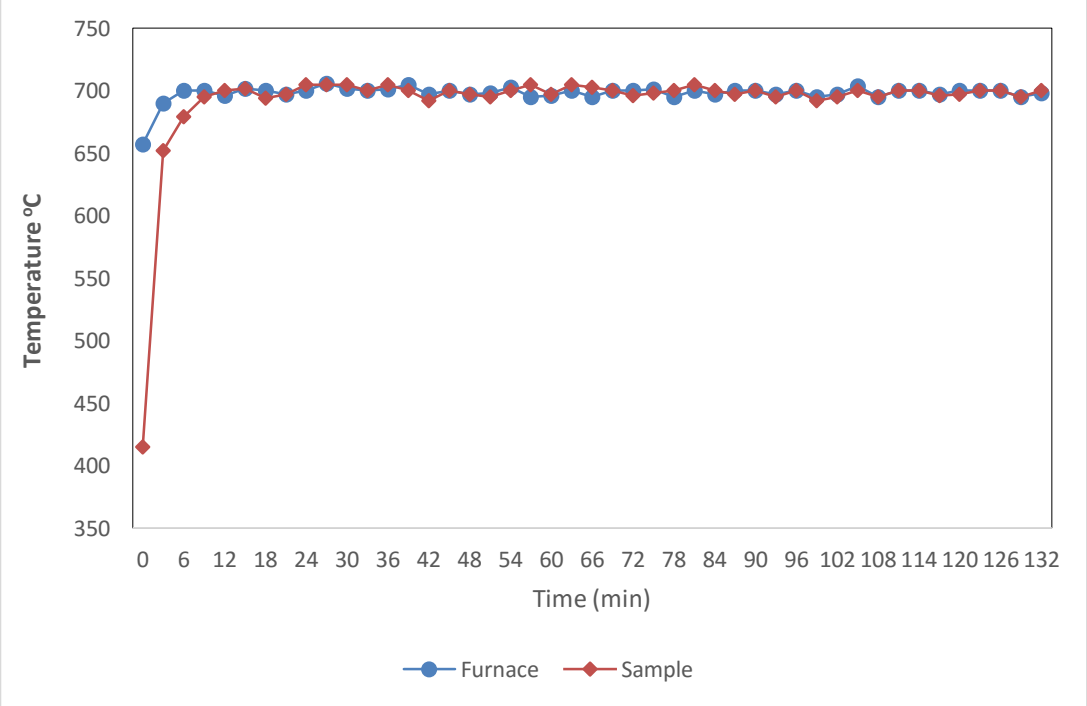

Figure A.16 Roast temperature plot for pure maghemite at 700°C and 100% O_2

APPENDIX B

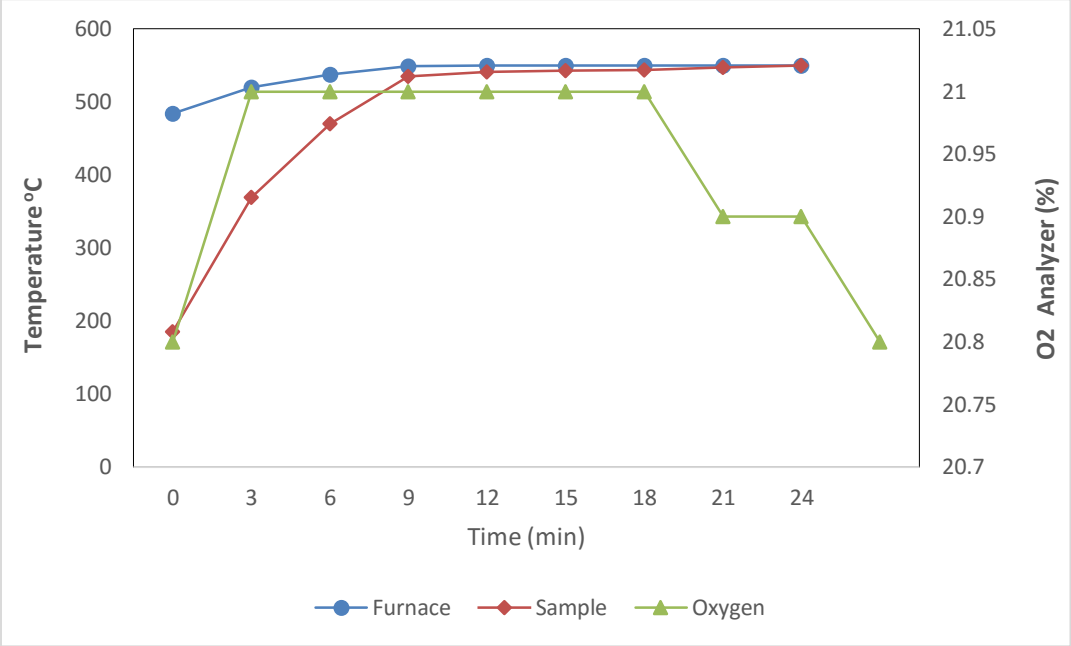

Figure B.1 Roast temperature and oxygen plot for MagCon sample at 550°C

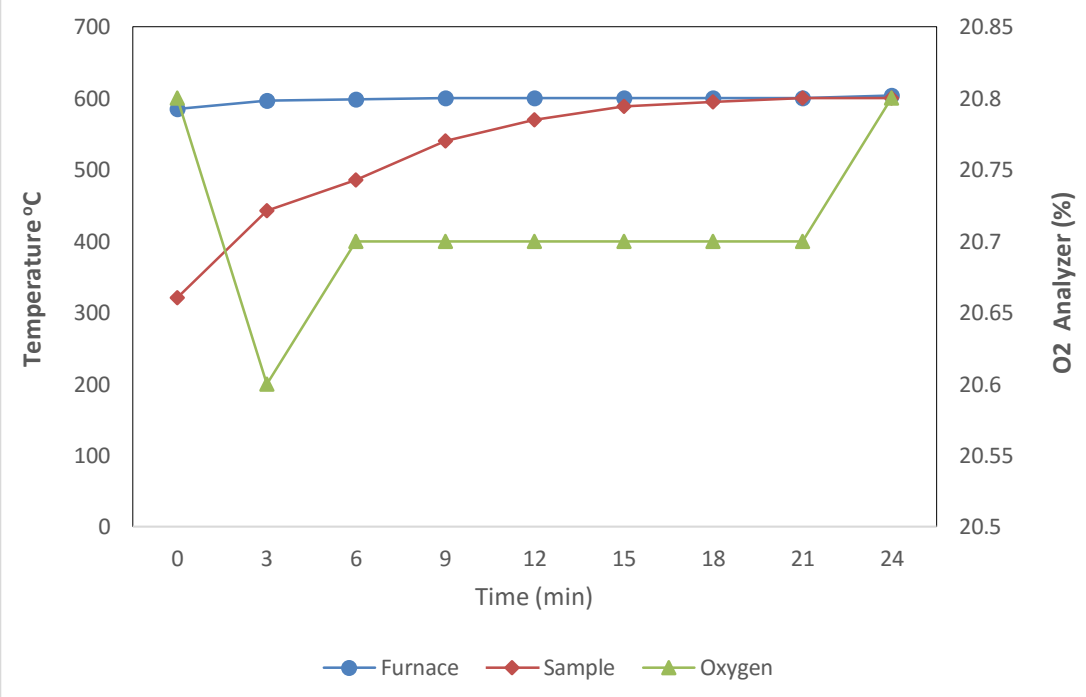

Figure B.2 Roast temperature and oxygen plot for Mag Con sample at 600°C

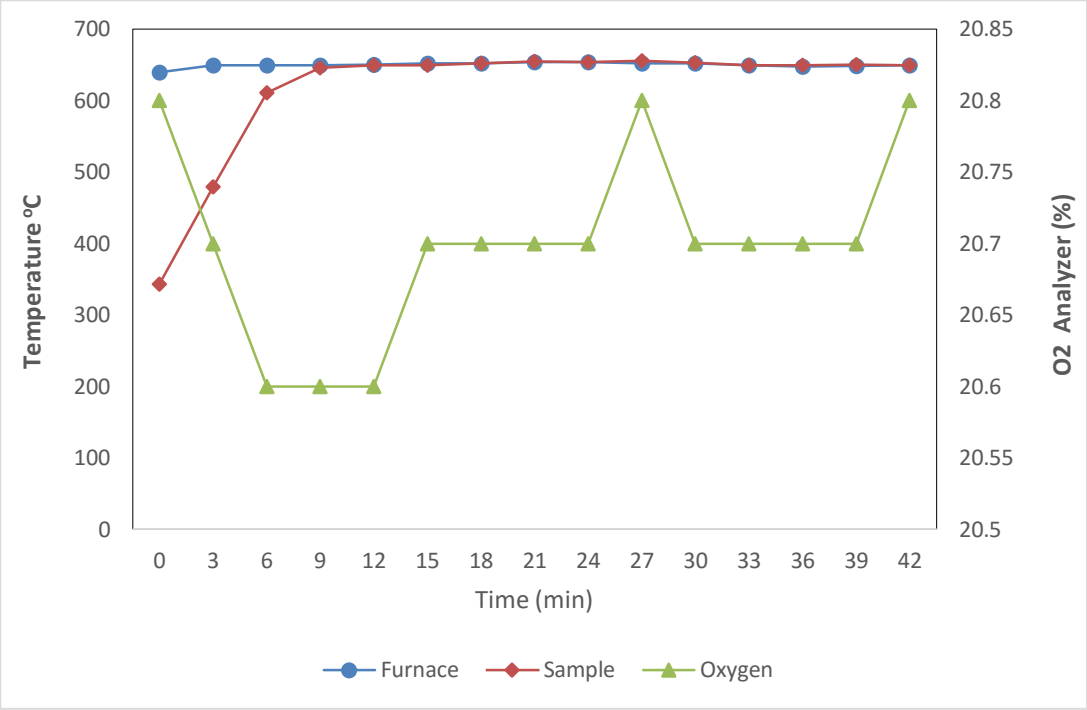

Figure B.3 Roast temperature and oxygen plot for Mag Con sample at 650°C

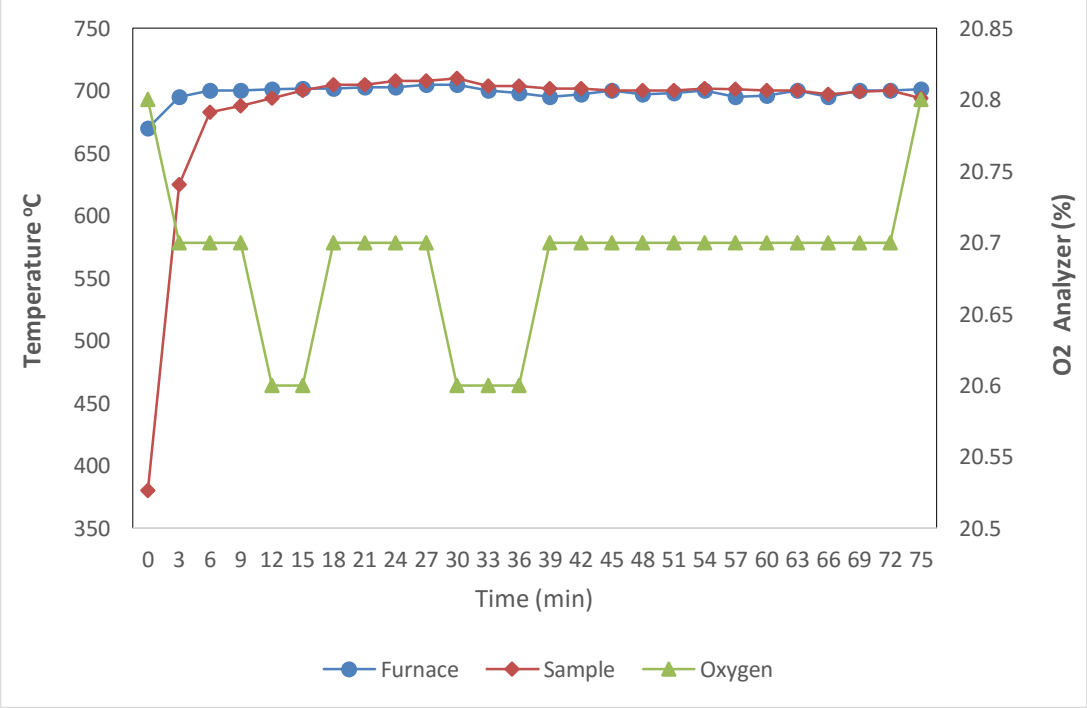

Figure B.4 Roast temperature and oxygen plot for Mag Con sample at 700°C

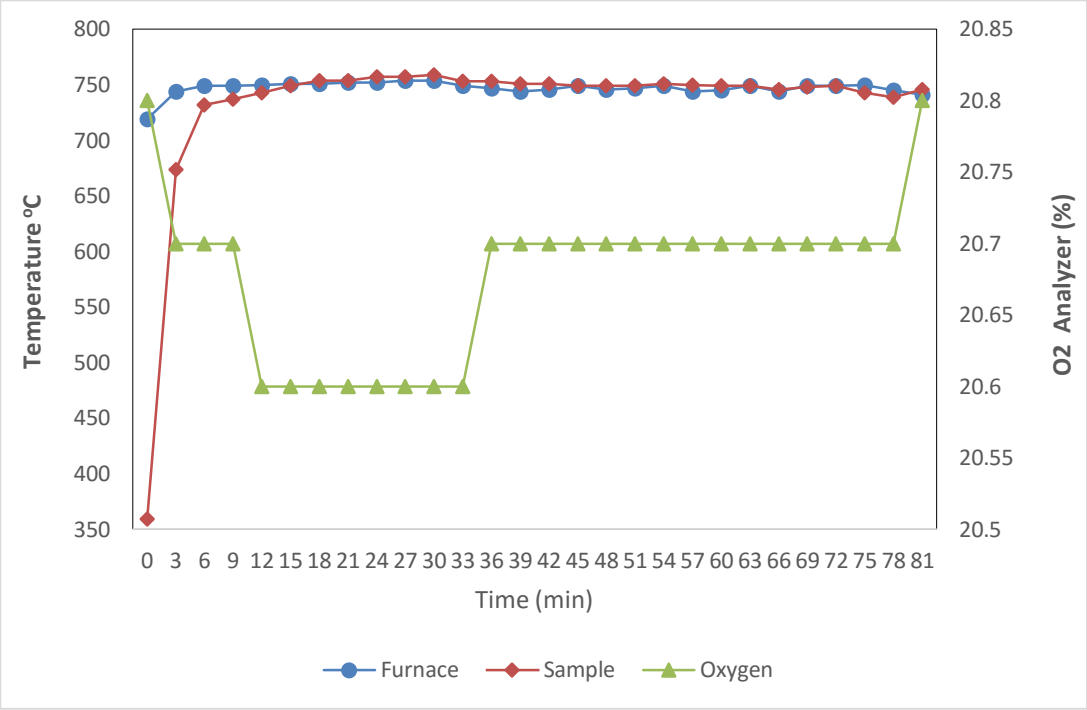

Figure B.5 Roast temperature and oxygen plot for Mag Con sample at 750°C

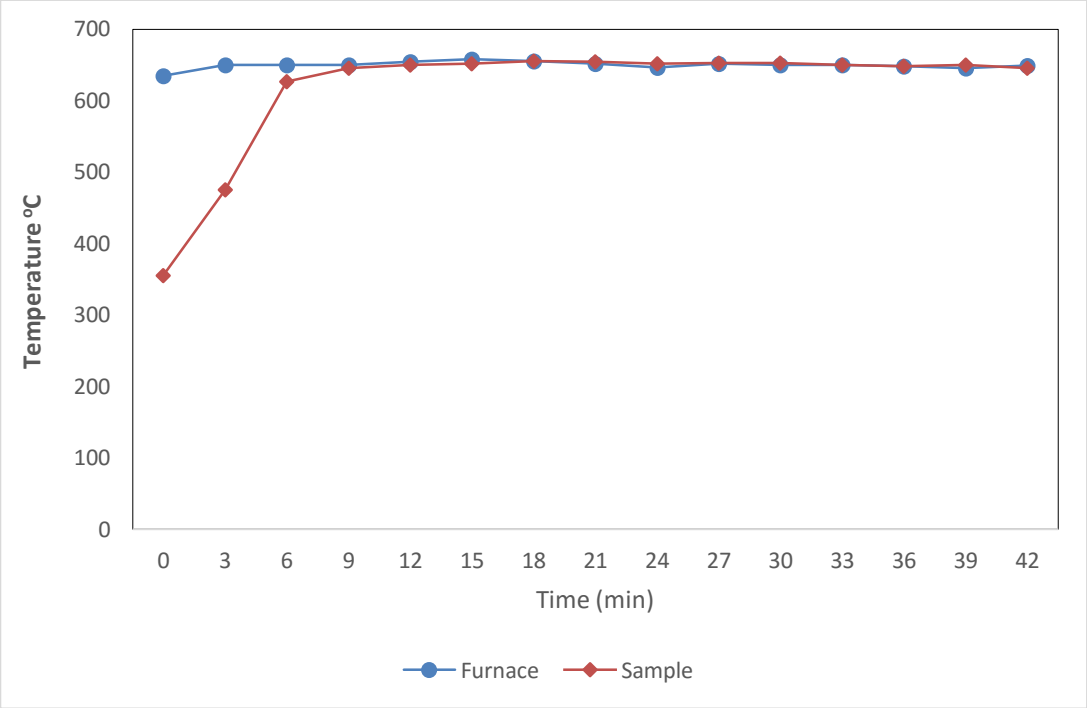

Figure B.6 Roast temperature and oxygen plot for Mag Con sample at 650°C and 50% O_2

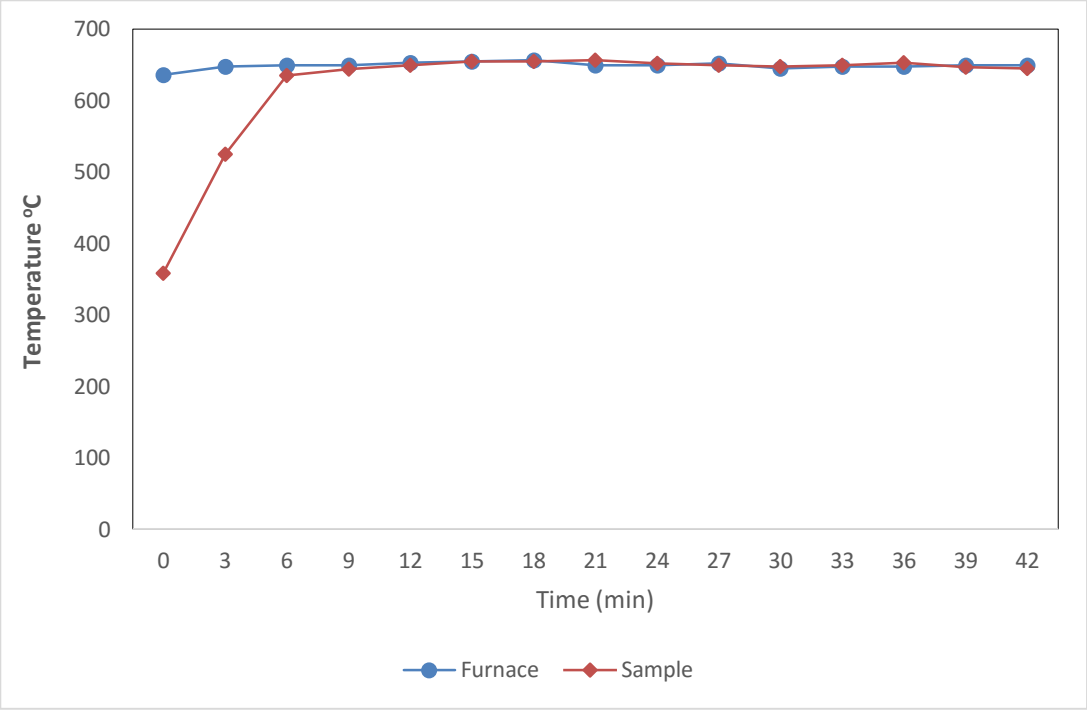

Figure B.7 Roast temperature and oxygen plot for Mag Con sample at 650°C and 75% O_2

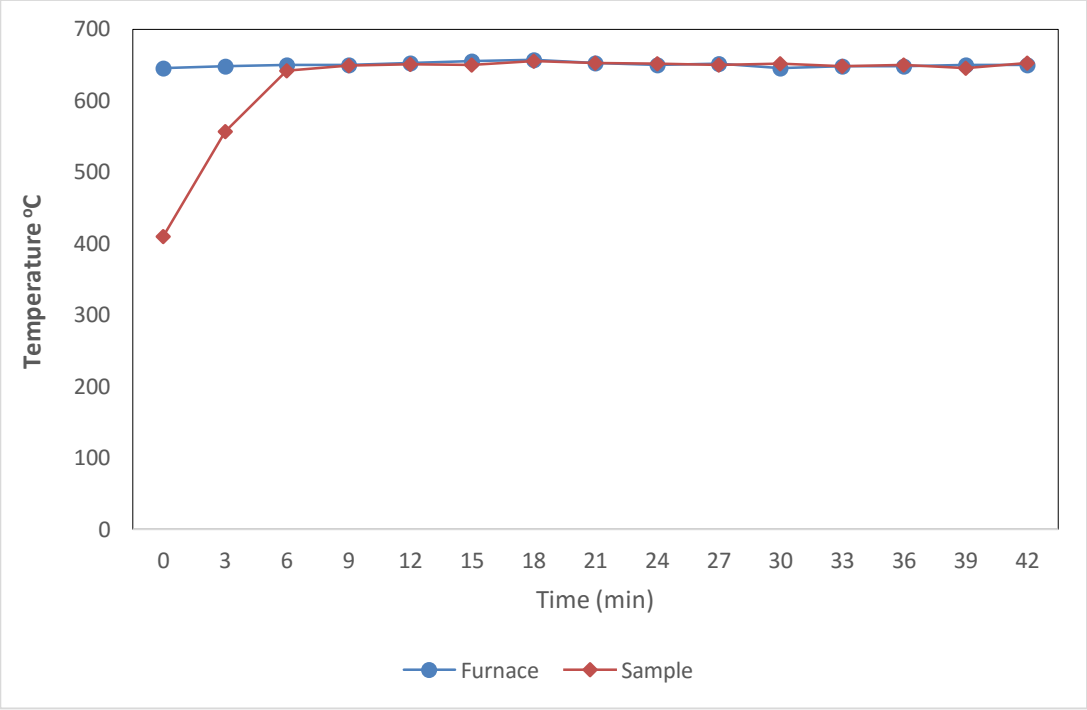

Figure B.8 Roast temperature and oxygen plot for Mag Con sample at 650°C and 100% O_2

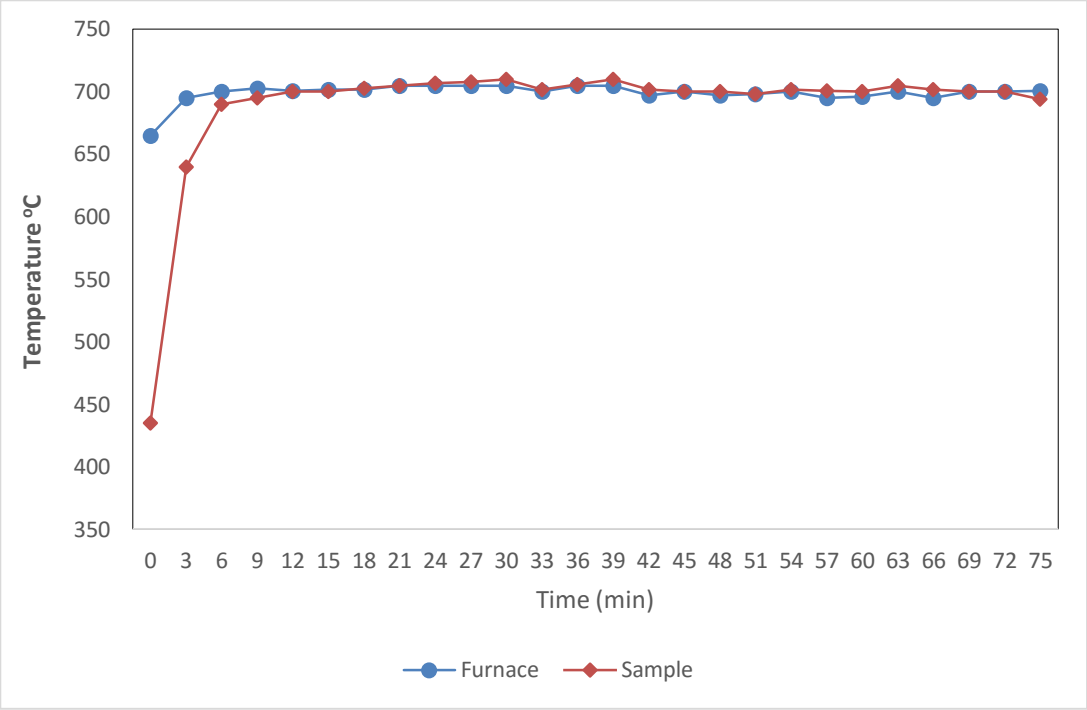

Figure B.9 Roast temperature and oxygen plot for Mag Con sample at 700ºC and 50% O_2

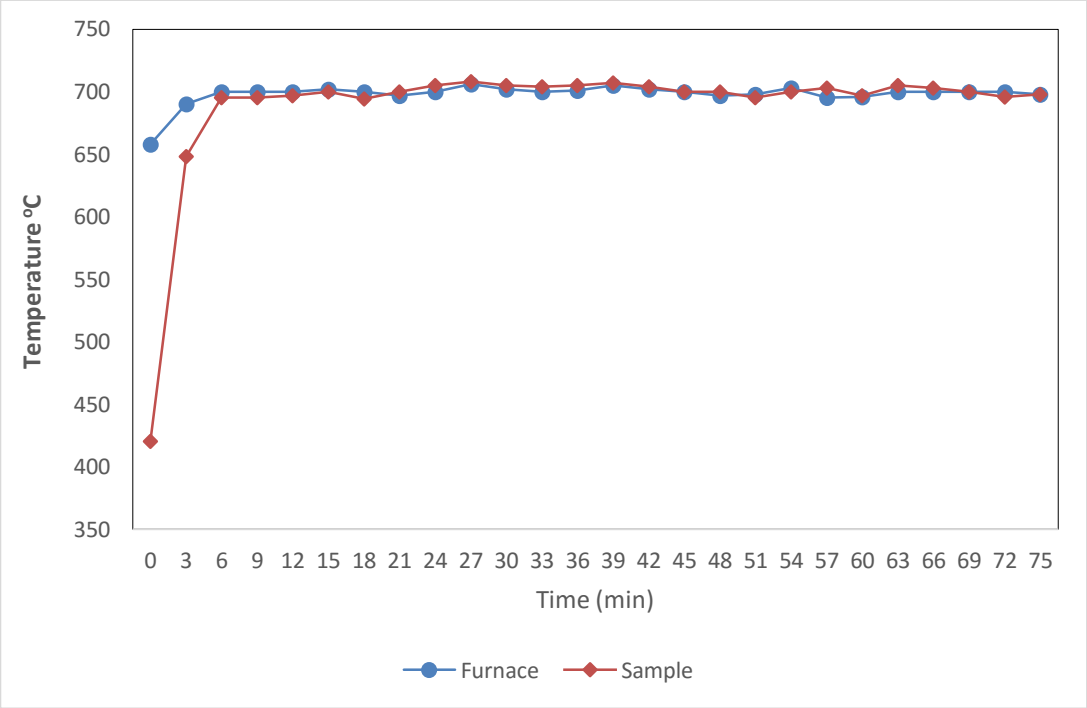

Figure B.10 Roast temperature and oxygen plot for Mag Con sample at 700ºC and 75% O_2

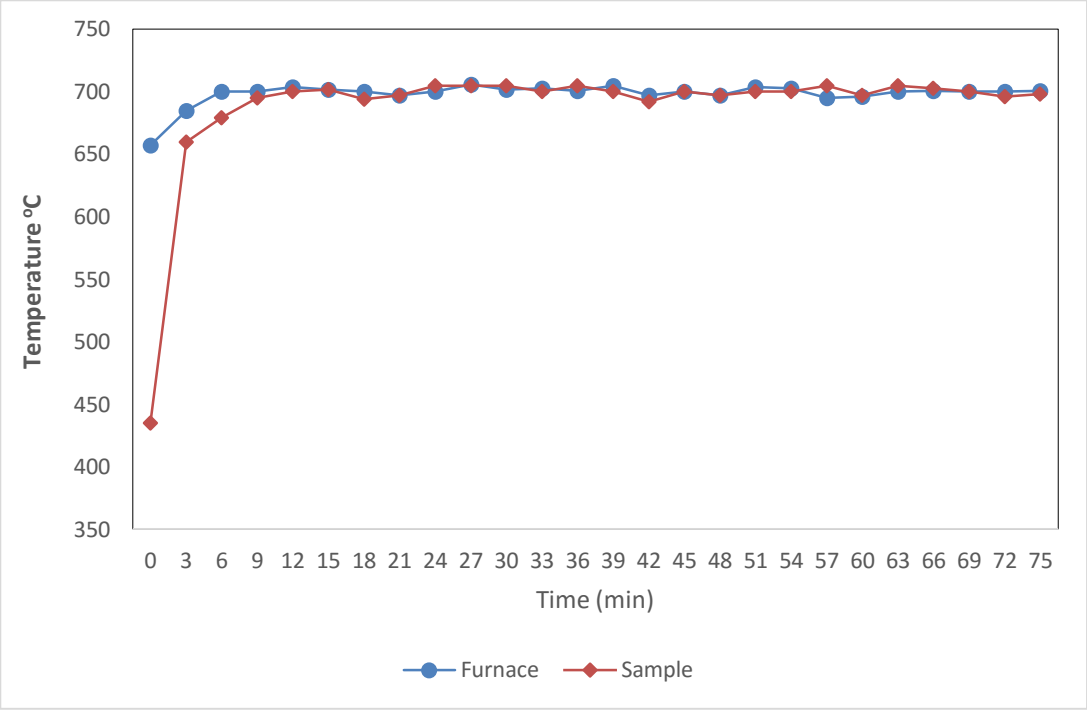

Figure B.11 Roast temperature and oxygen plot for Mag Con sample at 700ºC and 100% O_2

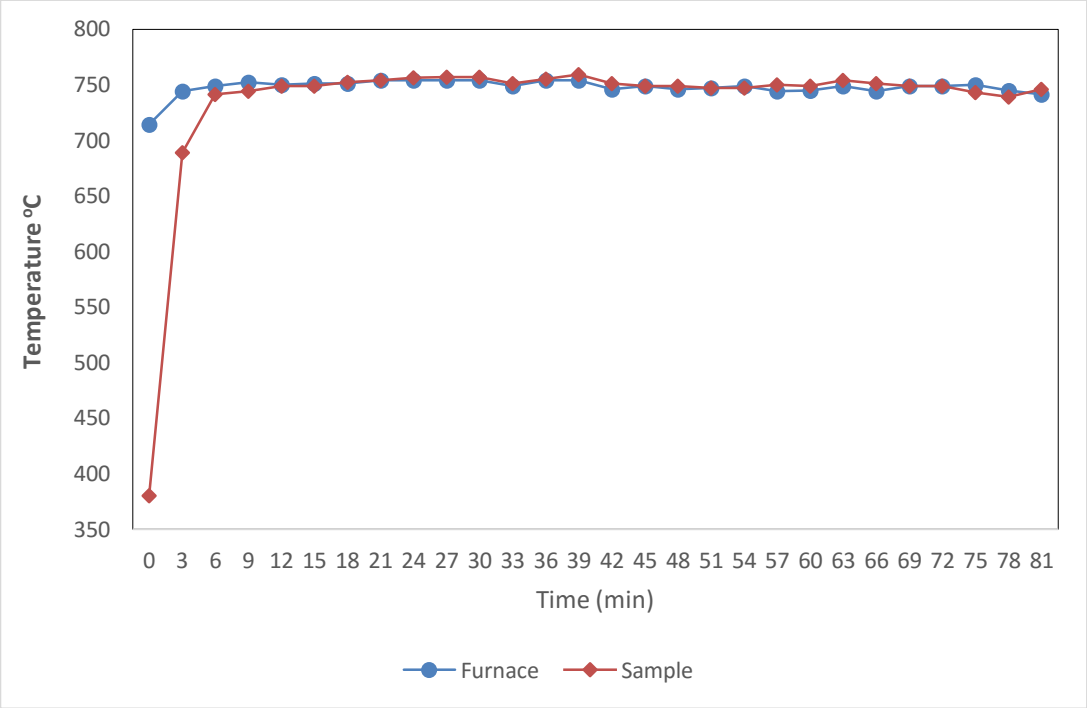

Figure B.12 Roast temperature and oxygen plot for Mag Con sample at 750ºC and 50% O_2

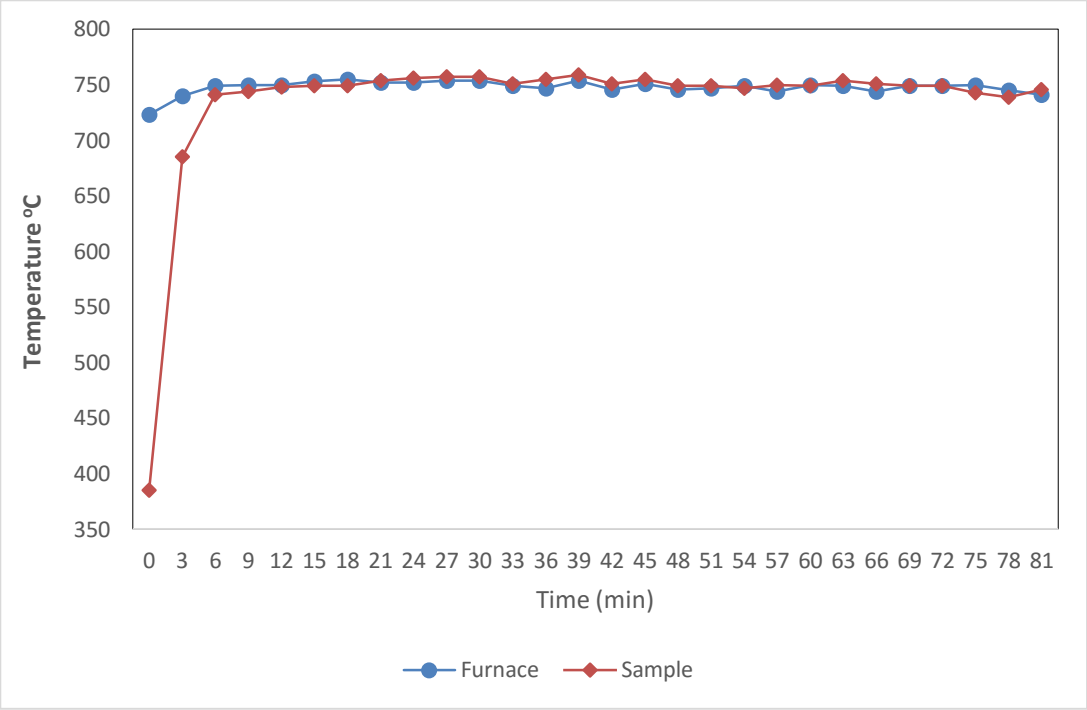

Figure B.13 Roast temperature and oxygen plot for Mag Con sample at 750°C and 75% O_2

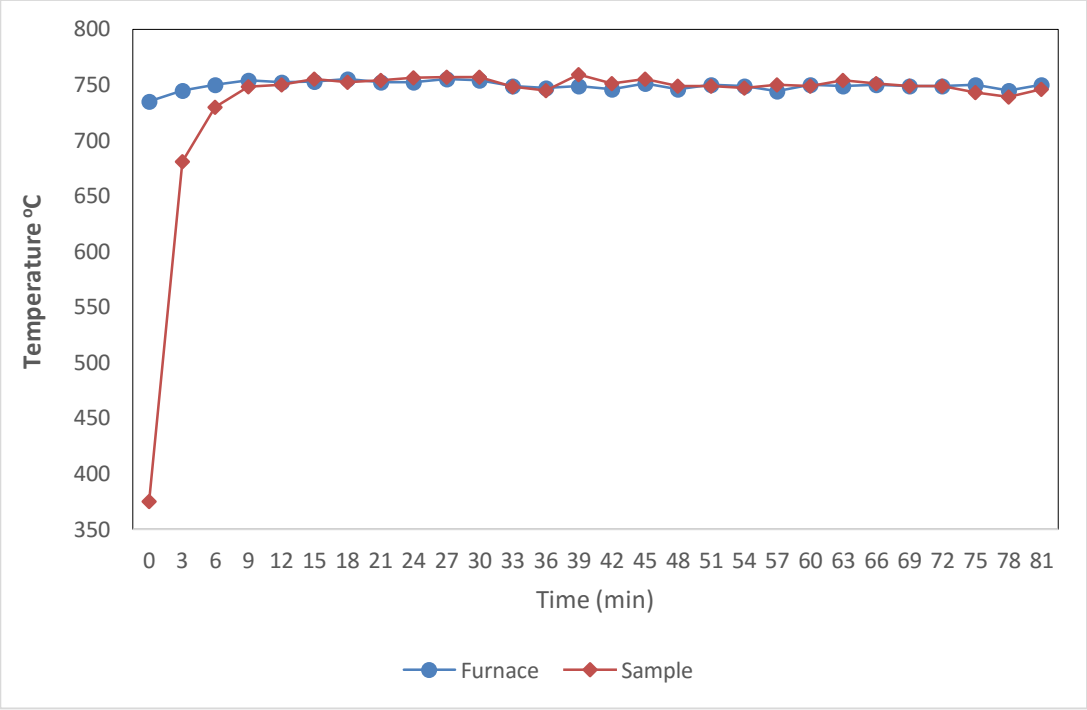

Figure B.14 Roast temperature and oxygen plot for Mag Con sample at 750°C and 100% O_2

APPENDIX C

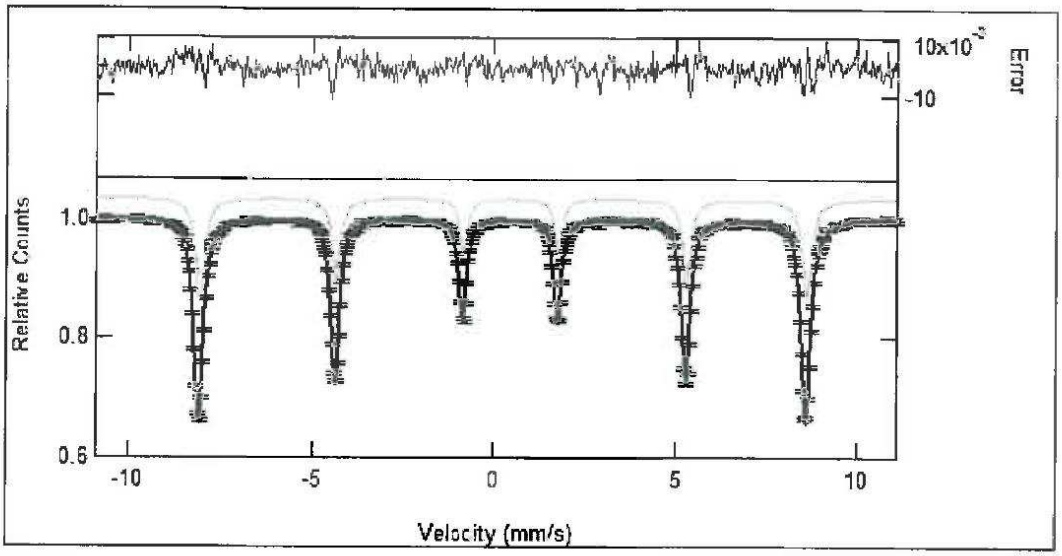

Figure C.1 Mossbauer spectra for pure hematite sample

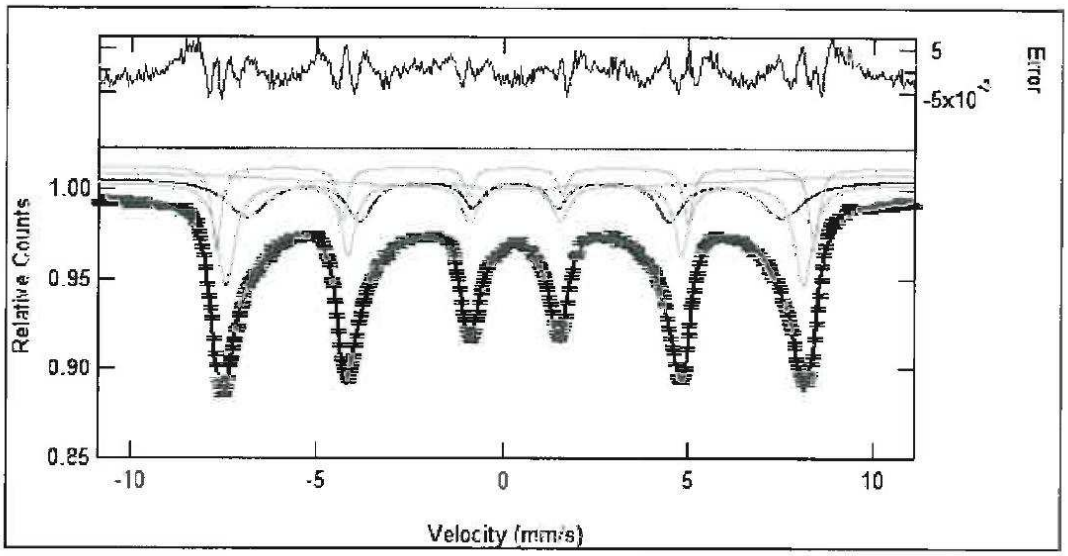

Figure C.2 Mossbauer spectra for pure maghemite sample

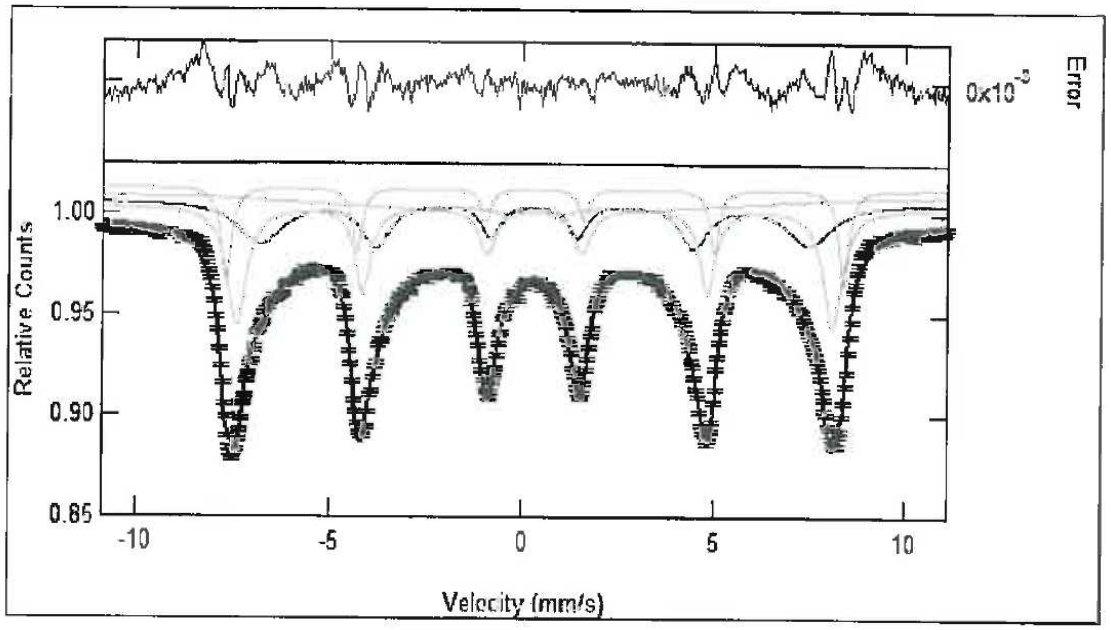

Figure C.3 Mossbauer spectra for pure maghemite sample at 450°C

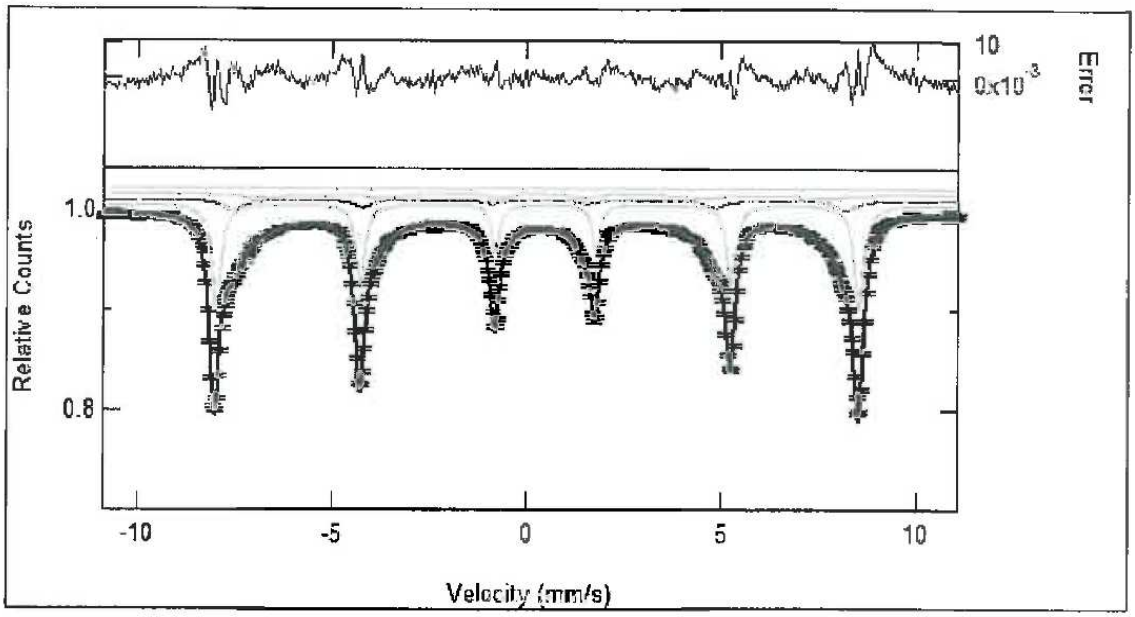

Figure C.4 Mossbauer spectra for pure maghemite sample at 600°C

Table C.1 Pure Hematite and Maghemite Mossbauer Data

Sample	% Maghemite	% Hematite
Pure Hematite	0	100
Pure Maghemite	100	0
Maghemite Calcine @ 450°C	98.5	1.5
Maghemite Calcine @ 600°C	64	36

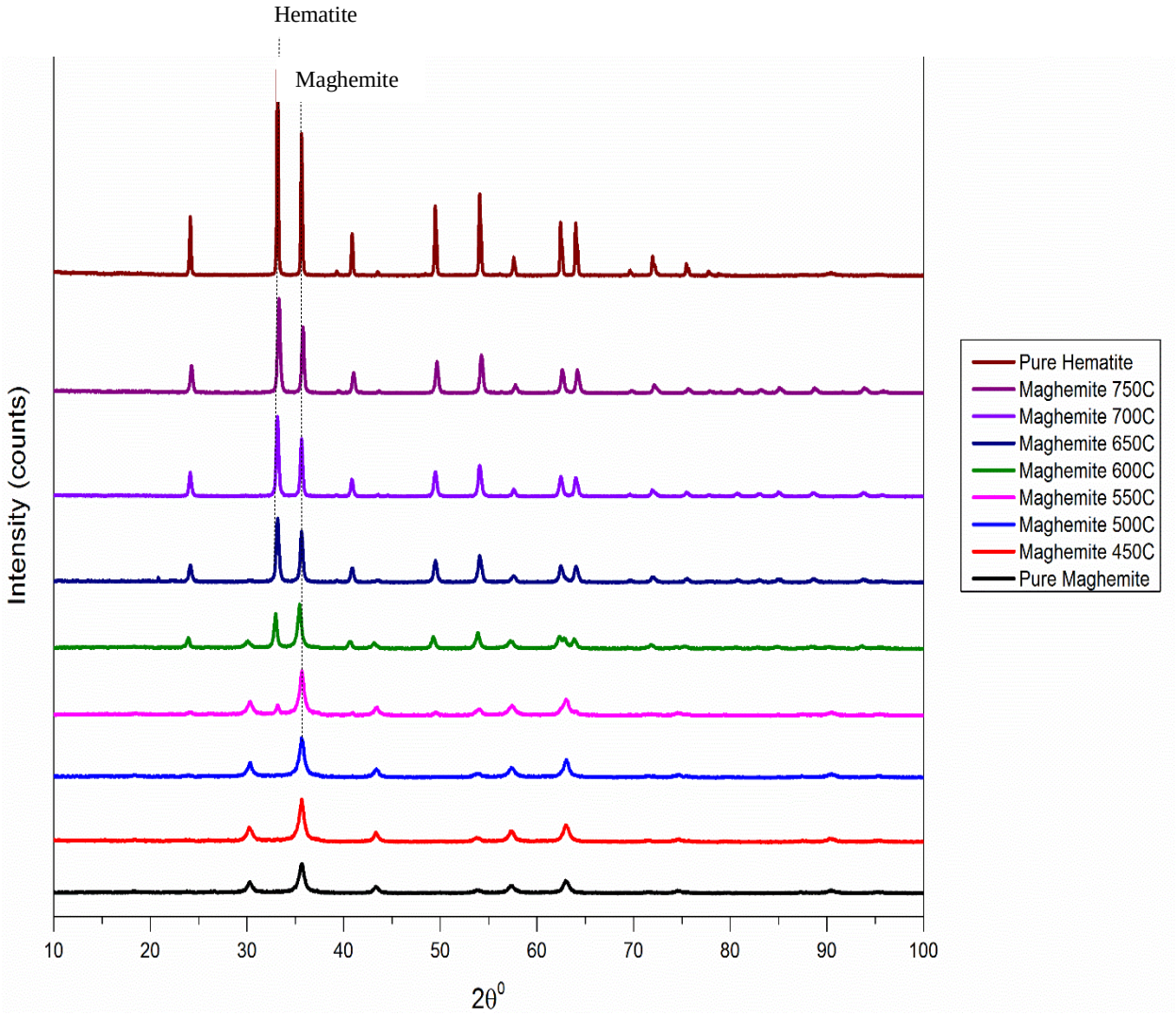

Figure C.5 XRD Results for Pure Maghemite at Various Temperatures

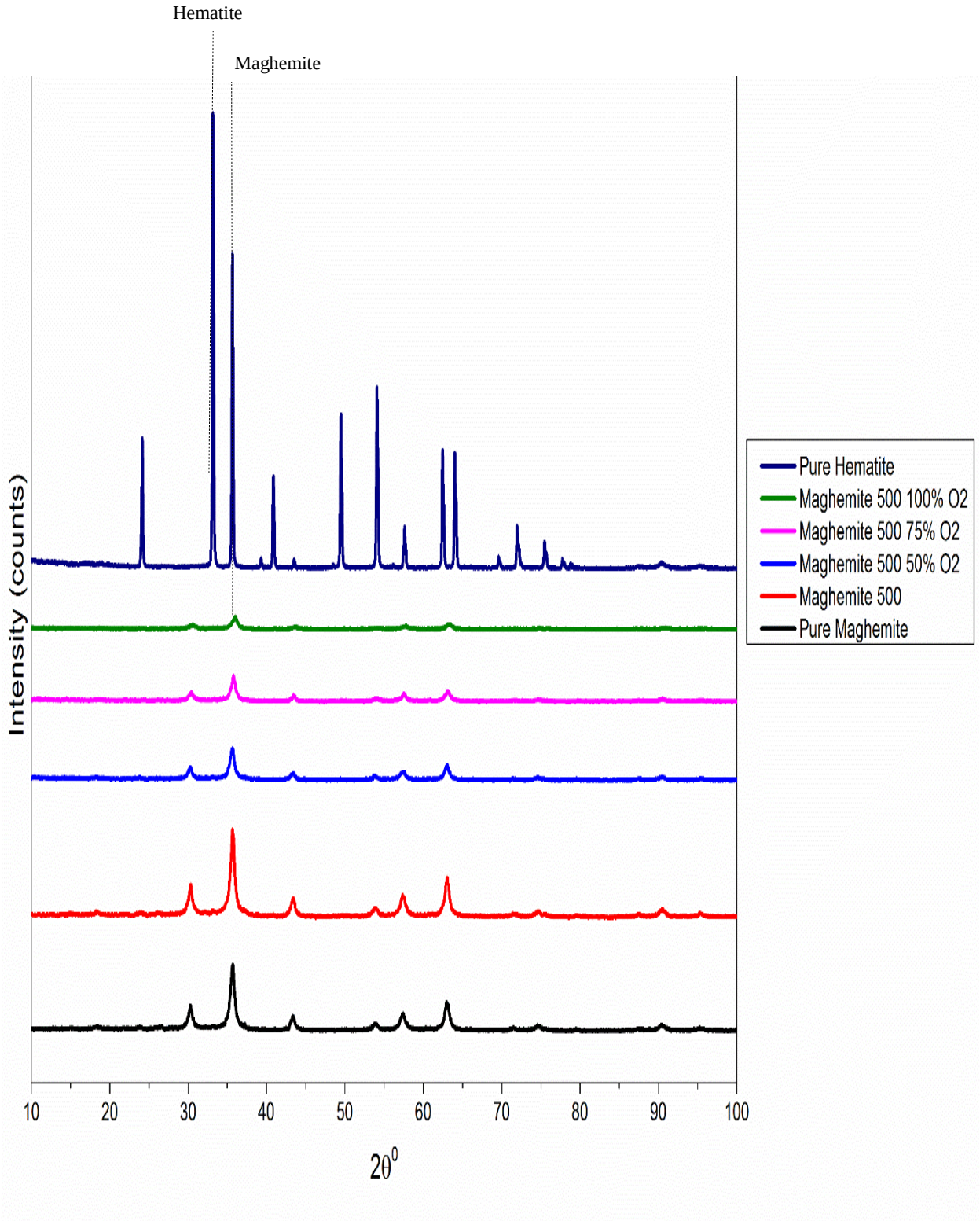

Figure C.6 XRD Results for Pure Maghemite Roasted at 500°C and Enriched with O_2

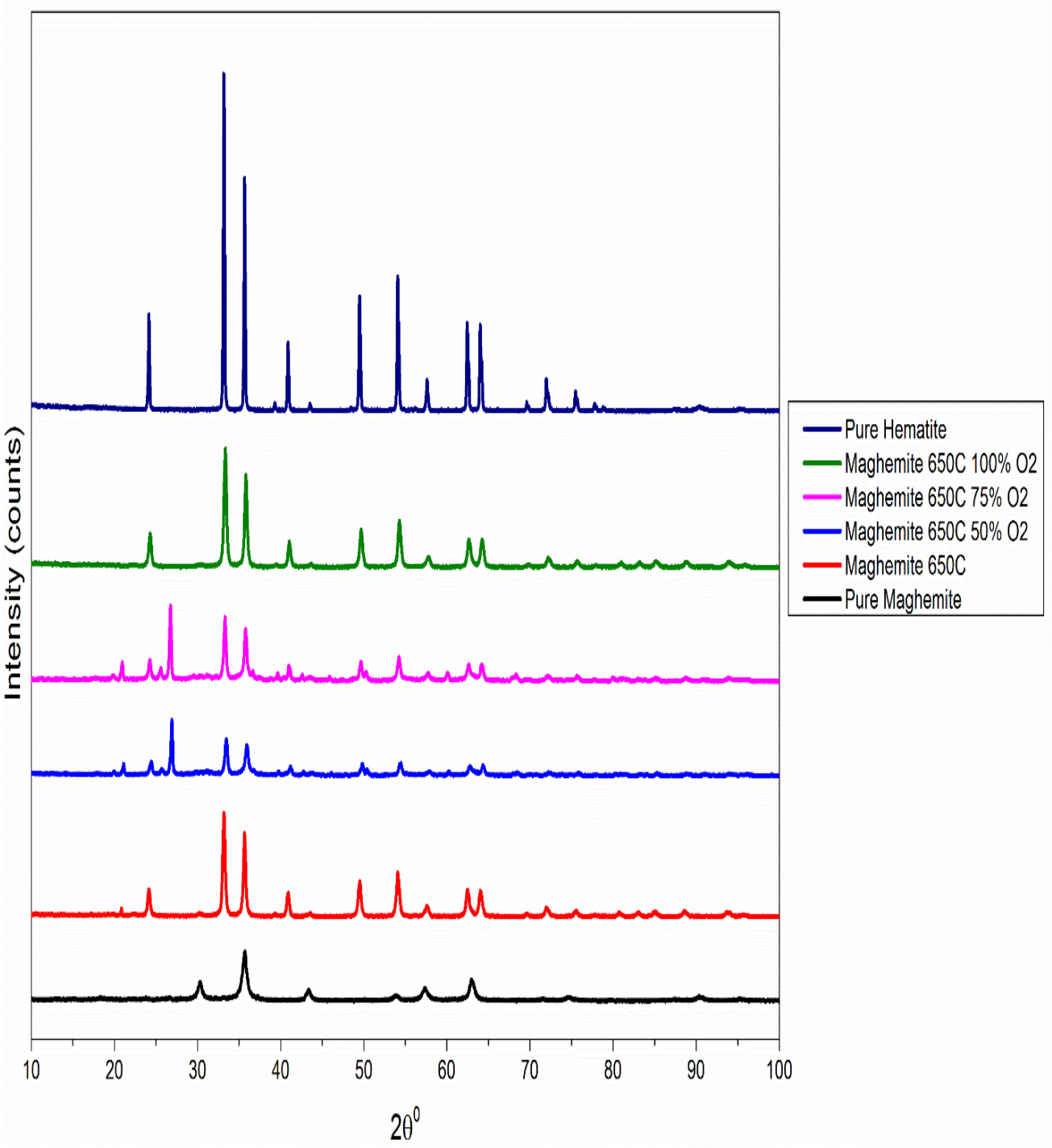

Figure C.7 XRD Results for Pure Maghemite Roasted at 650°C and Enriched with O_2

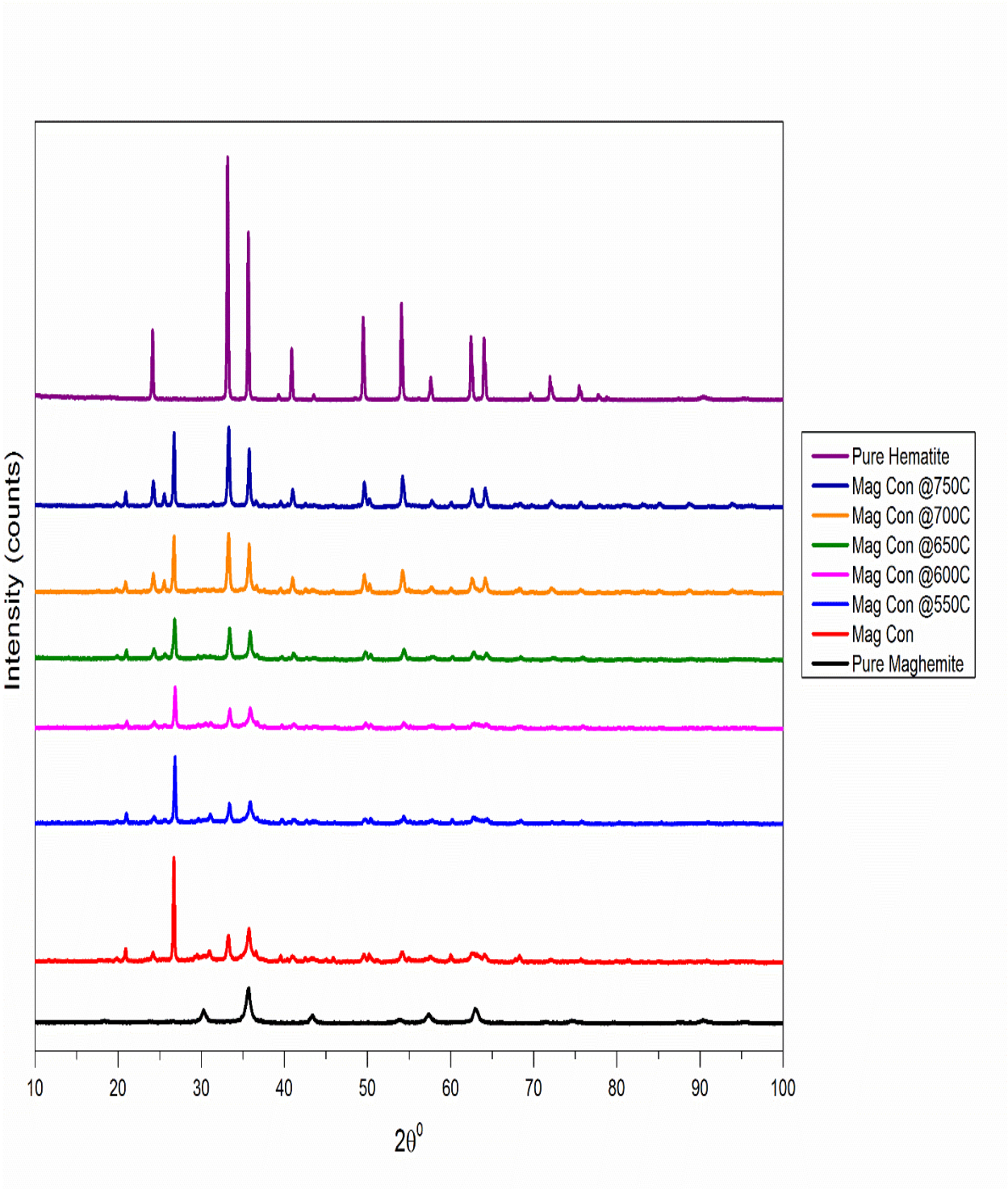

Figure C.8 XRD Results for Mag Con Roasted at Various Temperatures

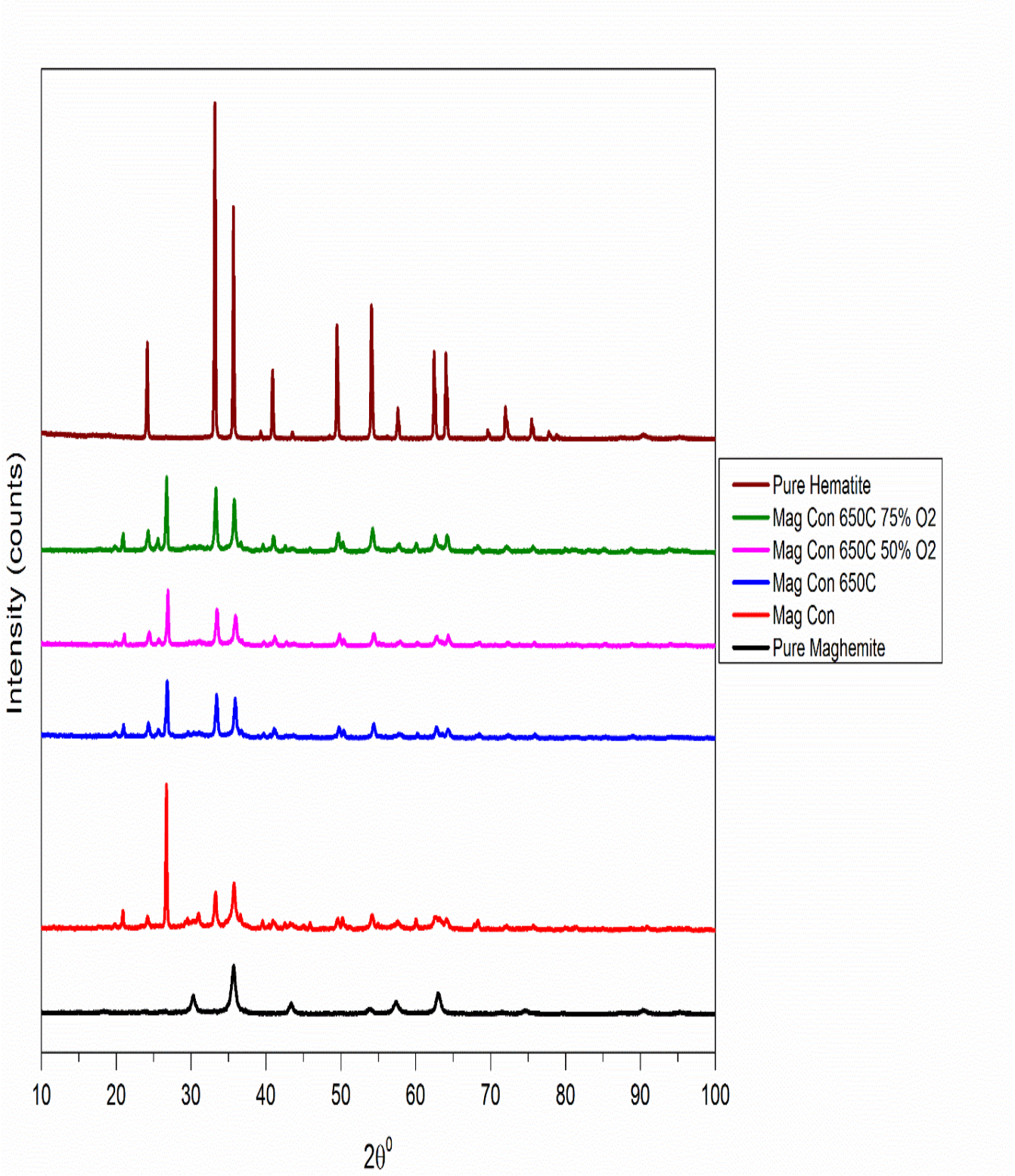

Figure C.9 XRD Results for Mag Con Roasted at 650°C and Enriched at indicated O_2 Percentages

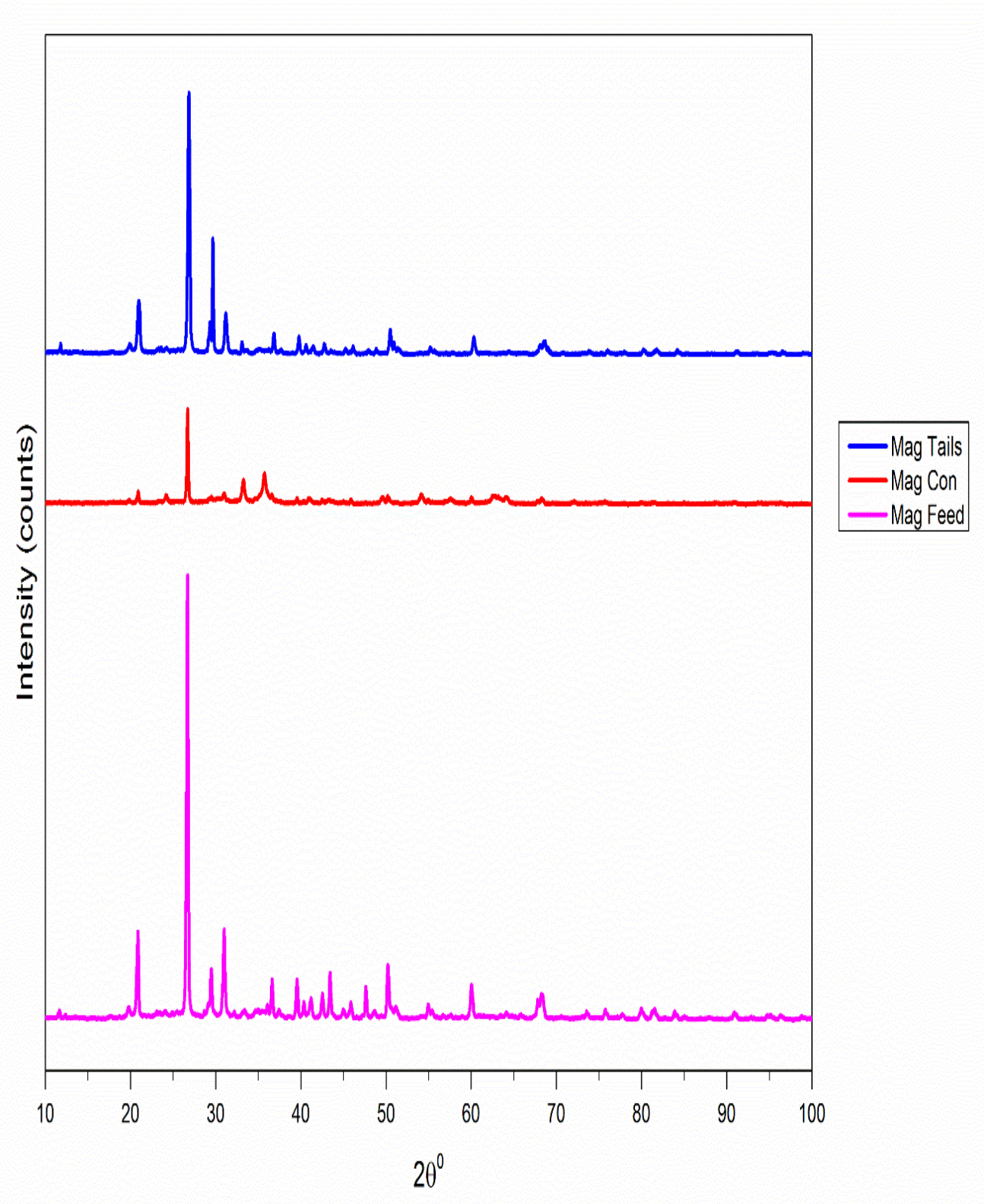

Figure C.10 XRD Results for Phases present in Mag Feed, Mag Con and Mag Tails